January 2019

The Effect Of Different Dianhydride Precursors On The Synthesis, Characterization And Gas Separation Properties Of PI And PBO Derived From BisAPAF

Maram Abdulhakim Qasem Al-Sayaghi

Follow this and additional works at: https://commons.und.edu/theses

THE EFFECT OF DIFFERENT DIANHYDRIDE PRECURSORS ON THE SYNTHESIS,
CHARACTERIZATION AND GAS SEPARATION PROPERTIES OF PI AND PBO
DERIVED FROM BISAPAF

By

Maram Abdulhakim Qasem Al-Sayaghi
Bachelor of Engineering, University of Leeds, UK, 2016

A Thesis
Submitted to the Graduate Faculty

of the

University of North Dakota

In partial fulfillment of the requirements

for the degree of

Master of Science
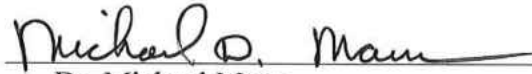
Grand Forks, North Dakota

May

2019

This thesis, submitted by Maram Al-Sayaghi in partial fulfillment of the requirements for the Degree of Master of Science from the University of North Dakota, has been read by the Faculty Advisory Committee under whom the work has been done and is hereby approved.
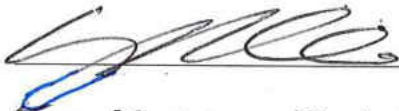
Dr. Ali Alshami

Dr. Michael Mann

Dr. Edward Kolodka

This thesis is being submitted by the appointed advisory committee as having met all of the requirements of the School of Graduate Studies at the University of North Dakota and is hereby approved.

Dean of the School of Graduate Studies

4/24/19
Date

TABLE OF CONTENT

LIST OF FIGURES

xi

LIST OF TABLES

ACKNOWLEDGEMENTS

ABSTRACT

The current processes used for natural gas separation and purification are considered energy intensive which could potentially be substituted by membrane technology. Aromatic polyimides are considered one of the most viable types of polymers used for the fabrication of membranes for gas separation mainly due to their outstanding properties. Moreover, aromatic polyimides could be thermally rearranged to form another class of polymers called polybenzoxazoles which are characterized by having enhanced gas separation properties. This research aimed to (1) synthesize and characterize three different aromatic polyimides via polycondensation reaction of a diamine (BisAPAF) with three different dianhydride precursors (PMDA, ODPA, BTDA), (2) fabricate free-standing polyimide membranes, and thermally rearrange them to polybenzoxazoles and (3) compare the gas separation properties (permeabilities and selectivities) of the membranes before and after the thermal rearrangement and compare the results to Robeson upper bounds. The tested gas pairs tested were CO_2/CH_4, N_2/CH_4 and CO_2/N_2. All the objectives of this research were successfully achieved, and it was found that chemical structure of the starting monomers plays a key role in the physicochemical properties of the synthesized polyimides which, consequently affected the gas separation properties. Among the three polyimides, APAF-BTDA showed the superior performance followed by APAF-PMDA and finally APAF-ODPA. This is believed to be due to the stability of the BTDA pendant group which resulted in high conversion and, hence, the best separation performance where they surpassed the Robeson upper bound for all gas pairs.

CHAPTER 1: EXECUTIVE SUMMARY

Natural gas is considered one of the primary fuels that currently supplies around 22% of the world's energy and its consumption is expected to continue increasing exponentially for at least the coming 30 years [1]. As the raw natural gas is extracted, it is usually accompanied with impurities such as carbon dioxide and nitrogen that need to be removed before being able to transport it through pipelines. This separation/purification step is currently done via conventional processes such as cryogenic distillation, pressure swing adsorption and absorption/stripping. These processes are energy intensive, complex and rather unsustainable. Therefore, separation using membranes is currently considered a potential viable alternative for the current conventional processes that could contribute towards a more sustainable future.

Generally, two types of membranes can be used for gas separation: polymeric and inorganic. Among the two, polymeric membranes are considered the most commonly used and investigated and that is mainly due to their superior properties and relative cost effectiveness. One of the most viable types of polymers that has been explored intensively are aromatic polyimides. They are well known by their exceptional thermal stability, chemical resistance, mechanical strength and electric properties. They are generally formed via a polycondensation reaction of two monomers, a diamine and a dianhydride. It was found that the properties of polyimides could be significantly manipulated by varying the starting monomers. These properties include molecular weights, glass transition temperatures, degradation

Temperatures, as well as the rigidity of the chains and the extent and distribution of fractional free volume that dictates the gas separation properties.

Furthermore, the gas separation properties of aromatic polyimides could significantly be enhanced via a thermal treatment which converts the polyimide into polybenzoxazole. During the conversion reaction, the polymer chains are rearranged to form a wide distribution of fractional free volume (FFV) which represents the distance between the polymer chains and sites through which the gases penetrate. This conversion causes the permeabilities of the gases to increase significantly. Thermal treatment also causes the polymer chains to be more rigid resulting in increasing the gases selectivities.

The hypothesis of this research concerns *varying the dianhydride precursors would affect the physicochemical properties of the polyimides and, ultimately, the gas separation performance of the membranes*. This was tested by using one diamine and three different dianhydrides precursors and their chemical structures are shown in Figure. 1. This was achieved via the following approaches:

- Synthesize the polyimide powders using the different monomers independently and ensure the procedure is reproduceable and repeatable. Then, characterize the polyimides using various analysis techniques and compare their properties.

- Fabricate free-standing polyimide membranes, and thermally rearrange them to polybenzoxazoles. Then, characterize the membranes before and after the thermal rearrangement thoroughly to verify their chemical structure.

- Preform gas permeability tests through all the polyimide membranes before and after thermal rearrangement. The gas pairs tested were CO_2/CH_4, N_2/CH_4 and CO_2/N_2.

Finally, compare the obtained data points to each other as well as to the Robeson upper bound, in an attempt to assess the extent of improvement against published results.

Diamine

2,2-Bis(3-amino-4-hydroxyphenyl)-
hexafluoro-propane (bisAPAF)

Dianhydrides

| 4,4'-oxydiphthalic anhydride (ODPA) | 3,3',4,4'- benzophenone tetracarboxylic dianhydride (BTDA) | pyromellitic dianhydride (PMDA) |
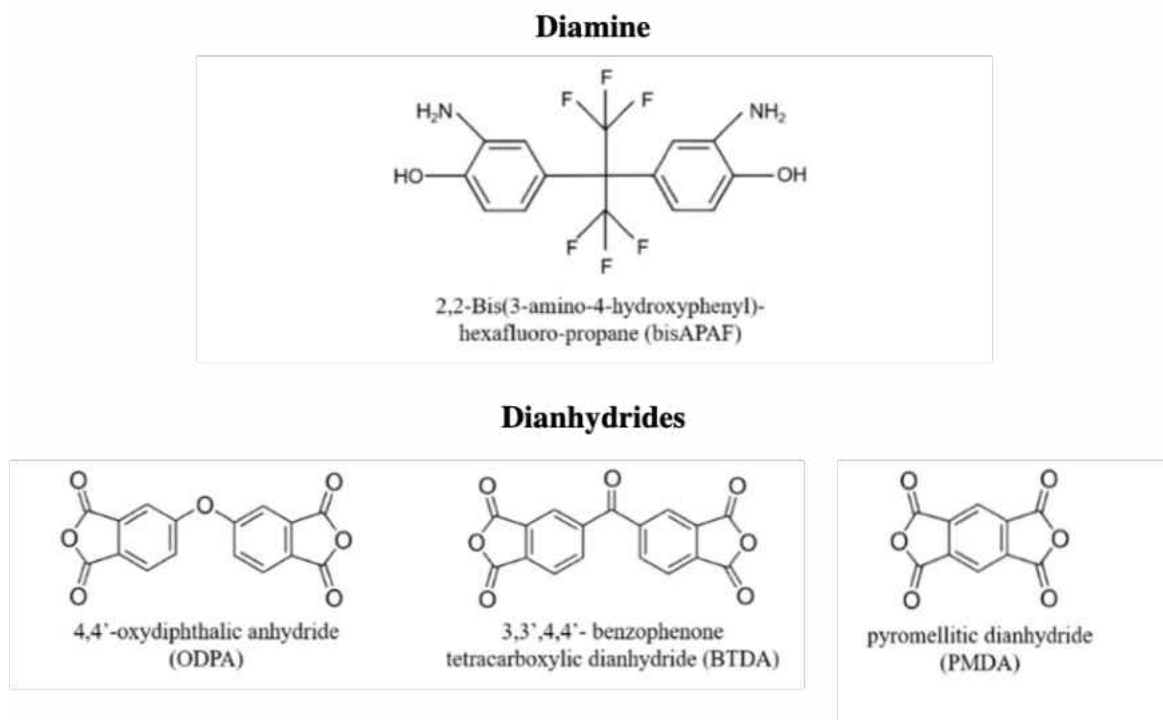
Figure 1. Chemical structures of the monomers used to synthesize the hydroxyl-polyimides (HPIs).

The thesis of research centers around the concept that *among the three dianhydride precursors, the polyimide membrane derived from BisAPAF and BTDA will provide more improved gas separation properties*. This was anticipated because the BTDA contains a very stable bridging group which would most likely result in high polymer chain rigidity.

This thesis consists of five main chapters other than executive summary. Chapter two is a literature review of the fundamentals of polyimide membranes for natural gas separation. It aims to provide the foundation needed to comprehend the rest of the thesis. It starts by discussing the main reason that drives this research and moves on to introducing all the relevant concepts. Chapter three represents the first research paper which was published at the

International Journal of Polymer Analysis and Characterization (IJPAC) in 2018. The paper concerns the synthesis of the polyimides using the different monomers, but its core is in the intensive characterization of the synthesized polyimide powders. Chapter four represents the second research paper which was submitted for publication in the Journal of Membrane Sciences (JMS). It goes through a more detailed synthesis methodology and discusses the fabrication of the free-standing membranes and the gas separation results. Chapter five then moves to discuss all the major challenges that emerged while conducting the experimental work along with all the potential solutions that were attempted. Chapter six then ends the thesis with some brief conclusions and a list of future recommendations.

CHAPTER 2: A REVIEW OF THE FUNDAMENTALS OF POLYIMIDE MEMBRANES FOR NATURAL GAS SEPARATION

2.1 Introduction

Natural gas is one of the world's primary fuels that currently accounts for the largest increase in the world's primary energy consumption [1]. This is mainly due to the abundance of natural gas resources and the advancement in production technologies especially hydraulic fracturing and horizontal drilling [1,2]. Natural gas currently supplies around 22% of the energy worldwide and more specifically, according to BP 2018 statistical review of world energy, the world's natural gas consumption in 2017 was 3156.0 MTOE, where the US consumed 635.8 MTOE which means the US alone consumed 20.15% of the world's natural gas [1,2]. Natural gas is primarily used in the electric power sector where it generates around a quarter of the entier sector's electricity and that is because it has a high fuel efficiency and it is considered cleaner than coal and other petroleum products [1-3]. For instance, natural gas yields 50% less carbon dioxide per unit produced than coal, and 25% less than oil [1,3]. Moreover, it is predominantly used in the industrial sector where it is a key feedstock to many processess and that is because it is used as a raw material that makes it a major ingredient for many products [1,2]. These reasons made these two sectors account for around 74% of the total increase in the world's natural gas consumption from 2012 through 2040 [1]. The natural gas future projection consumption is expected to continue increasing as shown in Figure. 2.
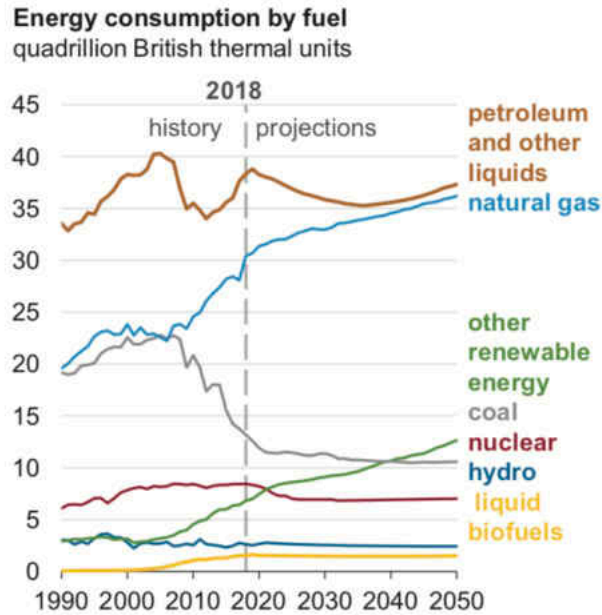
Figure 2. World energy current consumption and future projection by fuel [4].

There are a series of steps associated with the transportation of natural gas from production sites to consumers [5]. The first step is gathering the raw natural gas from the wellhead to the processing plant. The second step is the separation/purification of the natural gas where hydrocarbon gas liquids, water and nonhydrocarbon gases (impurities) are removed. The third step is transmitting the purified natural gas cross state boundaries and intrastate transmission pipelines from production and processing areas to storage and distribution centers. Finally, local distribution companies deliver natural gas to consumers through service lines.

The composition of raw natural gas varies considerably depending on the location from which it is extracted [6]. Natural gas primarily consists of methane and varying amounts of higher alkanes such as ethane, propane, butane and pentane. Moreover, it consists of impurities that include carbon dioxide, oxygen, nitrogen, hydrogen sulfide and some rare inert gases such as argon and helium. A typical gas composition is presented in Table. 1. As mentioned earlier, natural gas needs to be treated before being transported through pipelines in order to meet

certain pipeline specifications (Table. 1). These specifications are mainly concerned with impurities because separating them increase the calorific value of the fuel, prevent pipeline corrosion, enable the transportation of higher fuel volumes and create a cleaner fuel [7]. Some of the conventional processes used for natural gas separation/purification include adsorption, absorption and distillation (Figure. 3) [8]. However, separation via membranes is currently considered a potential viable alternative, especially when dealing with moderate to small gas streams [9-13].

Table 1. Typical natural gas composition and pipeline specifications.

Compound	Symbol	Percentage in Natural Gas [6]	Pipeline Specification [14]
Methane	CH_4	60-90	-
Ethane	C_2H_6	0-20	-
Propane	C_3H_8	0-20	-
Butane	C_4H_{10}	0-20	-
Carbon Dioxide	CO_2	0-8	< 2%
Oxygen	O_2	0-0.2	< 1%
Nitrogen	N_2	0-8	< 4%
Hydrogen Sulfide	H_2S	0-3	< 4 ppm =0.0004%
Rare Gases	Ar & He	0-2	< 4%
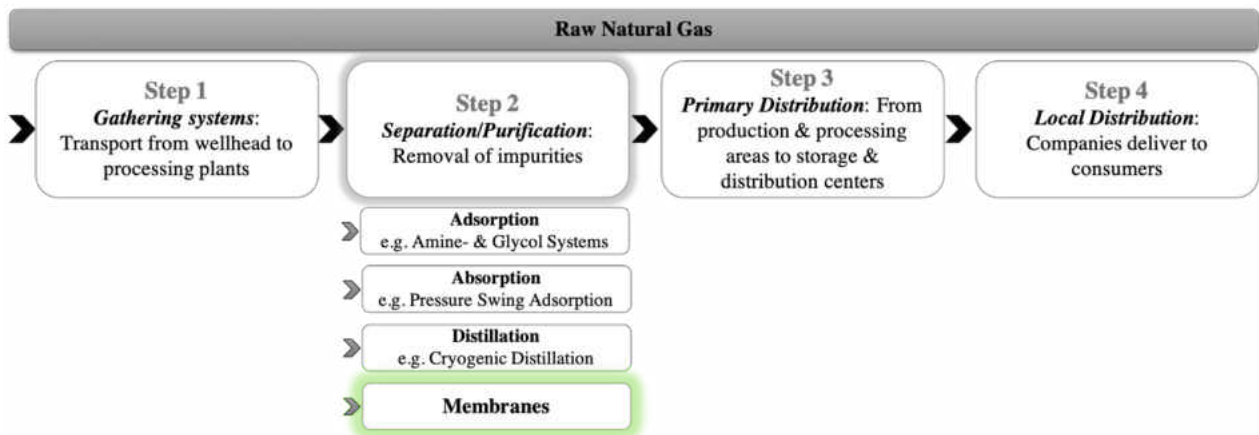
Figure 3. Summary of natural gas distribution scheme and technologies used for its separation [5,8].

Membranes have been studied intensively in the past few decades and that is mainly because they have several advantages over the conventional natural gas separation processes. Some of these advantages include: [15-17]

- Less energy intensive

- Small footprint

- Modular and easy to scale up

- Simple concept, operation and maintenance

- Does not require chemical additives

- Usually operate at under continuous steady-state conditions

- Doesnot involve phase changes (except for perevaporation)

- Potential recycling of the materials used

- Realatively inexpensive raw materials

The history of membrane technology is believed to have started as early as the 1820s and the "golden age" of membrane technology is believed to be between the 1960-1980 [15]. A detailed timeline of the development of membrane technology is presentenced in Table. 2.

The milestones in the industrial application of membrane systems specifically for gas separation started in 1980 and continued to our present day [17] . Some of these major milestones are presented in a time line between 1980 to 2010 (Figure. 4) [17].

Table 2. Timeline of the history of membrane technology.

Year	Description	Reference
1824	The osmosis phenomenon in natural membranes was discovered.	[15, 17]
1845	The anisotropy of natural membranes was researched.	[18]
1855	Fick's law of diffusion, which explains the diffusion of gases through fluid membranes, was introduced.	[19]
1861	The fundamentals of gases and vapor separation were investigated.	[19]
1865	The first synthetic membrane was made from nitrocellulosis.	[19]
1866	The solution-diffusion transport mechanism was introduced and gas separation in rubbery membranes was researched.	[18]
1867	Osmosis on synthetic membranes was researched.	[18]
1877	Osmosis on ceramic membranes was researched.	[18]
1887	The Van't Hoff equation for the osmotic pressure (π) was proposed.	[20]
1907	Ultrafiltration was introduced.	[18]
1911	The distribution law was introduced.	[18]
1926	Dialysis was researched intensively.	[18]
1931	Reverse osmosis (RO) was researched.	[18]
1934	Electrodialysis was researched.	[18]
1957	Gas separation on silicon rubber and pervaporation of azeotropic mixtures were studied.	[21]
1960	The first asymmetric integrally skinned cellulose acetate RO membranes were fabricated.	[22]
1962	Composite membranes were researched.	[21]
1963	Capillary membranes were studies.	[21]
1973	Mixed Matric Membranes (MMMs) were investigared.	[15]
1975	Pressure-driven processes were classified.	[18]
1977	Facilitated transport models were introduced.	[18]
1980	Membranes with immobilized carriers was instigated.	[18]
1989	The chain model of facilitated transport was introduced.	[21]
1990	Membrane hybrid processes and nanofiltration were introduced.	[18, 21]
2000	Carbon nanotube membranes were introduced.	[21]
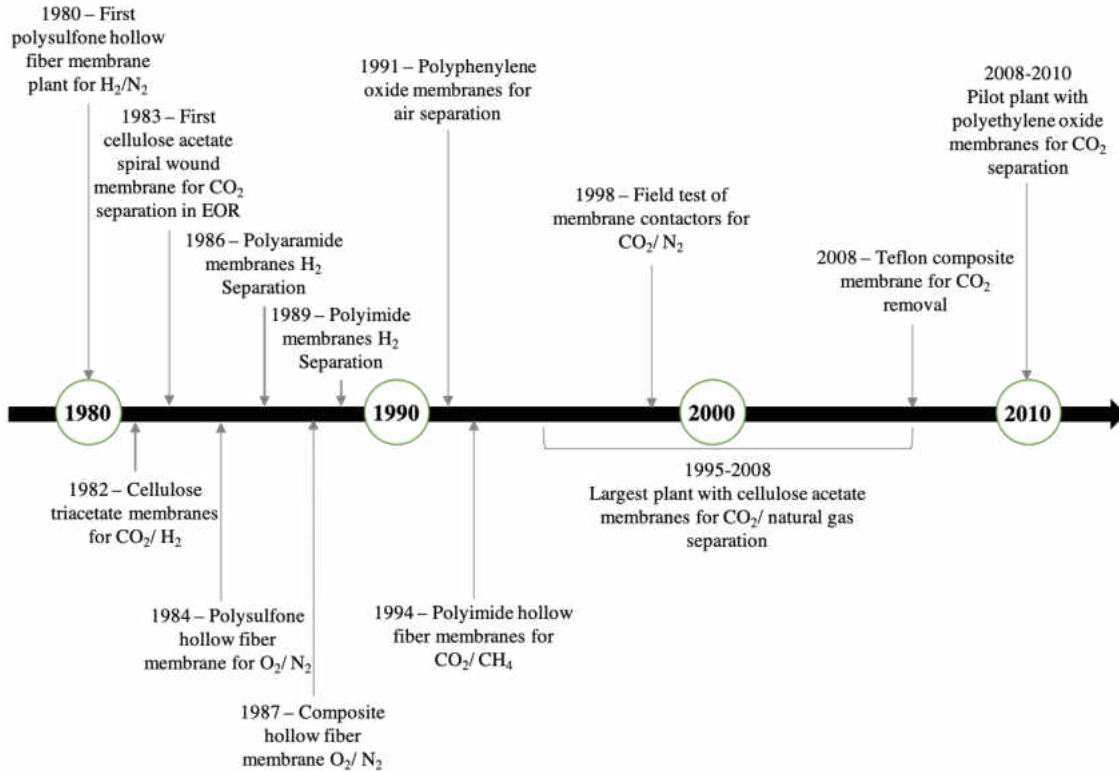
Figure 4. Timeline representing the milestones in the industrial application of membrane gas separation systems [17].

Gas separation using membranes has two major potential candidates that could be used [15]:

- *Polymeric Membranes*: The primary gas separation properties, permeability and selectivity, of polymeric membranes are governed by the nature of the material which includes the chemical structure of the precursors used. Moreover, the structural characteristics of the membrane, such as the thickness and the existence or nonexistence of pores, have a significant influence on the gas separation properties.

- *Inorganic Membranes*: The gas separation properties of inorganic membranes are primarily defined by the pore structure, pore size, pore volume, extent of tortuosity, surface roughness and the existence or nonexistence of constrictions. Furthermore, the most important properties that significantly impact the separation properties are the grade of hydrophilicity and/or hydrophobicity.

2.2 Polymeric Membranes

Polymeric membranes used for gas separation could be made of glassy or rubbery polymers. *Glassy polymers* are generally characterized by having stiff chains and relatively low fractional free volume (FFV), as indicated in Figure. 5, which causes the membranes to exhibits significantly high gas selectivity but relatively low gas permeability even at elevated pressures [15,24]. Moreover, they are usually used for applications that require polymers that are more permeable to the smaller components in a gas mixture where the FFV tend to sieve penetrant molecules mainly according to size [24]. More specifically, the selectivity of glassy membranes is based on solution-diffusion mechanism where the rate of gas transport depends on: (1) the affinity of the gas molecules to the material of the membrane together with (2) the rate of gas diffusion through the membrane matrix [15]. Thus, the gas permeation is a product of: (1) diffusivity which is linked to the FFV and the size of the penetrating gas molecules, and (2) solubility which is related to the chemical affinity between the polymer matrix and the gas molecules [15,24]. Some examples of glassy polymers include cellulose acetate (CA), polysulfone (PSF) and polyimides (PI) [15,25-27].

One the other hand, *rubbery polymers* are mainly characterized by having highly flexible chains and ultrahigh FFV (Figure. 5) which causes the membranes to demonstrate significantly high permeability and low selectivity [24]. This makes them mostly used in applications that require polymers that are more permeable to large components in the gas mixture which are weakly sieved based on size and rather on solubility [24]. In other words, the selectivity in rubbery membranes is based on the sorption phenomenon rather than gas diffusion where the chemical affinity between the gas molecules and the polymer chains is significant mainly due to the flexibility of the polymer chains especially for condensable gases

[15]. Some examples of rubbery polymers include poly(amide-6-b-ethylene oxide) (Pebax®),
polyvinylamine (PVAm) and poly(dimethyl siloxane) (PDMS) [28-30].
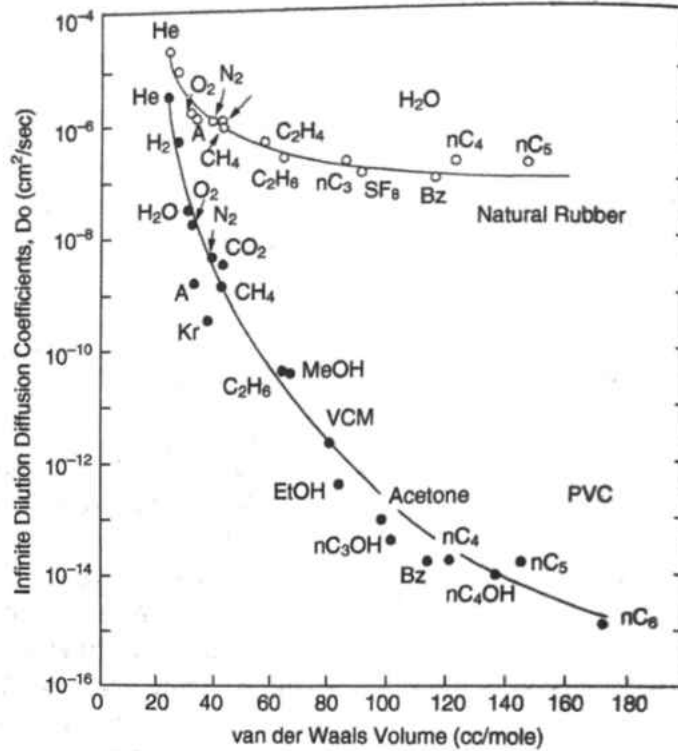
Figure 5. Permeation in glassy polymers Vs. rubbery polymers [17].

It is important to note that the transport phenomena of different gas species vary form
one polymer to another where the properties significantly depend on: (1) the free volume of
the polymer as well as (2) the segmental mobility of the polymer chains [17,31]. Additionally,
the degree of crystallinity, unsaturation and cross-linking as well as the nature of substituents
all affect the segmental mobility of the polymer chains which, consequently, affects the overall
separation properties.

There is a wide range of documented polymers that exhibit high gas separation;
however, there are only a few glassy polymers that are suitable for fabricating promising
membranes for various gas separation applications [15]. Some of the most commonly used
glassy polymeric membranes are presented in Figure. 6 [15].
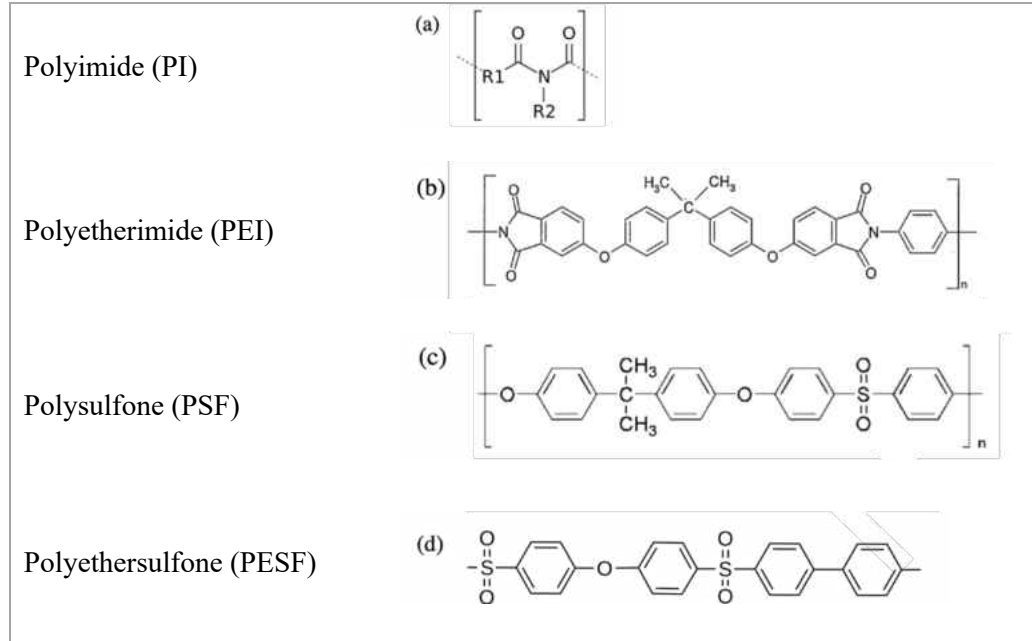
Figure 6. The chemical structures of (a) Polyimide (PI), (b) Polyetherimide (PEI), (c) Polysulfone (PSF) and (d) Polyethersulfone (PESF) [15].

2.2.1 Mass transfer principles in membranes

Gas separation via membranes is a rate-based process where the driving force is the pressure difference across the membrane. This pressure difference results in a corresponding difference in the concentration of the dissolved gas between the two sides of the membrane which causes the gas flow to diffuse through the membrane [17].

Moreover, the gas separation through a polymeric membrane is significantly affected by a number of factors that include the solubility and diffusivity of the gas species through the polymer matrix, chain packing of the polymer used and characteristics of the side/pendant groups such as their polarity, complexity, orientation and crystallinity [17,32].

2.2.1.1 Mass transfer diffusion

The term "diffusion" is defined as the process by which molecules in a media spread randomly from a region of high concentration to a region of lower concentration until a state of equilibrium is reached when the concentrations in both regions are equal [15,17]. Fick's

13

first law of diffusion (EQ.1) [33,34] describes this process by relating the diffusive flux and concentration assuming steady state.

$$J = -D \frac{\partial c}{\partial x}$$

Where J is the flux rate of the component (mol.s^{-1}), , D is the diffusion coefficient (cm^2.s^{-1}), c is the concentration of the diffused component in the membrane (mol.m^3) and x is the x-coordinate of the direction of the flow (cm). The negative sign indicates that the flow is in the opposite direction from the direction of increased concentration [15]. The diffusion coefficient (D), also called diffusivity, is dictated by the diffusion mechanism that takes place through a membrane. There are several diffusion mechanisms that could take place in membranes which are governed by the material of construction and the method of fabrications. Generally, five main mechanisms dominate the diffusion process across a membrane; namely: (a) Knudsen diffusion, (b) molecular sieving, (c) solution-diffusion, (d) surface diffusion and (e) capillary condensation [17]. These mechanisums are displayed in Figure. 7:
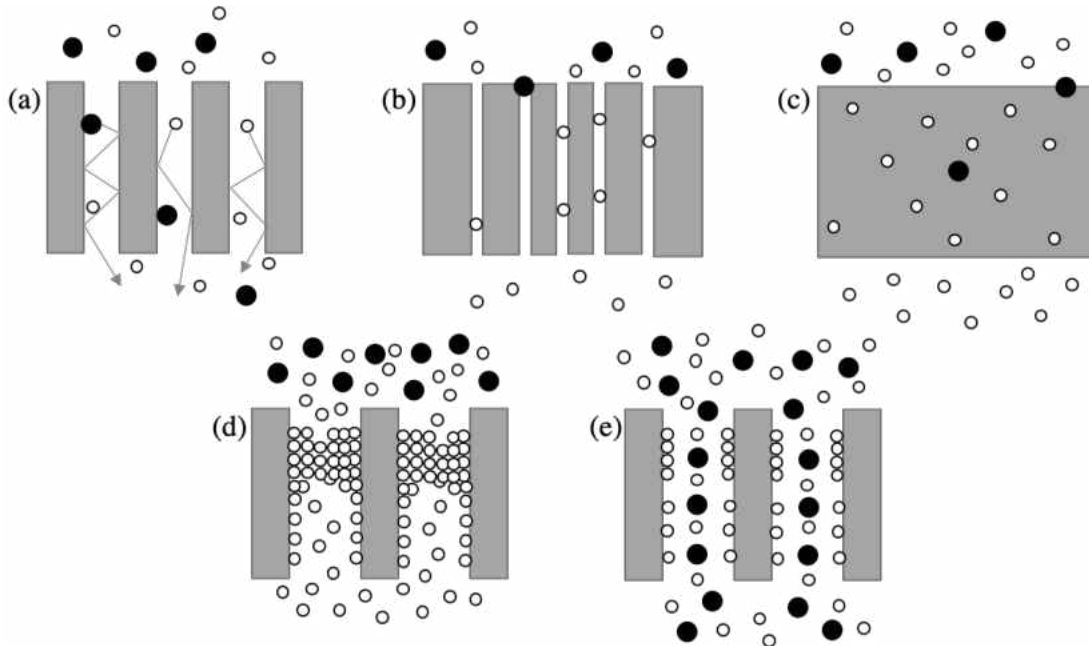
Figure 7. Main types of diffusion mechanisms: (a) Knudsen diffusion, (b) molecular sieving, (c) solution-diffusion, (d) surface diffusion and (e) capillary condensation (adapted from [17]).

14

In inorganic porous membranes, the potential diffusion mechanisms are Knudsen diffusion, molecular sieving, surface diffusion and capillary condensation [15,17]. Whereas, in polymeric membranes, the diffusion mechanisms are Knudsen diffusion and solution-diffusion [17] .

2.2.1.2 Knudsen diffusion

The Knudsen diffusion mechanism could occur in dense polymeric membranes through long pores that typically have narrow diameters of less than 50 nm [17]. More precisely, this mechanism takes place when the mean free path of the molecule is larger than the pore diameter [35]. This causes the collision of the gas molecules with the pore wall to occur more frequently than those collisions between the gas molecules themselves [35,36]. The Knudsen number (Kn) is defined as the ratio of the mean free path of the gas molecules and a representable physical length scale as shown in EQ. 2 [17].

$$K_n = \frac{\lambda}{r} \qquad\qquad EQ.\ 2$$

Where λ is the mean free path which is described as the average distance between collisions (EQ. 3) and r is the radius [17,36].

$$\lambda = \left(\frac{\eta}{P}\right)\left[\left(\frac{\pi\,K_B\,T}{2\,M}\right)^{1/2}\right] \qquad\qquad EQ.\ 3$$

Where η is the viscosity of the gas, P is the pressure, K_B is the Boltzmann constant, T is the temperature and M is the molecular weight.

The Knudsen permeance is calculated using EQ. 4 where the gas transport occurs in the gaseous state without the contribution of adsorption since the interaction between the diffusing molecules and the pore wall is considered negligible: [35]

$$\overline{P_K} = \frac{\varepsilon \, d_p}{\tau \, L} \left(\frac{8}{9 \, \pi \, M \, R \, T} \right)^{1/2} \qquad \qquad EQ. \ 4$$

Where ε is porosity, d_p pore diameter, τ is tortuosity, L is the thickness of the membrane and R is the gas constant. Moreover, the Knudsen selectivity is proportional to the ratio of the inverse square root of the molecular weight of the gas species (A and B) being separated (EQ. 5) [17,36].

$$\propto_K = \left(\frac{M_A}{M_B} \right)^{-1/2} \qquad \qquad EQ. \ 5$$

Some of the ideal separation factors of relevant gas pairs associated with natural gas based on a Knudsen flow were calculated using EQ. 5 and are presented in Table. 3. Nonetheless, the actual separation factors tend to be smaller and that is due to a number of reasons including: [17,36]

- Back diffusion

- Non-separation diffusion

- Concentration polarization on the feed or the permeant side

- Occurrence of viscous flow which mainly takes place in large pores

Table 3. Calculated separation factors based on Knudsen flow of selected binary gas mixtures associated with natural gas.

Gas Pair	Ideal Separation Factor
CO_2/CH_4	0.60
N_2/CH_4	1.07
CO_2/N_2	0.56
N_2/O_2	1.07

2.2.1.3 Solution-diffusion mechanism

The solution-diffusion mechanism (Figure. 7c) is mainly used to describe the gas transport through dense polymeric membranes, and it mainly takes place due to the

thermodynamic differences between the two sides of the membrane [37]. In other words, this mechanism relates the rate of gas transport to both the affinity of the gas molecules to the material of the membrane and the rate of gas diffusion through the matrix of the membrane [15]. This means that gas permeability through polymeric membranes is considered a product of both diffusivity, which is related to the fraction free volume (FFV) of the polymer and the size of the penetrating gas molecules, and solubility, that correlates to the chemical affinity between the polymer matric and the gas molecules [15,38,39]. Generally, gas permeation mechanism through dense polymeric membranes takes place through the following steps: [17,37]

- Step (1): Absorption of the permeating species into the membrane.

- Step (2): Diffusion of the gas species through the membrane.

- Step (3): Desorption of the permeating species from the surface of the membranes.

As mentioned earlier, Fick's first laws of diffusion (EQ. 1) describes diffusion in steady state. On the other hand, Fick's second law (EQ. 6) described the transport process in non-steady state which is ideal when dealing with isotropic membranes, and when the diffusion coefficient is dependent of the concentration, time and distance [17]. Fick's second law considers the rate of change of the penetrant concentration at a plane within a membrane [17,34].

$$\frac{\partial c}{\partial t} = D \left(\frac{\partial c^2}{\partial x^2} \right) \qquad \textit{EQ. 6}$$

The diffusion coefficient D is dependent on the concentration which means that the polymer-penetrant interaction occurs strongly with many organic penetrant molecules [17,34]. Hence, EQ. 6 becomes EQ. 7 after being modified:

$$\frac{\partial c}{\partial t} = D(c)\frac{\partial c^2}{\partial x^2} + \frac{\partial D(c)}{\partial c}\left(\frac{\partial c}{\partial x}\right)^2 \qquad\qquad EQ.\ 7$$

Generally, the term $\partial D(c)/\partial c$ is considered negligible compared to $D(c)$ and that is mainly because relatively small intervals of c are used while conducting experiments [17]. Therefore, the diffusion coefficient integral can be expressed as (EQ. 8):

$$\bar{D} = \int_{c_1}^{c_2} D(c)dc\ /\ c_1 - c_2 \qquad\qquad EQ.\ 8$$

Where c_1 and c_2 are the penetrant concentrations at the low and high concentration faces of the membrane, respectively.

At steady-state, the diffusion coefficient becomes independent of concentration and the diffusion flow is constant. This means that integrating Fick's first law (EQ. 1) yields in EQ. 9. [34]

$$J = \frac{D(c_1 - c_2)}{l} \qquad\qquad EQ.\ 9$$

Where l is the thickness of the membrane. Moreover, Henry's law (EQ. 10) is used to describe the penetrant distribution in case of gases and vapor transport [17,37].

$$c = S.p \qquad\qquad EQ.\ 10$$

Where c is the sorbed concentration, S is the solubility coefficient and p is the ambient pressure. Thus, one of the most commonly known and used permeation equations can be obtained by combining EQ. 9 with EQ. 10:

$$J = \frac{DS(p_1 - p_2)}{l} \qquad\qquad EQ.\ 11$$

Where p_1 and p_2 represent the pressures on the two sides of the membrane of thickness l. Furthermore, the term DS is the permeation coefficient (EQ. 12) which means that permeation equation could be written in terms of the permeability coefficient as shown in EQ. 13 [17,37].

$$P = D.S \qquad\qquad\qquad EQ.\ 12$$

$$J = \frac{P\ (p_1 - p_2)}{l} \qquad\qquad\qquad EQ.\ 13$$

Furthermore, the ideal selectivity, also known as permselectivity, is simply the ratio of the permeabilities of the tested gas pairs, as shown in EQ. 14, where the overall gas selectivity of polymeric membranes is governed by diffusivity and solubility [39].

$$\alpha_{A/B} = \frac{P_A}{P_B} = \frac{D_A S_A}{D_B S_B} \qquad\qquad\qquad EQ.\ 14$$

2.3 Polyimide Membranes

2.3.1 Properties of polyimides membranes

Polyimides are glassy high-temperature polymers made of imide monomers. They are well known for their outstanding thermal stability, chemical resistance, mechanical toughness and electric properties [40]. Polyimides are mainly formed from diamines and dianhydrides which are chosen to tailor the final properties of the polymer. More specifically, they consist of aromatic rings and/or aliphatic compounds together with imide linkages which contain two carbonyl groups attached to one nitrogen atom. There are various monomers that could be used to form polyimides, some of which are presented in Table. 4.

Depending on the nature of the monomers used to derive polyimides, they could be generally classified into three classes: fully aromatic, semi-aromatic and fully aliphatic polyimides as shown in Figure. 8 [41]. Fully aromatic polyimides are derived from aromatic diamines and dianhydrides, semi-aromatic polyimides are derived from a combination of aromatic and aliphatic monomers (either the diamines or the dianhydrides could be aromatic while the other is aliphatic) and fully aliphatic polyimides are those derives from aliphatic

diamines and dianhydrides. Among the three classes, fully aromatic polyimides are the most

commercially used and for this reason, they will be discussed primarily in the rest of the paper.
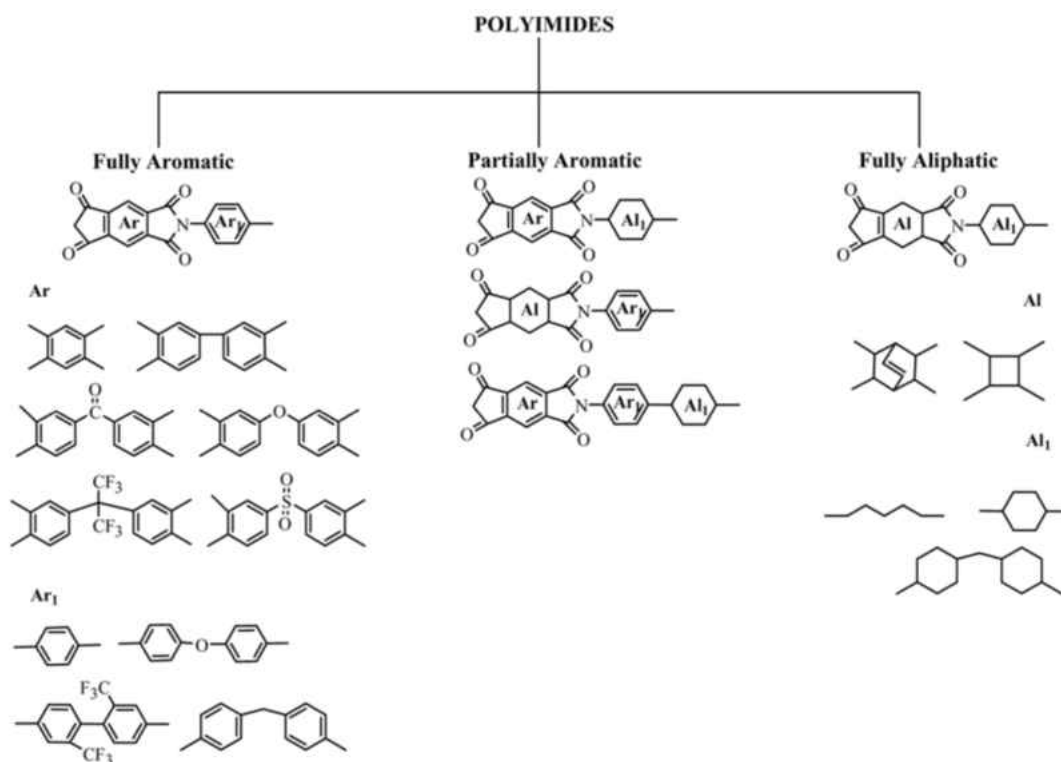
Figure 8. Polyimides can be generally classified into three classes: fully aromatic, semi aromatic and fully aliphatic [41].

Table 4. Some of the most common monomers used to make polyimides.

Abbreviation	Monomer	References
6FDA	4,4'-(Hexafluoroisopropylidene) diphthalic anhydride	[42-46]
BisAPAF	2,2-Bis(3-amino-4-hydroxyphenyl)hexafluoropropane	[47-51]
NDA	1,4,5,8-Naphthalenetetracarboxylic dianhydride	[52-54]
TABOB	1,3,5-Tris(4-aminophenoxy) benzene	[55]
DATPA	4,4′-Diaminotriphenylamine	[56][4-7]
ODPA	4,4'-Oxydiphthalic anhydride	[48, 57-59]
BTDA	3,3',4,4'- Benzophenone tetracarboxylic dianhydride	[48, 57, 60-61]
PMDA	Benzene-1,2,4,5-tetracarboxylic dianhydride	[48, 57, 62, 63]
BPDA	3,3',4,4'-biphenyl tetracarboxylic dianhydride	[48, 57, 61,63,78]
DAD	2,3,5,6-Tetramethyl-1,3-phenylenediamine	[65,66]
6FpA	4,4′-(9-Fluorenylidene) bis (2-methyl-6-isopropylaniline)	[67,68]
6FmA	4,4′-(9-Fluoroenylidene)bis(2-isopropylaniline)	[69]

DAM	2,4,6-Trimethyl-1,3-phenylenediamine	[70,71]
DDBT	Dimethyl-3,7-diaminodibenzothiophene-5,5′-dioxide	[72-74]
MDA	Methylenedianiline	[75,76]
MPD	4,4′-Phenylenediamine	[77,78]
ODA	4,4′-Oxydianiline	[5,6,62,64]
HAB	3,3′-Dihydroxy-4,4′-diamino-biphenyl	[79,80]
DAB	3,3′-Diaminobenzidine	[81,82]
BPADA	Bisphenol A diphthalic anhydride	[83-85]
DABP	Diaminobenzophenone	[86,87]
PPD	p-Phenylene diamine	[88,89]
DAP	2,4-Diaminophenol dianhydrochloride	[90-92]
PDA	p-Phenylenediamine	[93,94]
TMPDA	2,3,5,6-Tetramethyl-1,4-phenylenediamine	[95,96]
BDAF	2,2-bis-(Aminophenoxyphenyl)hexafluoropropane	[97,98]
Durene	2,3,5,6-Teramethyl-1,4-phenylene diamine	[99-101]
DAPI	Diaminophenylindane	[102,103]
TAPA	Tris(4-aminophenyl)amine	[6]
DSDA	3,3′,4,4′-Diphenylsulfonetetracarboxylic dianhydride	[104,105]

Aromatic polyimides are known for their exceptional thermal stability (> 500 ºC) which is mainly attributed to its heterocyclic imide rings on the backbone [41,106]. Furthermore, the existence of rigid imides and aromatic rings in polyimides provide excellent mechanical resistance [41,106,107]. A polymer that consists of two monomers usually contains a charge transfer complex: a donor and an acceptor as shown in Figure. 9 [41]. The donor tends to have plenty of electrons to move around and that is due to the existence of the nitrogen groups. Whereas, the acceptor tends to draw away it's electrons density due to their carbonyl groups. This donor and acceptor dynamic allow the acceptors to draw the electrons form the donors and hold them tightly together causing the polymer chains to stack together like strips of paper. The formation of charge transfer complex between the adjacent units in the polymer chains

causes the donors and acceptors to pair up, as presented in Figure. 9b, which holds the chains very tightly together and restricts their movement. This corresponds to exceptional thermal, mechanical and chemical properties. However, the same reasons that give aromatic polyimides their exceptional thermal, mechanical and chemical properties causes them to be insoluble in their fully imidized form which results in low processability [41,108].
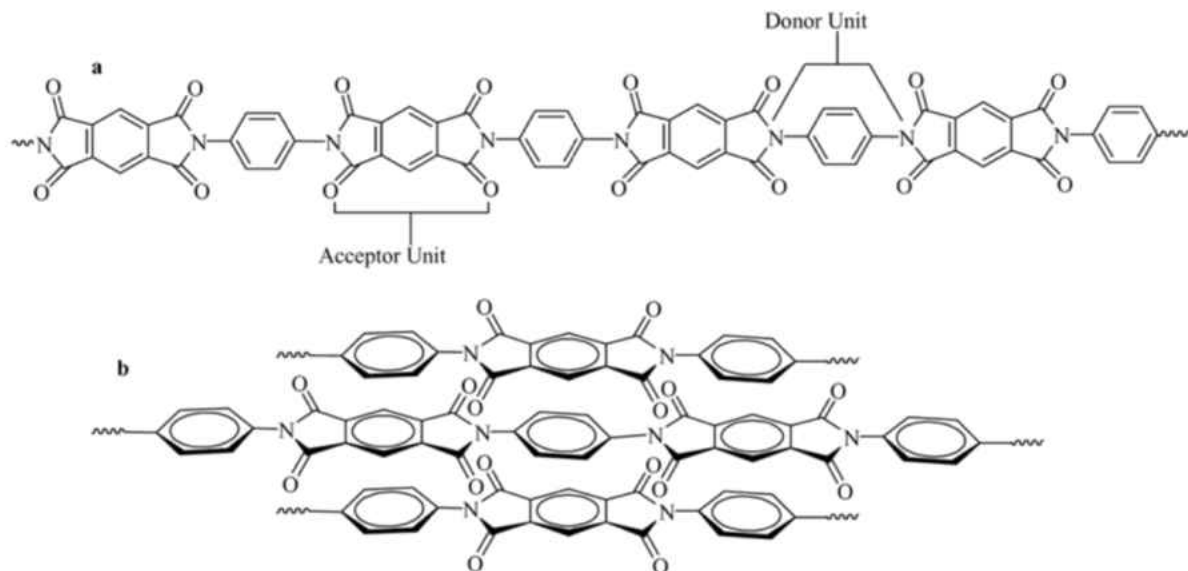
Figure 9. The underlying donor/acceptor system in polyimides and the resulting interchain locking. (a) The nitrogen molecules have high electron density than the carbonyl groups which lends it to the acceptor while the carbonyl groups draw the electron density away from the acceptor unit. (b) Interchain interlocking of the polyimide backbone causing the chains to stack as shown allowing the carbonyl of the acceptor on one chain to interact with the nitrogen of the donor on the adjacent chains [41].

In addition, the inter and intra molecular charge transfer (CT) interaction that takes place between the aromatic ring and the five membered ring of the imide group (Figure. 10) are responsible for the coloration of the aromatic polyimides [41,107]. Moreover, aromatic polyimides cannot be used in areas where colorlessness is a key requirement mainly because they absorb visible light intensely [41]. Also, the CT interactions are also the main reasons behind the good dielectric constants of aromatic polyimides [41,106].

Aromatic polyimides are typical of most commercial polyimides where one of the most known trademarked name is Kapton®, 4,4'-poly-oxydiphenylene-pyromellitimide, which was

originally developed by DuPont^{TM} Company in the late 1960s, and its chemical structure is presented in Figure. 10 [40]. Kapton® is characterized by having high molecular weight, light weight and exceptional thermal stability in a wide range of temperatures (-269 to +400 ºC) [41]. Some other properties of Kapton® are presented in Table. 5.
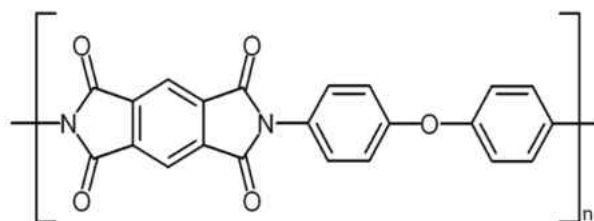
Figure 10. Chemical structure of Kapton® [40].

Table 5. The effect of gamma radiation on Kapton polyimide films [109,110].

Property	Radiation Exposure				
	Control, 1 mm Film	10^4 Gy, 1h	10^5 Gy, 10h	10^6 Gy, 4 Days	10^7 Gy, 42 Days
Tensile Strength (MPa)	207	207	214	214	152
Elongation (%)	80	78	78	79	42
Tensile Modulus (MPa)	3172	3275	3378	3275	2903
Volume Resistivity Ω-cm × 10^{13} at 200 °C	4.8	6.6	5.2	1.7	1.6
Dielectric Constant 1 kHz at 23 °C	3.46	3.54	3.63	3.71	3.50
Dielectric Factor 1 kHz at 23 °C	0.0020	0.0023	0/0024	0.0037	0.0029
Dielectric Strength V/µm (kV/mm)	256	223	218	221	254

2.3.2 Chemistry & synthesis of polyimides membranes

Aromatic polyimides could be one of two types: condensation or addition, depending on the type of reaction used to synthesize them. Condensation polyimides are synthesized via step-growth polymerization and are characterized by having a linear-like structure [111]. At first, the reaction forms a polyamic acid which is then converted into polyimide when heated to a temperature above 150 °C [111]. On the other hand, addition polyimides are produced by

heat activated addition polymerization of diimides and are known for having a network-like structure [106,111]. They are synthesized from bismaleimide (BMI) and nadimide precursors where a free-radical addition polymerization takes place at around 200 °C causing the double bonds to form a thermosetting network polymer [107,111]. The BMI reacts differently at high temperatures whereas the nadimide group tends to decompose first to form cyclopentadiene and maleimide, which then copolymerize to form the network polyimide structure. Among the two types, condensation polyimides are the most commonly used because it is well established. For instance, Kapton® is considered a condensation polyimide since it is made via the condensation reaction of a diamine with a dianhydride as shown in Figure. 11.
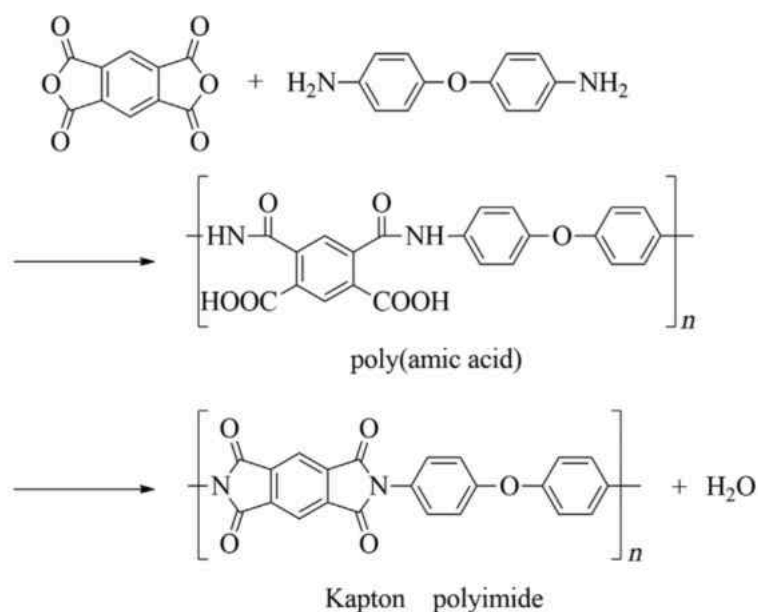
Figure 11. The condensation reaction of Kapton® and the chemistry of the polyamic acid and polyimide [112].

The method used to prepare aromatic polyimides consists of two main steps: (1) synthesis of poly(amic acids) and (2) conversion of the poly(amic acids) to polyimides [108,112,113] .

2.3.2.1 Synthesis of hydroxyl poly(amic acids)

Hydroxyl poly(amic acids) (HPAA) are generally prepared via the condensation reaction of diamines and dianhydrides in an appropriate dipolar aprotic solvent at ambient to low temperatures because the reaction is exothermic [112-118]. Some of the most commonly used solvents in the synthesis of HPAA are listed in Table. 6 [112,113]. It is worth mentioning that it is critical to dissolve the diamine first followed by the dianhydride due to the moisture sensitivity of the dianhydride [118]. The process of synthesizing HPAA overcome one of the major issues associated with aromatic polyimides and that is their poor solubility which is mainly due to the extended rigid planar aromatic and heteroaromatic structures, as mentioned previously [112]. Overcoming this issue enabled the birth of the first significant commercial polyimide film product (Kapton®) to the market and ever since it is considered the method of choice in most of the polyimide film production [112].

Table 6. Potential solvents used for poly (amic acid) synthesis [112,113].

Solvents

N-methyl-2-pyrrolidone (NMP)	Pyridine
N, N-dimethylforamide (DMF)	Dimethyl sulfone
N, N-diethylformamide	Hexamethylphosphoramide
N, N-dimethylacetamide (DMA)	Tetramethylene sulfone
N, N-dimethylmethoxyacetamide	*N*-acetyl-2-pyrrolidone
N-methylcaprolactam	Dimethyl sulfoxide

The HPAA reaction mechanism consists of two mains steps; first, the nucleophilic attack of the amino group present on the carbonyl of the anhydride group and, second, the opening of the anhydride ring from the amic acid group as presented in Figure. 12. This reaction is considered an irreversible equilibrium reaction mainly because a high-molecular weight HPAA resin is produced readily and rapidly at ambient temperatures [112]. Moreover, the irreversible reaction is several orders of magnitudes faster than the reversible reaction

(Figure. 12) and that is essential because having a large difference in the reaction rates enables the production of the high-molecular weight HPAA which otherwise would not [112]. This is the reason it is necessary to understand and examine the driving forces that favors the forward reaction over the reverse reaction. Furthermore, the acylation reaction of amines is an exothermic reaction which means that its equilibrium is favored at low temperatures [112]. Additionally, the equilibrium is favored at high monomer concentrations, usually 1:1, in order to obtain high-molecular weight HPAA and that is because the reverse reaction is a first-order reaction whereas the forward reaction in dipolar solvents is a second-order [59,108,112,113]. Some main factors that influence the molecular weight of the HPAA include the purity of the monomers used, the thorough exclusion of moisture, the solvent choice and maintain low to moderate temperatures [113].
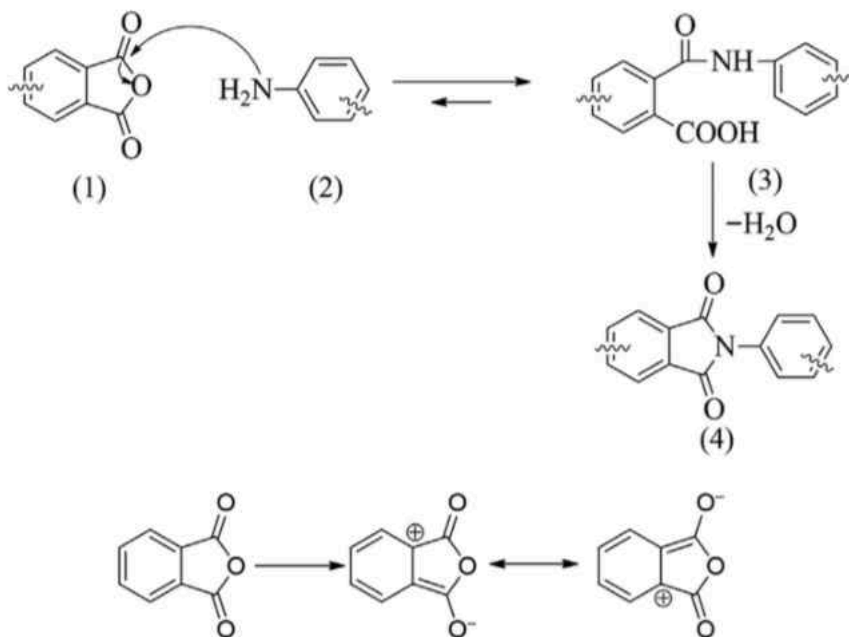
Figure 12. The reaction mechanism of the formation of polyimides [112].

2.3.2.2 Conversion of the polyamic acids to polyimides

The conversion of the HPAA to polyimide could be achieved by one of three main routes: thermal, azeotropic or chemical imidization [112-118]. However, a fourth route (ester-acid imidization) is currently considered a potential route too [118]. All the four potential imidization routes are discussed below.

i.   *Thermal imidization*

The thermal imidization route is considered the most commonly used pathway for converting HPAA solutions into free-standing polyimide films [112]. Thermal imidization takes place in three main stages: (1) solvent evaporation, (2) imidization and (3) annealing [112,113,118]. Stage (1) starts by casting the HPAA solution on a support, usually a glass plate, and allowing it to dry and gradually heat at low temperatures in order to evaporate the solvent where the more solvent is removed, the higher the mechanical properties and glass transition temperatures (Tg) of the films are [112,116]. Then, stage (2) starts as the HPAA solution continues to be heated to around 180 °C where the imidization reaction takes place during which the evaporation of the hydrogen-bonded solvents on HPAA as well as the dehydration of the produced water takes place [112,113,118]. A key factor that determines the enhancement of the mechanical properties and Tg is the interplay between the solvent evaporation and the imidization reaction. In other words, stage (2) converts the HPAA into polyimide. The temperature continues to increase to around 350-400 °C where stage (3) takes place as the complete imidization is achieved by annealing to those temperatures [112,113,118]. During the third stage, the polyimide is technically converted into thermally rearranged (TR) polyimide known as polybenzoxazole (PBO) [118]. It is important to note that heating the HPAA results in shifting the equilibrium towards the left (Figure. 13) since the

polycondensation reaction of the diamine with the dianhydride is exothermic. This reversion is usually responsible for obtaining low molecular weights and high levels of anhydride and amino groups [112].
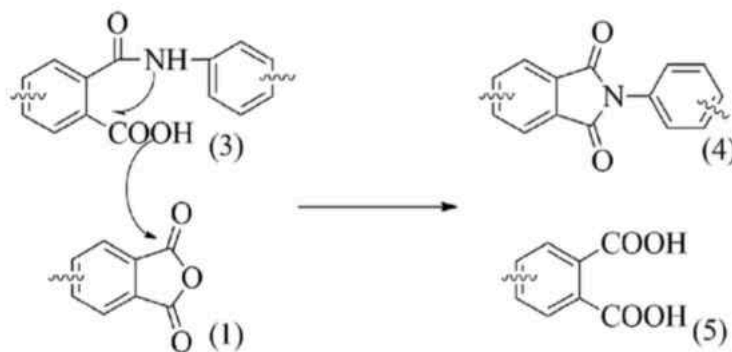
Figure 13. The mechanism of the thermal ring-closure of amic acid to imide [112].

ii.   *Azeotropic imidization*

Similar to the thermal imidization route, the azeotropic imidization starts by preparing the HPAA but instead of casting it, it is converted directly into polyimide in the liquid state by using o-xylene [118]. The o-xylene forms an azeotropic mixture with the water released by the ring-closure reaction (Figure. 14), silanol and siloxane byproducts in order to distill it easily from the HPAA solution usually using a dean-stark extractor [48,59,108,118]. This occurs at temperature of around 180 °C for around 6 hours where dehydration and imidization takes place [48,59,108,118]. After that, the polyimide solution is cooled to room temperature and precipitated in water: methanol solution and then in water for several hours resulting in a powder polyimide [59,108]. The powder is then dried for 24 hours at 120 °C and finally re-dissolved in a solvent, cast on a plate and thermally treated at temperature between 60 °C and 250 °C where the imidization reaction takes place. Finally, the films are converted into TR polyimides (PBO) of temperatures of up to 450 °C [118].

The thermal and azeotropic imidization methods are summarized in Figure. 14 and it is important to note the final mechanical and gas separation properties of polyimides synthesized via azeotropic imidization are more enhanced than those made via thermal imidization. This is mainly because the azeotropic imidization route effectively removes more water than the thermal imidization route.
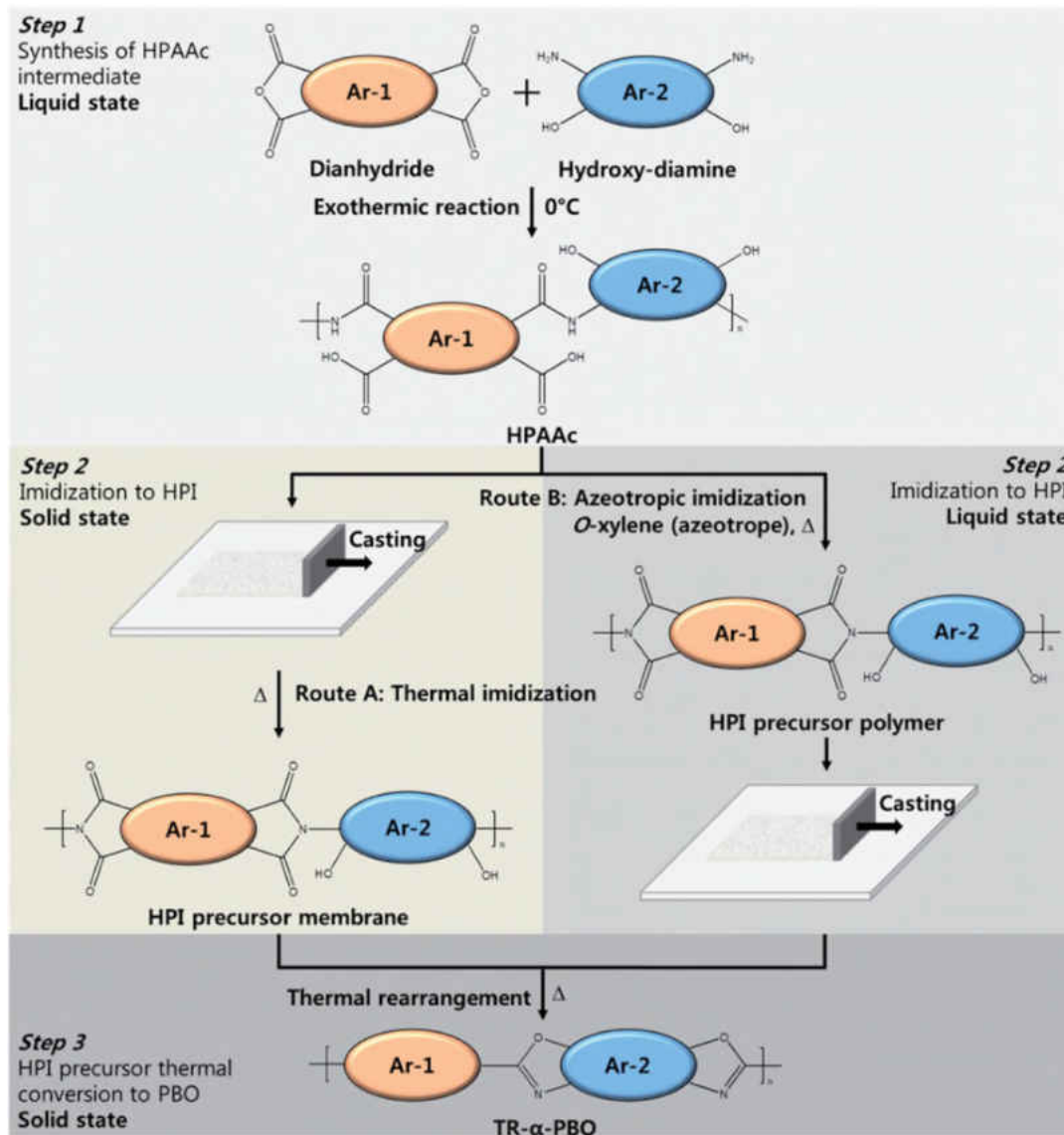
Figure 14. The synthesis of polybenzoxazole (PBO*) via thermal imidization (Route A) (tPBO) and azeotropic imidization (Route B) (aPBO). Ar-1 and AR-2 are the aromatic moiety of the dianhydride and the diamine, respectively [118].

iii.   *Chemical imidization*

The main concept behind the chemical imidization process is that the cyclodehydration of the HPAA is achieved via chemical dehydration at ambient temperature [112]. This is commonly done using a mixture of reagents of acid anhydrides and tertiary amines in an aprotic dipolar solvent (Table. 7) [112,119-123]. Some of the most commonly used dehydration agents are presented in Table. 7 [112,113].

Table 7. Some dehydration agents used during the chemical imidization route [112,113].

Acid Anhydrides	Amine Catalysts
Acetic anhydride	Pyridine
Propionic anhydride	Methylpyridines
n-butyric anhydride	Lutidine
Benzoic anhydride	Trialkylamines
Acetic benzoic anhydride	*N*-methyl moroholine

Similar to the previous imidization routes, chemical imidization starts by the synthesis of the HPAA solution. After which, the acid anhydride is introduced to the solution to react with the amic acid moiety of HPAA. Then, the carboxylic acid is eliminated under basic conditions from the amine catalyst at room temperature which takes place via a ring-closing cyclodehydration reaction resulting in granular or fibrous ester-functionalized polyimides [118] . Moreover, the acylation of the carboxylic group of the amic acid forms the imides as shown in Figure. 15 [112]. All this results in the addition of a pair of bulky side groups at the otho-position which will eventually be eliminated during the final stage when TR takes place [118]. Depending on the type of acid anhydride used during the reaction, the bulky side groups by-products will vary. As these side groups are eliminated during TR, they leave behind large cavities in the polymer matrix which enhances the gas transport properties [118]. Some previous studies [118-123] proved that there is a very strong correlation between the FFV of

the thermally rearranged polyimides (PBO) and the size of the ortho-position ester group. This means that the largest side group by-product results in the largest FFV and vice versa.
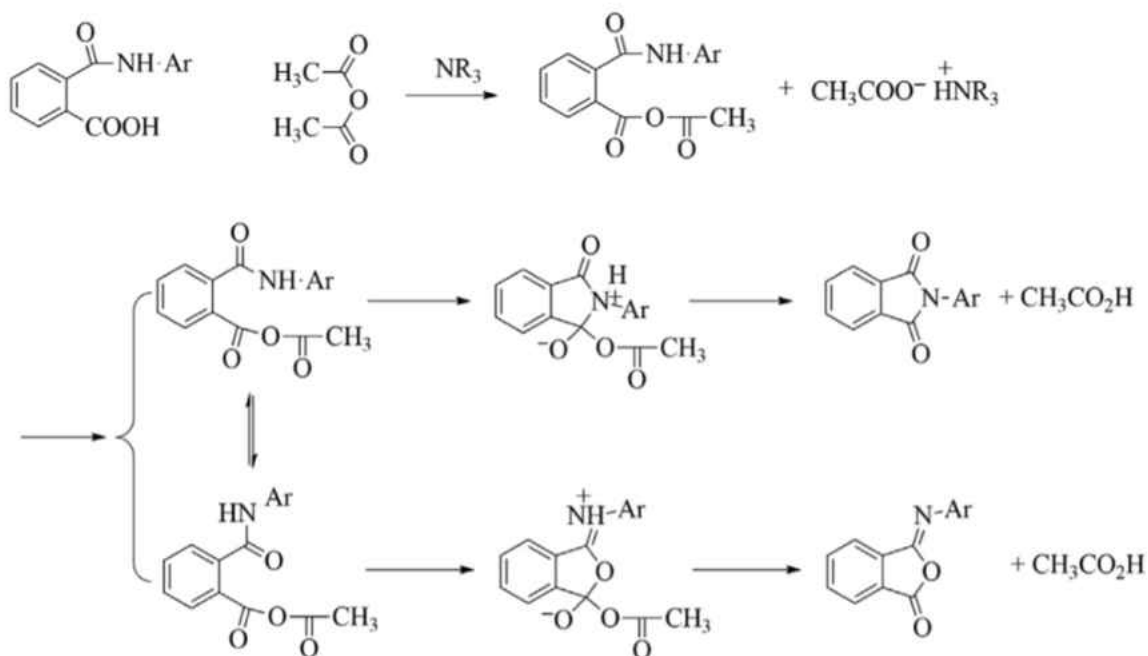
Figure 15. The mechanism of the chemical imidization of amic acid to imide (R: ethyl; Ar: phenyl) [112].

iv.   *Ester-acid imidization*

The poor stability of the anhydride precursors is one of the major issues associated with polyimide synthesis. Generally, this issue could be minimized by strictly following the sequence of adding the diamine first followed by the dianhydride when preparing the HPAA [118]. Another potential solution is the thermal treatment of the dianhydrides which results in the cyclization of potential o-diacid impurities that usually emerges the hydrolysis of the dianhydrides [118,124]. Moreover, the ester-acid imidization route presents another potential solution where it could be used to avoid the hydrolysis of dianhydrides under hydrated conditions [118,124].

Unlike any of the previously discussed imidization routs, the ester-acid imidization route starts by mixing the dianhydride in an absolute acid in the presence of triethylamine

(TEA) under reflux at high temperatures in order to produce an ester-acid intermediate as shown in Figure. 16 [118]. After that, the ester-acid intermediate is reacted with the diamine and is allowed to imidize at elevated temperatures while using o-dichlorobenzene (o-DCB) as the azeotrope. This finally results in the formation of a polyimide which is then thermally rearranged into a PBO.
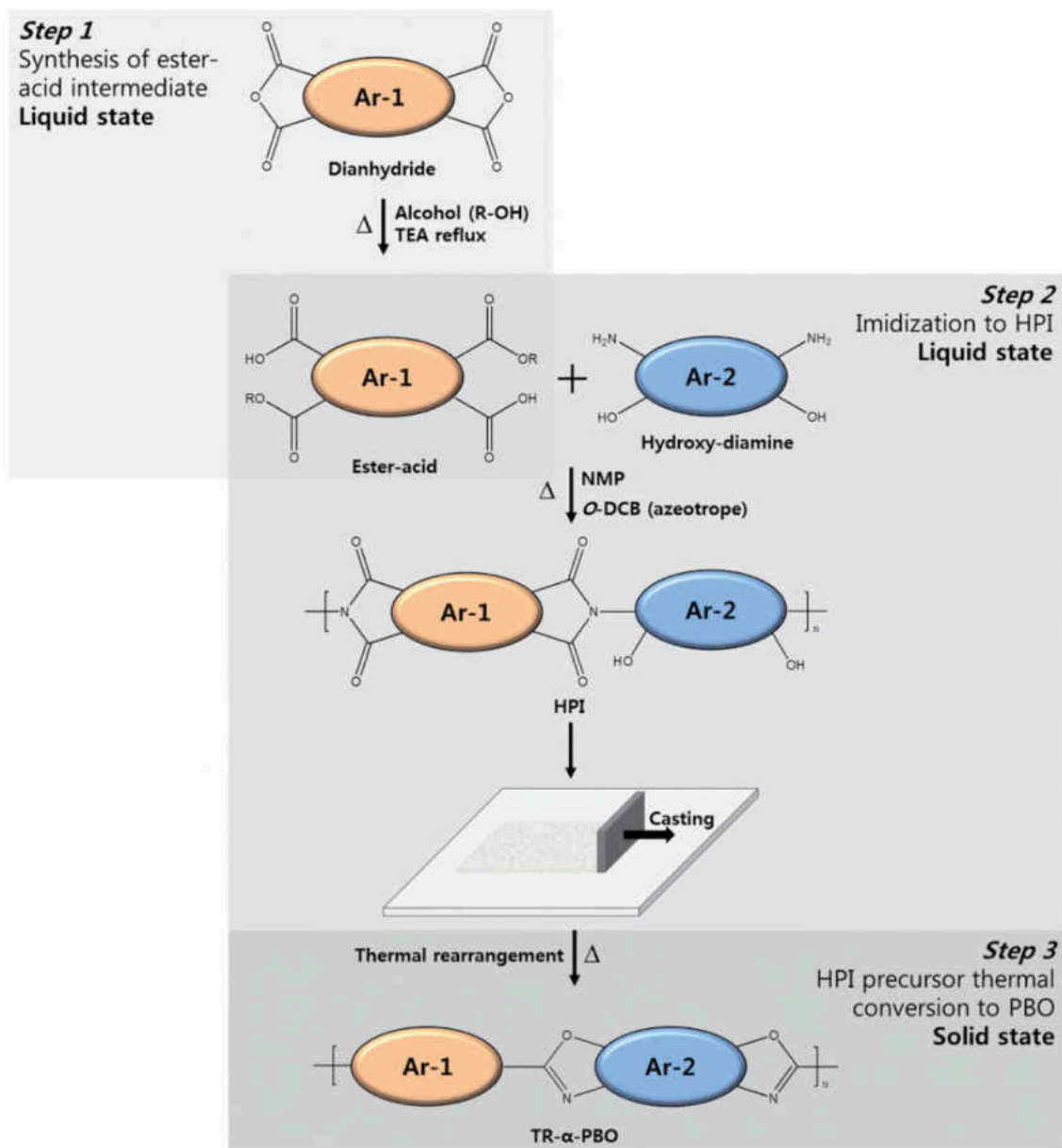
Figure 16. The synthesis of polyimide and polybenzoxazole (PBO) using the ester-acid method where Ar-1 is the aromatic moiety of the anhydride, and Ar-2 is the aromatic moiety of the diamine [118].

2.3.3 *Thermal rearrangement of polyimides membranes*

Aromatic polyimides containing ortho-positioned functional groups can undergo a thermal conversion reaction known as thermal rearrangement (TR) to form polybenzoxazole (PBO) as shown in Figure. 17. This new class of polymers was discovered by Lee and his team [38,47,48,59,61,89,91,94,125-127] by accident in 2007.
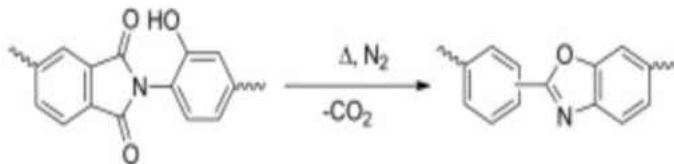
Figure 17. General mechanism of the TR of poly(hydroxyimides) [128].

During the thermal conversion reaction, the precursor polymer is converted into a rigid unique microporous structure that is characterized by having high FFV distribution and large cavities that are separated by narrow necks resulting in higher permeabilities [128]. More specifically, the formed structure is known to be rod-like with high-torsional energy barriers to rotational energy between two individual phenylene-heterocyclic rings [48,129]. Such a feature is crucial when considering gas separation applications because it could lead to large differences in the mobility of the pendant groups depending on their size and, hence, result in relatively higher selectivities [48,129]. This increase in both permeabilities and selectivities enables TR aromatic polyimides to lower the permeability/selectivity tradeoff [130,131]. However, there is a misconception that the increase in the permeabilities and selectivities is with same magnitude. The fact is that TR tends to increase the permeabilities significantly, as mentioned earlier; nevertheless, TR tends to increase the rigidity of the polymer chains where the rigid-rod benzoxazole structure is responsible for slightly increasing and mostly maintaining a relatively unchanged selectivity [80] . Hence, polyimide membranes which

undergo TR witness a significant increase in permeability of gases while mainly maintaining their selectivities.

PBOs are classified as sglassy aromatic polymers that consist of heterocyclic rings prepared by an in situ thermal treatment of polyimides at elevated temperatures [118]. According to Park et al. [48], in order for a polyimide to thermally rearrange it should contain a hydroxyl group where the hydroxyl-imide ring rearrange to a carboxyl-benzoxazole intermediate followed by decarboxylation. At temperatures between 350 and 450 °C, the fully aromatic PBO is obtained.

The exact mechanism of TR is still being investigated; however, a potential mechanism is presented in Figure. 18 [48]. It is important to note that how exactly does the polymer structure change with TR and what exactly is affected by it at the atomistic and molecular level is still challenging. Specially in terms of the FFV, Tg, configuration and conformation. Understanding the relationship between structure and properties of the starting and final structures becomes even more complex if a chemical reaction occurs during TR [118]. This is mainly due to the fact that the physical properties of TR polymeric membranes are significantly dictated by the backbone structure of the polymer and the imidization route [118]. For instance, polyimide films synthesized from the same starting diamine and dianhydride have different morphologies when derived using the thermal and the chemical imidization routes. The films obtained via thermal imidization showed microdomains of an almost spherical shape, while those obtained by chemical imidization exhibited a net-like structure which are governed by the extent of TR [112].
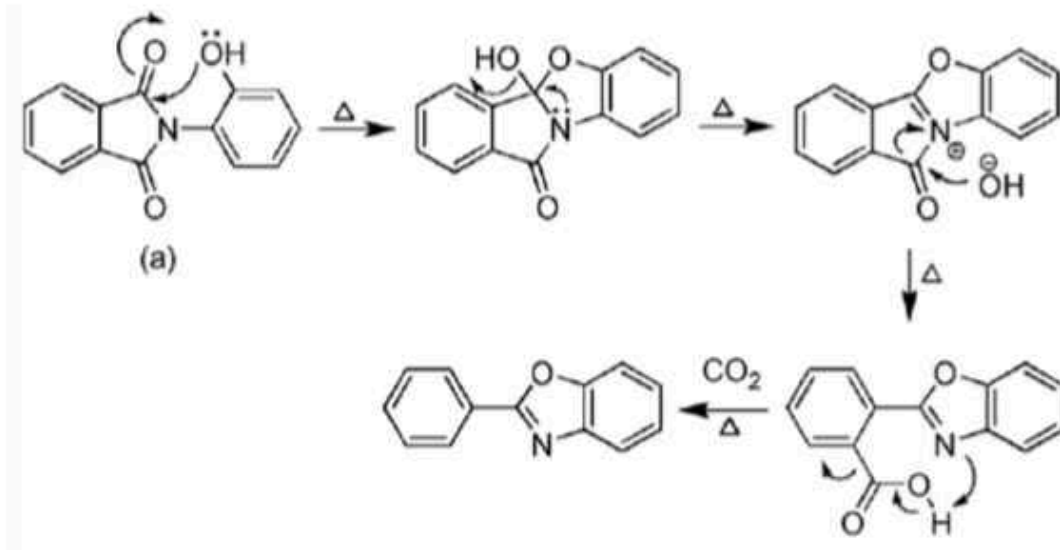
Figure 18. The potential general mechanism of the TR of hydroxyl-containing polyimides to PBO [48].

2.4 Polyimide membranes for gas separation

The majority of the suggested applications of polyimide-based membranes are related to gas separation. The mambrane gas separation depends on the material from which it is made of which dictates: (1) the permeability and separation factors, (2) the structure and the thickness of the membrane which governs the permeance, (3) the configuration of the membranes and whether they are flat or hollow fibers, for instance, and (4) the module and the system design it will be used at [17].

Membranes are used in a wide range of applications and they are most favorable when: [17,32]

- Moderate purity recovery is sufficient
- The component meant to be separated is in a relatively considerable concentration
- The feed is available at the desired pressure
- The residue stream is needed at higher pressure
- The feed stream does not contain substances that could compromise the integrity of the membrane
- The selectivity of the membrane is sufficient

The most important gas pairs associated with natural gas separation/purification processes are CO_2/CH_4, N_2/CH_4 and CO_2/N_2 and it has been reported that polyimide-based membranes are considered one of the most successful for CO_2/CH_4 and CO_2/N_2 applications [15,132,133]. However, they are not yet successful in the separation of N_2/CH_4 and it is important to note that the separation of this gas pair is considered challenging to almost all polymeric membrane and not only polyimide-based ones. This difficulty is mainly attributed to the fact that N_2 and CH_4 are substantially similar in the sense that they have almost identical dielectric constants of 1.0 and 1.1 respectively, which means that their solubilities are very similar [134-137]. This is essential because the first step in the solution-diffusion mechanism is the sorption of *preferential* permeate, via solubility, at the upstream surface of the membrane [36,130]. Therefore, both species are soluble in the polymeric membranes and hence will not separate. Moreover, both N_2 and CH_4 have very close kinetic diameters of 0.38 nm and 0.36 nm respectively which means that the diffusion of both species through the fractional free volume would be relatively similar [17].

Generally, membranes are associated with a permeability-selectivity trade-off relationship where high permeabilities usually correspond to low selectivities and vice versa. Robeson [138] suggested that every gas pair has an upper bound known as "Robeson upper bound" or "Robeson upper limit". The upper bound correlation curve can be calculated using EQ (15): [138]

$$P_i = k\alpha_{ij}^n \hspace{4cm} EQ.\ (15)$$

Where P_i is the permeability of gas species i, k is the front factor, α_{ij}^n is the ideal selectivity and n is the upper bound slope. The values of k and n for the gas pairs considered in this research are presented in Table. 8.

Table 8. Tabulated values of the front factor (k) and the upper bound slope (n) [138].

Gas Pair	k (Barrer)	n
CO_2/CH_4	5,369,140	-2.636
CO_2/N_2	30,967,000	-2.888
N_2/CH_4	2,570	-4.507

Figure. 19 compiles the gas separation properties of some of the most known TR polymers. Such plots could be used to demonstrate the suitability of some TR polymers for a wide range of industrially related gas separation processes [118]. For example, looking at the CO_2/CH_4 plot in Figure 19, it is clearly observed that some TR polymers exceed the upper bound which suggests that they are excellent candidates for CO_2/CH_4 separation. However, it should be noted that when most TR-polymers are exposed to natural gas in actual field conditions, they tend to exhibit very modest separation. Moreover, real field conditions usually deteriorate the membrane separation performance which is mainly because of the action of CO_2 and higher hydrocarbons contaminants present in the natural gas. As the higher hydrocarbons sorb into the polymeric membrane, they act as plasticizers where they increase the chain mobility of the polymer and reduce the diffusivity-selectivity of the polymer. As mentioned earlier, polymeric membranes are generally not suitable for the gas separation of N_2/CH_4 and that could be clearly observed from Figure. 20 where there are almost no polymeric membranes that clearly and completely exceeds the upper bound. Figures (21) were plotted in an attempt to summarize a number of gas separation data points of dense polyimides and TR-

polyimides that were collected from various sources. A detailed table of all the permeability

and selectivity values is in available in Appendix. 1.
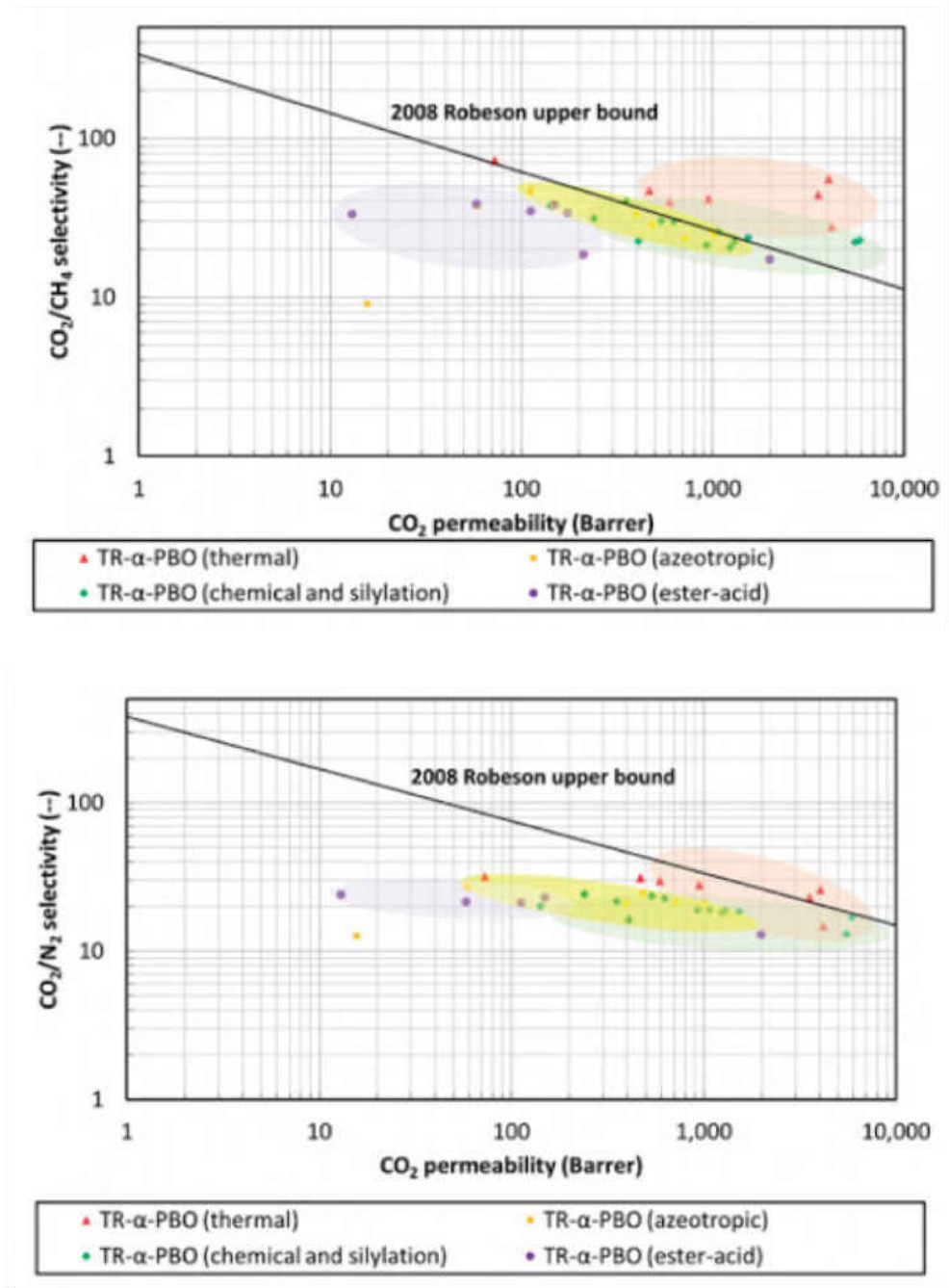
Figure 19. Upper bound correlation between CO_2/CH_4 (top) and CO_2/N_2 (bottom) separation for a number of TR polyimide membranes characterized based on the their imidization route [118].
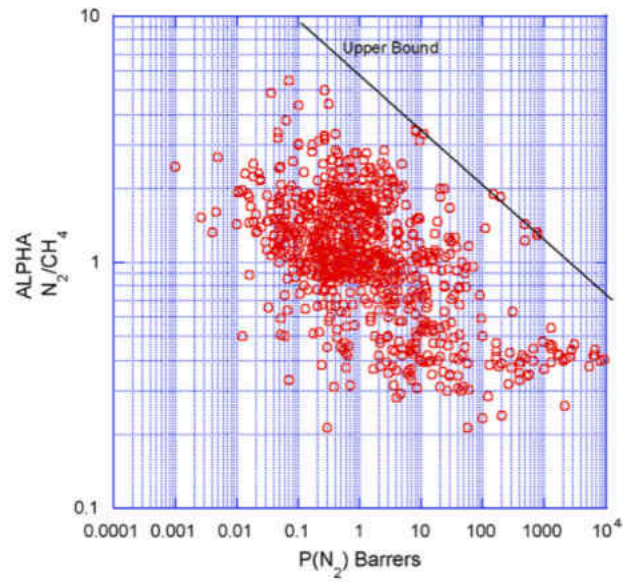
Figure 20. The upper bound correlation for N_2/CH_4 separation using a number of polymeric membranes [138].
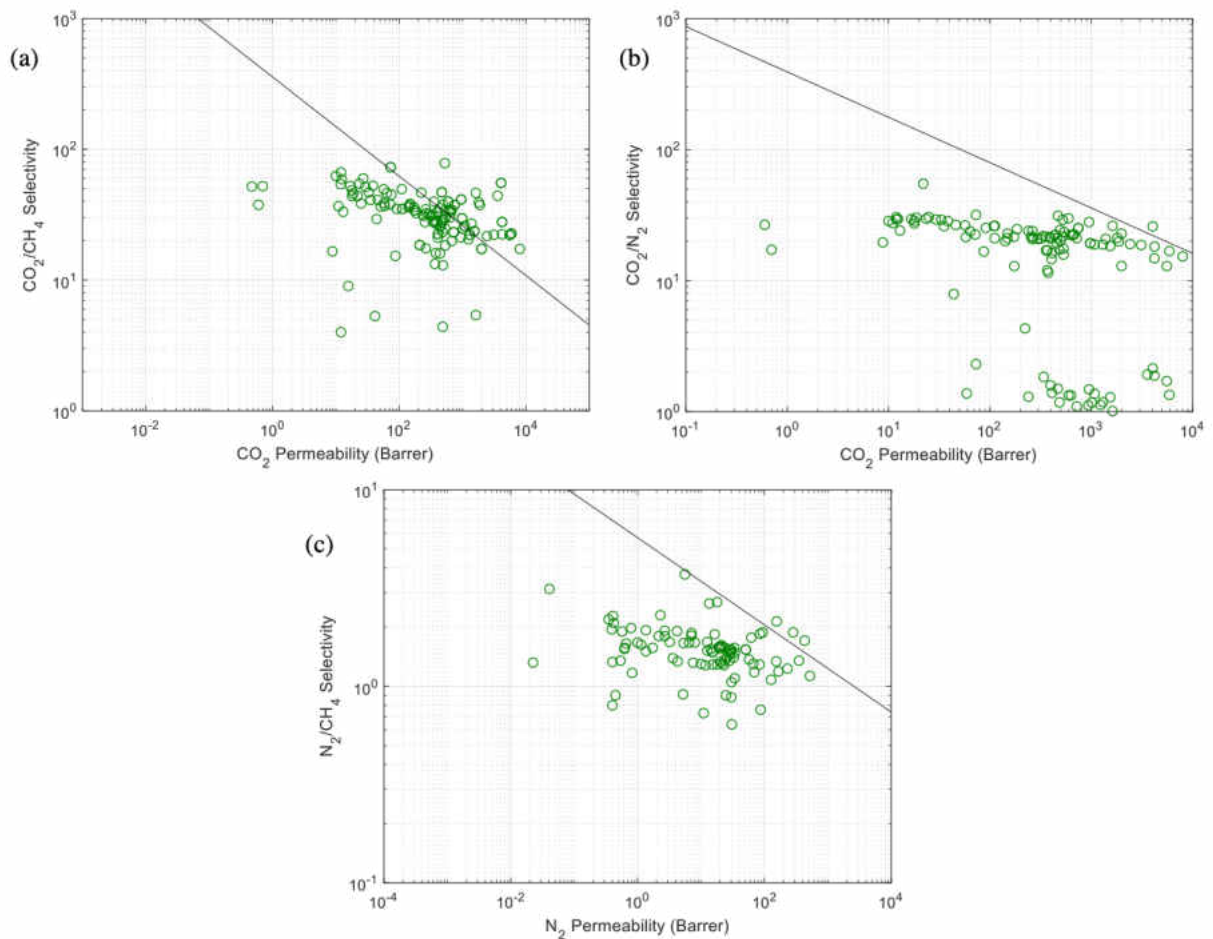
Figure 21. Upper bound correlation between (a) CO_2/CH_4, (b) CO_2/N_2 and (c) N_2/CH_4 gas separation for a number of TR polyimide membranes characterized based on the their imidization route.

2.5 Surface modification of polyimides

   To address some of the limitations that occur in polyimides, various surface modifications have been performed. The ultimate goal of surface modification is improving the separation performance of the membrane. This is done by either sealing defects or tailoring the functional groups on the membrane surface to a particular gas species. In doing this, both diffusivity and solubility of gases is influenced, ideally leading to improved permeability and selectivity. Surface modification is a promising method for gas separation polyimides for that reason.

2.5.1 Coating

   Coating is one method of surface modification that is typically used to repair surface defects such as pin holes. Pin holes in membranes can be caused by trapped gases or moisture that escape during membrane formation, leaving behind a large hole in the membrane surface. These defects can be sealed by coating the surface with a highly permeable but non selective polymer. This is typically achieved by dip coating in a dissolved coating polymer. One of the most common polymers used for membrane coating include silicone rubber, or poly(dimethylsiloxane) [139]. Interestingly, coating with a silicon rubber has also shown to reduce the effects of aging in polyimide membranes. Rowe et al. showed that increasing the thickness of the coating layer resulted in higher O_2, N_2, and CH_4 permeability after aging [140]. Kim et al. [141] found success in silicone coating on 6FDA-based polyimides for CO_2/N_2 separation. They found a slight decrease in both CO_2 and N_2 permeance with a simultaneous increase in CO_2/N_2 selectivity, confirming defects were sealed [141]. The performance of membranes coated with the silicone was also influenced by the solvent used to dissolve the coating, thus, care should be taken in solvent selection when coating.

Another coating that has been explored is polydopamine. In this case, the aim is not to seal defects, but to influence the functionality of the membrane surface. On its own, polydopamine tends to increase the surface free energy [142]. However, polydopamine has been used as a binding agent for other various coatings and particle phases such as silver nanoparticles and aquaporin. Although interesting, these are different classes of membrane and are not discussed further.

2.5.2 Crosslinking

Chemical crosslinking is one way to influence gas solubility in the polymer membrane. New functional groups are introduced, or rearranged, by reacting with a crosslinking compound. Crosslinking also tends to suppress plasticization, which can be especially beneficial for natural gas processing [143]. Diamine crosslinking is the most frequently reported chemical cross-linking reaction. For example, Chung et al. reacted linear aliphatic amines with a 6FDA-durene polyimide to partially replace the imide groups with amide groups [144]. This greatly influenced the presence of hydrogen bonding potential on the surface of the polyimide, leading to greatly enhanced H_2/CO_2 selectivity. The crosslinking reaction that was proposed is show in Figure. 22.

It is worth noting that crosslinking by reactions in the liquid phase can potentially result in penetration of the reaction below the surface of the membrane, potentially leading to poorer performance from increased free volume. To prevent this, the same group also achieved conversion of imide groups into amide groups by the vapor phase reaction of ethylenediamine with polyimide [145]. Other vapor phase cross linking agents have also been examined [146].
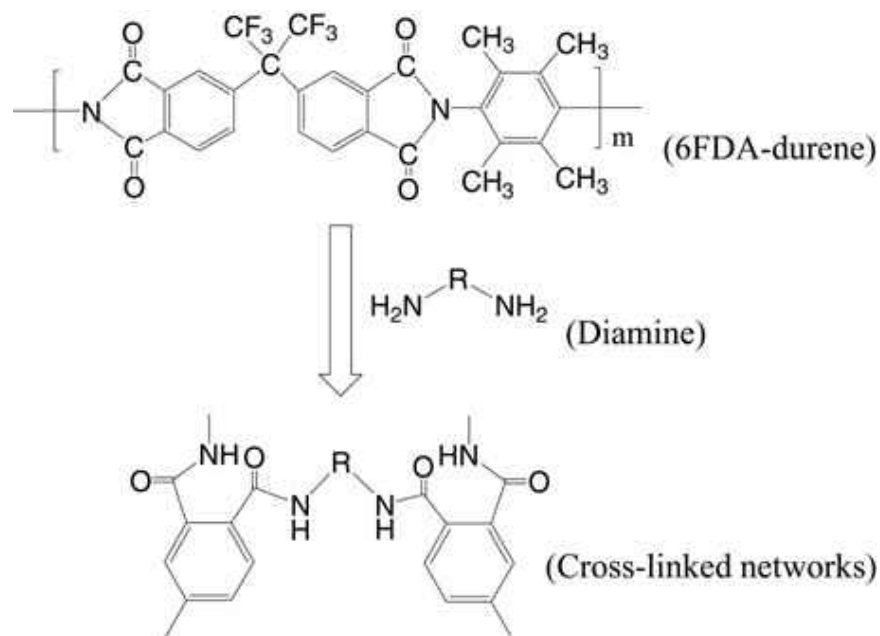
Figure 22: Crosslinking reaction between diamine and 6FDA based polyimide [144].

Another major crosslinking agent for polyimides is diols, such as 1,4-butylene glycol, ethylene glycol, and 1,40cyclohexanedimethanol to name a few [143]. Diol crosslinking is most successful in polyimides with carboxyl groups due to the esterification reaction that can take place shown in Figure. 23.
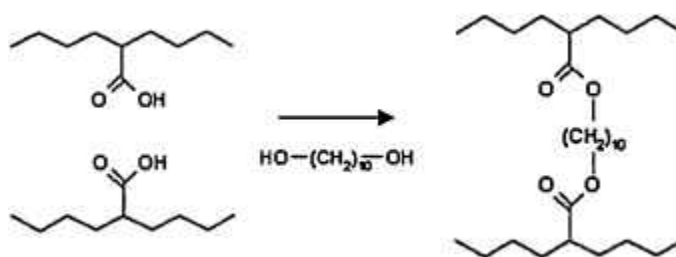
Figure 23: Diol crosslinking of carboxyl containing polyimide. [143].

Other forms of crosslinking such as thermal and UV crosslinking have also been investigated. Instead of chemically reacting a species to the polyimide, heat of UV light is introduced to a pristine polyimide and crosslinking takes place internally. Generally, both methods result in bond formation between the pendant group of the polyimide with neighboring chains.

2.5.3 Ion Irradiation

Another polyimide surface modification method is by introduce carbon molecular sieve-like pores in the surface of the membrane with ion beam irradiation. This method essentially locally carbonizes the polyimide to produce amorphous molecular sieving networks. Won et al. found that the ion beam dosage greatly influenced the gas separation properties. Higher doses of ions seemed to turn the selective top layer of a polyimide into a barrier layer, effectively reducing the gas permeability while greatly increasing selectivity [147]. This ion treatment has also shown to alter the surface conductivity of polyimides. Kakitani et al. [148] demonstrated the surface of polyimide membranes became conductive due to carbonization with argon ion irradiation. Again, this was said to be a result of the local carbonization of the surface, creating highly carbonaceous networks. As expected, the type of ion used for irradiation, dose, and type of polyimide, and the desired gas separation application are all important factors to consider as each combination can potentially produce unique results.

2.5.4 Nanocomposites and Mixed Matrix Polyimides

Recently, the introduction of a particle phase into the polyimide membrane has shown to yield interesting surface properties. The surface free energy tends to be influenced by the hydrophobicity of the particle phase. The membrane surface tends to become rougher with particle loading creating more effective surface area for gas penetration. Interesting dielectric properties are also seen in polyimide nanocomposites, which can be manipulated by altering particle size and particle functionality. This is a potential method to facilitate tunable interaction between the membrane surface and a specific gas to achieve enhanced separation. None the less, the most notable influence of particle phase on polyimide nanocomposites is the

addition of multiple mechanistic pathways through the membrane via the particle free volume. This typically results in improved permeability with comparable selectivity as pristine membranes. For this reason, the most important factor to consider in mixed matrix membrane fabrication is the compatibility between the particle phase and polymer phase. For more information on mixed matrix polyimides, see [149].

2.6 Conclusions

Membrane technology can be used in various gas separation applications one of which is natural gas purification to meet pipeline specifications. Aromatic polyimides are considered one of the leading polymeric materials for membrane fabrication and gas separation applications and that's due to their resilient properties. There are different types of diffusion mechanisms that take place through membranes; however, the two main mechanisms that take place through polymeric membranes are Knudsen diffusion and solution-diffusion mechanisms where both the size of the gas molecule and its condensability governs the separation. Moreover, the properties of aromatic polyimides are mainly governed by the structure and stability of the starting monomers as well as the imidization route used during the synthesis. Another advantage for using aromatic polyimides is that they could be thermally converted into polybenzoxazole which are known for their enhanced gas separation properties and they allowed the gas permeabilities and selectivities to surpass Robeson upper bound especially when dealing with CO_2/CH_4 and CO_2/N_2 gas pairs. Furthermore, there are multiple surface modification techniques that could be used to mitigate the defects associated with polyimide membranes fabrication.

References

[1] International Energy Outlook 2016, ProQuest eLibrary Editorial Websites, (2010).

[2] International Energy Agency (iea), Natural gas, (2018).

[3] J.G. Speight, Gas processing : environmental aspects and methods, England, 1993.

[4] BP, BP Statistical Review of World Energy (2018).

[5] International Energy Agency (iea), Natural Gas Explained: natural Gas Pipelines, (2018).

[6] CROFT Production Systems, Natural Gas Composition, (2015).

[7] Y. Xiao, B.T. Low, S.S. Hosseini, T.S. Chung, and D.R. Paul. The strategies of molecular architecture and modification of polyimide-based membranes for CO2 removal from natural gas—A review. Progress in Polymer Science, 34 (2009) 561.

[8] Hongqun Yang Zhenghe Xu Maohong Fan Rajender Gupta Rachid B Slimane Alan E Bland Ian Wright. Progress in carbon dioxide separation and capture : A review.20 (2008) 14.

[9] R. Baker, Membrane Technology and Applications, GB, Wiley, 2012.

[10] R. Spillman, Chapter 13 Economics of gas separation membrane processes, in Anonymous , Membrane Science and Technology, Elsevier B.V, 1995, pp. 589-667.

[11] J.P. Agostini, F.J.C. Fournie. Permeation Membranes Can Efficiently Replace Conventional Gas Treatment Processes. Journal of Petroleum Technology, 39 (1987) 707.

[12] T.E. Cooley, W.L. Dethloff. Field tests show membrane processing attractive. Chem. Eng. Prog.; (United States), 81:10 (1985).

[13] R. E. Babcock, R. W. Spillman, C. S. Goddin and T. E. Cooley. Natural Gas Cleanup: A Comparison of Membrane and Amine Treatment Processes. (1988).

[14] Michelle Michot Foss, Chief Energy Economist, CEE Head 1650 Highway 6, Suite 300 Sugar Land, and Texas 77478 Tel 281-313-9763 Fax 281-340-3482 energyecon@beg.utexas.edu www.beg.utexas.edu/energyecon/lng, INTERSTATE NATURAL GAS—QUALITY SPECIFICATIONS & INTERCHANGEABILITY,.

[15] E.P. Favvas, F.K. Katsaros, S.K. Papageorgiou, A.A. Sapalidis, and A.C. Mitropoulos. A review of the latest development of polyimide based membranes for CO2 separations. Reactive and Functional Polymers, 120 (2017) 104.

[16] S. Alexander Stern, Polymers for gas separations: the next decade, Journal of Membrane Science, 94 (1994) 1.

[17] A.F. Ismail, K. Khulbe, T. Matsuura, and K.C. Khulbe, Gas Separation Membranes, (2015).

[18] LI DONGFEI, Dual-layer asymmetric hollow-fiber membranes for gas separation, (2005).

[19] T.A. Saleh, V.K. Gupta, Nanomaterial and Polymer Membranes: Synthesis, Characterization, and Applicatons, Cambridge, Elsevier, 2016.

[20] A. Fick. On liquid diffusion. (1855).

[21] Jacobus Henricus Van't Hoff. Osmotic Pressure and Chemical Equilibrium, (Nobel Prize in Chemistry). (1901).

[22] T. Uragami, Science and technology of separation membranes, , 2017.

[23] Loeb, S. Sourirajan, Sea water demineralization by means of an osmotic membrane, Adv. Chem. Ser. 38 (1962) 117–132.

[24] Freeman and Pinnau; Polymer Membranes for Gas and Vapor Separation ACS Symposium Series; American Chemical Society: Washington, DC, 1999.

. American Chemical Society,.

[25] A. Hasimi, A. Stavropoulou, K.G. Papadokostaki, and M. Sanopoulou. Transport of water in polyvinyl alcohol films: Effect of thermal treatment and chemical crosslinking. European Polymer Journal, 44 (2008) 4098.

[26] G. Alefeld, Hydrogen in metals, Berlin [u.a.], Springer, 1978.

[27] Pengpeng Liu, Xingbo Ge, Rongyue Wang, Houyi Ma, and Yi Ding. Facile Fabrication of Ultrathin Pt Overlayers onto Nanoporous Metal Membranes via Repeated Cu UPD and in Situ Redox Replacement Reaction. Langmuir : the ACS journal of surfaces and colloids, 25 (2009) 561.

[28] J.-. Duval, B. Folkers, M.H.V. Mulder, G. Desgrandchamps, and C.A. Smolders. Adsorbent filled membranes for gas separation. Part 1. Improvement of the gas separation properties of polymeric membranes by incorporation of microporous adsorbents. Journal of Membrane Science, 80 (1993) 189.

[29] M. Jia, K. Pleinemann, and R. Behling. Preparation and characterization of thin-film zeolite–PDMS composite membranes. Journal of Membrane Science, 73 (1992) 119.

[30] S.F. Nitodas, E.P. Favvas, G.E. Romanos, M.A. Papadopoulou, A.Ch. Mitropoulos, N.K. Kanellopoulos, Synthesis and characterization of hydrogen selective silica-based membranes, J. Porous. Mater. 15 (2008) 551–557.

.

[31] P.M. Budd, N.B. McKeown. Highly permeable polymers for gas separation membranes. Polymer Chemistry, 1 (2010) 63.

[32] P. Bernardo, E. Drioli, and G. Golemme. Membrane Gas Separation: A Review/State of the Art. Industrial & Engineering Chemistry Research, 48 (2009) 4638.

[33] A. Fick, Concerns diffusion and concentration gradient, Ann. Phys. Lpz. 170 (1850) 59.

[34] S.C. George, S. Thomas. Transport phenomena through polymeric systems. Progress in Polymer Science, 26 (2001) 985.

[35] S.T. Oyama. Review on Mechanisms of Gas Permeation through Inorganic Membranes. Journal of the Japan Petroleum Institute, 54 (2011) 298.

[36] A. Javaid. Membranes for solubility-based gas separation applications. Chemical Engineering Journal, 112 (2005) 219.

[37] J.G. Wijmans, R.W. Baker. The solution-diffusion model: a review. Journal of Membrane Science, 107 (1995) 1.

[38] S. Kim, Y.M. Lee. Rigid and microporous polymers for gas separation membranes. Progress in Polymer Science, 43 (2015) 1.

[39] B.D.Freeman,Basisofpermeability/selectivitytradeoffrelationsinpolymericgas separation membranes, Macromolecules 32 (1999) 375–380.

[40] L.W. McKeen, The effect of sterilization on plastics and elastomers, third edition, Waltham [Mass.], William Andrew, 2012.

[41] Anu Stella Mathews, Il Kim, and Chang Sik Ha. Synthesis, Characterization, and Properties of Fully Aliphatic Polyimides and Their Derivatives for Microelectronics and Optoelectronics Applications. Macromol. Res, 15 (2007) 114.

[42] C.A. Scholes, G.W. Stevens, and S.E. Kentish. Membrane gas separation applications in natural gas processing. Fuel, 96 (2012) 15.

[43] K. Tanaka, M. Okano, H. Toshino, H. Kita, and K. Okamoto. Effect of methyl substituents on permeability and permselectivity of gases in polyimides prepared from methyl-substituted phenylenediamines. Journal of Polymer Science Part B: Polymer Physics, 30 (1992) 907.

[44] Masako Miki, Hideki Horiuchi, and Yasuharu Yamada. Synthesis and Gas Transport Properties of Hyperbranched Polyimide–Silica Hybrid/Composite Membranes. Polymers, 5 (2013) 1362.

[45] J.P. Jampol'skij, Materials science of membranes for gas and vapor separation, Chichester, Wiley, 2006.

[46] T. Suzuki, Y. Yamada, and K. Itahashi. 6FDA-TAPOB hyperbranched polyimide-silica hybrids for gas separation membranes. Journal of Applied Polymer Science, 109 (2008) 813.

[47] S.H. Han, N. Misdan, S. Kim, C.M. Doherty, A.J. Hill, and Y.M. Lee. Thermally Rearranged (TR) Polybenzoxazole: Effects of Diverse Imidization Routes on Physical Properties and Gas Transport Behaviors. Macromolecules, 43 (2010) 7657.

[48] H.B. Park, S.H. Han, C.H. Jung, Y.M. Lee, and A.J. Hill. Thermally rearranged (TR) polymer membranes for CO2 separation. Journal of Membrane Science, 359 (2010) 11.

[49] R. Swaidan, B. Ghanem, E. Litwiller, and I. Pinnau. Effects of hydroxyl-functionalization and sub-Tg thermal annealing on high pressure pure- and mixed-gas CO2/CH4 separation by polyimide membranes based on 6FDA and triptycene-containing dianhydrides. Journal of Membrane Science, 475 (2015) 571.

[50] F. Alghunaimi, B. Ghanem, N. Alaslai, M. Mukaddam, and I. Pinnau. Triptycene dimethyl-bridgehead dianhydride-based intrinsically microporous hydroxyl-functionalized polyimide for natural gas upgrading. Journal of Membrane Science, 520 (2016) 240.

[51] J.H. Hodgkin, B.N. Dao. Thermal conversion of hydroxy-containing polyimides to polybenzoxazoles. Does this reaction really occur? European Polymer Journal, 45 (2009) 3081.

[52] N.L. Le, Y. Wang, and T. Chung. Synthesis, cross-linking modifications of 6FDA-NDA/DABA polyimide membranes for ethanol dehydration via pervaporation. Journal of Membrane Science, 415-416 (2012) 109.

[53] S.S. Chan, T. Chung, Y. Liu, and R. Wang. Gas and hydrocarbon (C 2 and C 3) transport properties of co-polyimides synthesized from 6FDA and 1,5-NDA (naphthalene)/Durene diamines. Journal of Membrane Science, 218 (2003) 235.

[54] J. Ren, R. Wang, T. Chung, D.F. Li, and Y. Liu. The effects of chemical modifications on morphology and performance of 6FDA-ODA/NDA hollow fiber membranes for CO2/CH4 separation. Journal of Membrane Science, 222 (2003) 133.

[55] T. Suzuki, M. Miki, and Y. Yamada. Gas transport properties of hyperbranched polyimide/hydroxy polyimide blend membranes. European Polymer Journal, 48 (2012) 1504.

[56] K. Okamoto, K. Tanaka, H. Kita, M. Ishida, M. Kakimoto, and Y. Imai. Gas Permeability and Permselectivity of Polyimides Prepared from 4,4'-Diaminotriphenylamine. Polymer Journal, 24 (1992) 451.

[57] M.A.Q. Al-Sayaghi, J. Lewis, C. Buelke, and A.S. Alshami. Physicochemical and thermal effects of pendant groups, spatial linkages and bridging groups on the formation and processing of polyimides. International Journal of Polymer Analysis and Characterization, 23 (2018) 566.

[58] Z.P. Smith, G. Hernández, K.L. Gleason, A. Anand, C.M. Doherty, K. Konstas, et al. Effect of polymer structure on gas transport properties of selected aromatic polyimides, polyamides and TR polymers. Journal of Membrane Science, 493 (2015) 766.

[59] C.Y. Soo, H.J. Jo, Y.M. Lee, J.R. Quay, and M.K. Murphy. Effect of the chemical structure of various diamines on the gas separation of thermally rearranged poly(benzoxazole-co-imide) (TR-PBO-co-I) membranes. Journal of Membrane Science, 444 (2013) 365.

[60] C. Leu, Z. Wu, and K. Wei. Synthesis and Properties of Covalently Bonded Layered Silicates/Polyimide (BTDA-ODA) Nanocomposites. Chemistry of Materials, 14 (2002) 3016.

[61] Y.K. Kim, H.B. Park, and Y.M. Lee. Preparation and characterization of carbon molecular sieve membranes derived from BTDA–ODA polyimide and their gas separation properties. Journal of Membrane Science, 255 (2005) 265.

[62] Z. Xu, L. Xiao, J. Wang, and J. Springer. Gas separation properties of PMDA/ODA polyimide membranes filling with polymeric nanoparticles. Journal of Membrane Science, 202 (2002) 27.

[63] Y. Hirayama, T. Yoshinaga, Y. Kusuki, K. Ninomiya, T. Sakakibara, and T. Tamari. Relation of gas permeability with structure of aromatic polyimides I. Journal of Membrane Science, 111 (1996) 169.

[64] J. Hayashi, H. Mizuta, M. Yamamoto, K. Kusakabe, S. Morooka, and S. Suh. Separation of Ethane/Ethylene and Propane/Propylene Systems with a Carbonized BPDA−pp'ODA Polyimide Membrane. Industrial & Engineering Chemistry Research, 35 (1996) 4176.

[65] S. Carturan, M. Tonezzer, A. Quaranta, G. Maggioni, M. Buffa, and R. Milan. Optical properties of free-base tetraphenylporphyrin embedded in fluorinated polyimides and their ethanol and water vapours sensing capabilities. Sensors & Actuators: B. Chemical, 137 (2009) 281.

[66] S. Kulkarni Sudhir, Fu Shilu, J. Koros William, and J.E.S. Sanders, Carbon molecular sieve membranes made from 6FDA and DETDA-based precursor polymers, , US9527045B2, 2016.

[67] J K Adewole, A L Ahmad. Polymeric membrane materials selection for high-pressure CO2 removal from natural gas. Journal of Polymer Research, 24 (2017) 1.

[68] M. López-Badillo, J.A. Galicia-Aguilar, E. Ortiz-Muñoz, G. Hernández-Rodríguez, and F.H. Del Valle-Soto. Chemical Cross-Linking of 6FDA-6FPA Polyimides for Gas Permeation Membranes. International Journal of Chemical Reactor Engineering, (2018).

[69] X. Zhao, J. Liu, H. Li, L. Fan, and S. Yang. Synthesis and properties of fluorinated polyimides from 1,1-bis(4-amino-3,5-dimethylphenyl)-1-(3,4,5-trifluorophenyl)-2,2,2-trifluoroethane and various aromatic dianhydrides. Journal of Applied Polymer Science, 111 (2009) 2210.

[70] J.H. Kim, W.J. Koros, and D.R. Paul. Physical aging of thin 6FDA-based polyimide membranes containing carboxyl acid groups. Part I. Transport properties. Polymer, 47 (2006) 3094.

[71] C. Zhang, Y. Dai, J.R. Johnson, O. Karvan, and W.J. Koros. High performance ZIF-8/6FDA-DAM mixed matrix membrane for propylene/propane separations. Journal of Membrane Science, 389 (2012) 34.

[72] K. Tanaka, A. Taguchi, J. Hao, H. Kita, and K. Okamoto. Permeation and separation properties of polyimide membranes to olefins and paraffins. Journal of Membrane Science, 121 (1996) 197.

[73] K. Okamoto, N. Tanihara, H. Watanabe, K. Tanaka, H. Kita, A. Nakamura, et al. Vapor permeation and pervaporation separation of water-ethanol mixtures through polyimide membranes. Journal of Membrane Science, 68 (1992) 53.

[74] J. Hao, K. Tanaka, H. Kita, and K. Okamoto. The pervaporation properties of sulfonyl-containing polyimide membranes to aromatic/aliphatic hydrocarbon mixtures. Journal of Membrane Science, 132 (1997) 97.

[75] S. Xu, Y. Wang. Novel thermally cross-linked polyimide membranes for ethanol dehydration via pervaporation. Journal of Membrane Science, 496 (2015) 142.

[76] S. Zhang, H. Zhang, Y. Zhang, J. Li, and X. Huang. Sulfonated polyimide membranes with different non-sulfonated diamines for vanadium redox battery applications. Electrochimica Acta, 150 (2014) 114.

[77] M. Langsam, W.F. Burgoyne. Effects of diamine monomer structure on the gas permeability of polyimides. I. Bridged diamines. Journal of Polymer Science Part A: Polymer Chemistry, 31 (1993) 909.

[78] Y. Zhang, Y. Su, J. Peng, X. Zhao, J. Zhao, J. Liu, et al. Composite nanofiltration membranes prepared by interfacial polymerization with natural material tannic acid and trimesoyl chloride. Journal of Membrane Science, 429 (2013) 235.

[79] L. ZHOU, P.K. COUGHLIN, C. LIU, R. SERBAYEVA, and M. TANG, POLYMER MEMBRANES DERIVED FROM AROMATIC POLYIMIDE MEMBRANES, , MY157508A, 2016.

[80] Y.M. Xu, N.L. Le, J. Zuo, and T. Chung. Aromatic polyimide and crosslinked thermally rearranged poly(benzoxazole-co-imide) membranes for isopropanol dehydration via pervaporation. Journal of Membrane Science, 499 (2016) 317.

[81] H. Wang, D.R. Paul, and T. Chung. Surface modification of polyimide membranes by diethylenetriamine (DETA) vapor for H2 purification and moisture effect on gas permeation. Journal of Membrane Science, 430 (2013) 223.

[82] L. Shao, T. Chung, S.H. Goh, and K.P. Pramoda. Polyimide modification by a linear aliphatic diamine to enhance transport performance and plasticization resistance. Journal of Membrane Science, 256 (2005) 46.

[83] Y. Li, X. Wang, M. Ding, and J. Xu. Effects of molecular structure on the permeability and permselectivity of aromatic polyimides. Journal of Applied Polymer Science, 61 (1996) 741.

[84] S. Xiao, X. Feng, and R.Y.M. Huang. 2,2-Bis[4-(3,4-dicarboxyphenoxy) phenyl]propane dianhydride (BPADA)-based polyimide membranes for pervaporation dehydration of isopropanol: Characterization and comparison with 4,4′-(hexafluoroisopropylidene) diphthalic anhydride (6FDA)-based polyimide membranes. Journal of Applied Polymer Science, 110 (2008) 283.

[85] Y. Xu, C. Chen, P. Zhang, B. Sun, and J. Li. Pervaporation Properties of Polyimide Membranes for Separation of Ethanol + Water Mixtures. Journal of Chemical & Engineering Data, 51 (2006) 1841.

[86] H. Ohya, I. Okazaki, M. Aihara, S. Tanisho, and Y. Negishi. Study on molecular weight cut-off performance of asymmetric aromatic polyimide membrane. Journal of Membrane Science, 123 (1997) 143.

[87] B. Fang, K. Pan, Q. Meng, and B. Cao. Preparation and properties of polyimide solvent-resistant nanofiltration membrane obtained by a two-step method. Polymer International, 61 (2012) 111.

[88] F. Aziz, A.F. Ismail. Preparation and characterization of cross-linked Matrimid® membranes using para-phenylenediamine for O2/N2 separation. Separation and Purification Technology, 73 (2010) 421.

[89] Y. Zhuang, J.G. Seong, Y.S. Do, W.H. Lee, M.J. Lee, M.D. Guiver, et al. High-strength, soluble polyimide membranes incorporating Troger's Base for gas separation. Journal of Membrane Science, 504 (2016) 55.

[90] N. Alaslai, B. Ghanem, F. Alghunaimi, E. Litwiller, and I. Pinnau. Pure- and mixed-gas permeation properties of highly selective and plasticization resistant hydroxyl-diamine-based 6FDA polyimides for CO2/CH4 separation. Journal of Membrane Science, 505 (2016) 100.

[91] Sang Hee Park, Kwang Je Kim, Won Wook So, Sang Jin Moon, and Soo Bok Lee. Gas Separation Properties of 6FDA-Based Polyimide Membranes with a Polar Group. Macromol. Res, 11 (2003) 157.

[92] K. Kim, S. Park, W. So, D. Ahn, and S. Moon. CO2 separation performances of composite membranes of 6FDA-based polyimides with a polar group. Journal of Membrane Science, 211 (2003) 41.

[93] Y. Xu, C. Chen, and J. Li. Experimental study on physical properties and pervaporation performances of polyimide membranes. Chemical Engineering Science, 62 (2007) 2466.

[94] Y. Zhuang, J.G. Seong, Y.S. Do, H.J. Jo, Z. Cui, J. Lee, et al. Intrinsically Microporous Soluble Polyimides Incorporating Tröger's Base for Membrane Gas Separation. Macromolecules, 47 (2014) 3254.

[95] X. Duthie, S. Kentish, C. Powell, K. Nagai, G. Qiao, and G. Stevens. Operating temperature effects on the plasticization of polyimide gas separation membranes. Journal of Membrane Science, 294 (2007) 40.

[96] X. Duthie, S. Kentish, S.J. Pas, A.J. Hill, C. Powell, K. Nagai, et al. Thermal treatment of dense polyimide membranes. Journal of Polymer Science Part B: Polymer Physics, 46 (2008) 1879.

[97] YANG Xiang-dong YE Hong LI Yan-ting LI Juan LI Ji-ding ZHAO Bing-qiang LIN Yang-zheng. An asymmetric membrane of polyimide 6FDA-BDAF and its pervaporation desulfurization for n-heptane/thiophene mixtures. 农业科学学报：英文版, 14 (2015) 2529.

[98] H. Ye, J. Li, Y. Lin, J. Chen, and C. Chen. PERVAPORATION SEPARATION FOR TOLUENE/n-HEPTANE MIXTURE BY POLYIMIDE MEMBRANES CONTAINING FLUORINE. Chinese Journal of Polymer Science, 26 (2008) 705.

[99] W. Lin, T. Chung. Gas permeability, diffusivity, solubility, and aging characteristics of 6FDA-durene polyimide membranes. Journal of Membrane Science, 186 (2001) 183.

[100] S. Japip, H. Wang, Y. Xiao, and T. Shung Chung. Highly permeable zeolitic imidazolate framework (ZIF)-71 nano-particles enhanced polyimide membranes for gas separation. Journal of Membrane Science, 467 (2014) 162.

[101] L. Shao, L. Liu, S. Cheng, Y. Huang, and J. Ma. Comparison of diamino cross-linking in different polyimide solutions and membranes by precipitation observation and gas transport. Journal of Membrane Science, 312 (2008) 174.

[102] R. Swaidan, B. Ghanem, M. Al-Saeedi, E. Litwiller, and I. Pinnau. Role of Intrachain Rigidity in the Plasticization of Intrinsically Microporous Triptycene-Based Polyimide Membranes in Mixed-Gas CO2/CH4 Separations. Macromolecules, 47 (2014) 7453.

[103] S. Sridhar, R.S. Veerapur, M.B. Patil, K.B. Gudasi, and T.M. Aminabhavi. Matrimid polyimide membranes for the separation of carbon dioxide from methane. Journal of Applied Polymer Science, 106 (2007) 1585.

[104] C.P. Ribeiro, B.D. Freeman, D.S. Kalika, and S. Kalakkunnath. Aromatic polyimide and polybenzoxazole membranes for the fractionation of aromatic/aliphatic hydrocarbons by pervaporation. Journal of Membrane Science, 390 (2012) 182.

[105] J. Fang, H. Kita, and K. Okamoto. Gas permeation properties of hyperbranched polyimide membranes. Journal of Membrane Science, 182 (2001) 245.

[106] K.L. Mittal, Polyimides, New York [u.a.], Plenum Press, 1984.

[107] C. Feger, Polyimides, Amsterdam u.a, Elsevier, 1989.

[108] A. Tena, S. Shishatskiy, D. Meis, J. Wind, V. Filiz, and V. Abetz. Influence of the Composition and Imidization Route on the Chain Packing and Gas Separation Properties of Fluorinated Copolyimides. Macromolecules, 50 (2017) 5839.

[109] Summary of properties of Kapton® polyimide film, H-38492–2; DuPont™; 2006.

[110] L.W. McKeen, The effect of sterilization on plastics and elastomers, third edition, Waltham [Mass.], William Andrew, 2012.

[111] W. Volksen, Volksen W. (1994) Condensation polyimides: Synthesis, solution behavior, and imidization characteristics. In: Hergenrother P.M. (eds) High Performance Polymers. Advances in Polymer Science, vol 117. Springer, Berlin, Heidelberg, , High Performance Polymers, 2005.

[112] S. Yang, L. Yuan, Chapter 1 - Advanced Polyimide Films, Advanced Polyimide Materials, (2018) 1.

[113] C.E. Sroog. Polyimides. Progress in Polymer Science, 16 (1991) 561.

[114] D.R. Lloyd, Materials science of synthetic membranes, Washington, DC, 1986.

[115] Curro, J.G. Lagasse, R. R and Simah, R.Diffusion model for volume recovery in glasses. Macromolecules. 15(6). 1982, pp. 1621-1626.

[116] Wang, H. Chug, T and Paul, D.R. Physical aging and plasticization of thick and thin films of the thermally rearranged ortho-functional polyimide 6FDA-HAB. Journal of Membrane Science. 2014. 458 pp. 27-35.

[117] Keller, P.R. Membrane Technology and Industrial Separation Techniques. 1976. London: Noyes Data Corporation, pp. 164-180.

[118] E. Drioli, G. Barbieri, and A. Brunetti, Membrane engineering for the treatment of gases, 2nd edition, volume 2, , Royal Society of Chemistry, 2017.

[119] E.A. Laszlo. Process for preparing polyimides by treating polyamide-acids with lower fatty monocarboxylic acid anhydrides. USA. US3179630, 1965.

[120] L.E. Andrew. Aromatic polyimides from meta-phenylene diamine and para-phenylene diamine. USA. US3179633, 1965. .

[121] E.A. Laszlo. Aromatic polyimide particles from polycyclic diamines. US3179631, 1965.

[122] R.H. William. Process for preparing polyimides by treating polyamide-acids with aromatic monocarboxylic acid anhydrides: Google Patents,

1965.

[123] R.J. Angelo. Treatment of aromatic polyamide-acids with carbodiimides: Google Patents, 1966.

[124] T.M. Moy, C.D. DePorter, and J.E. McGrath. Synthesis of soluble polyimides and functionalized imide oligomers via solution imidization of aromatic diester-diacids and aromatic diamines. Polymer, 34 (1993) 819.

[125] C.H. Park, E. Tocci, Y.M. Lee, and E. Drioli. Thermal Treatment Effect on the Structure and Property Change between Hydroxy-Containing Polyimides (HPIs) and Thermally Rearranged Polybenzoxazole (TR-PBO). The journal of physical chemistry. B, 116 (2012) 12864.

[126] C.H. Park, E. Tocci, S. Kim, A. Kumar, Y.M. Lee, and E. Drioli. A Simulation Study on OH-Containing Polyimide (HPI) and Thermally Rearranged Polybenzoxazoles (TR-PBO):

Relationship between Gas Transport Properties and Free Volume Morphology. The journal of physical chemistry. B, 118 (2014) 2746.

[127] M. Calle, C.M. Doherty, A.J. Hill, and Y.M. Lee. Cross-Linked Thermally Rearranged Poly(benzoxazole-co-imide) Membranes for Gas Separation. Macromolecules, 46 (2013) 8179.

[128] D.F. Sanders, Z.P. Smith, C.P. Ribeiro, R. Guo, J.E. McGrath, D.R. Paul, et al. Gas permeability, diffusivity, and free volume of thermally rearranged polymers based on 3,3′-dihydroxy-4,4′-diamino-biphenyl (HAB) and 2,2′-bis-(3,4-dicarboxyphenyl) hexafluoropropane dianhydride (6FDA). Journal of Membrane Science, 409-410 (2012) 232.

[129] M. Kusama, T. Matsumoto, and T. Kurosaki. Soluble Polyimides with Polyalicyclic Structure.3. Polyimides from (4arH,8acH)-Decahydro-1t,4t:5c,8c-dimethanonaphthalene-2t,3t,6c,7c-tetracarboxylic 2,3:6,7-Dianhydride. Macromolecules, 27 (1994) 1117.

[130] B.D. Freeman, Basis of Permeability/Selectivity Tradeoff Relations in Polymeric Gas Separation Membranes, Macromolecules, 32 (1999) 375.

[131] T. Woock, S. Bjorgaard, B. Tande, and A. Alshami. Purification of natural gas using thermally rearranged polybenzoxazole and polyimide membranes – a review: part 2. Membrane Technology, 2016 (2016) 7.

[132] E.P. Favvas, Chapter 5th: Nanomaterials and their applicability as membranes' fillers, in: A.-N. Chowdhuryi, J. Shapter, A. Bin Imran (Eds.), Innovations in Nanomaterials, Nova Science Publishers, Inc., New York, U.S.A., 2015, pp. 105–157 (ISBN: 978-1-63483-548-0).

[133] J.D. Wind, D.R. Paul, and W.J. Koros. Natural gas permeation in polyimide membranes. Journal of Membrane Science, 228 (2004) 227.

[134] C.E. Powell, G.G. Qiao. Polymeric CO2/N2 gas separation membranes for the capture of carbon dioxide from power plant flue gases. Journal of Membrane Science, 279 (2006) 1.

[135] T. Hirose, Y. Mi, S.A. Stern, and A.K. St. Clair. The solubility of Carbon Dioxide and Methane in polyimides at elevated pressures. Journal of Polymer Science Part B: Polymer Physics, 29 (1991) 341.

[136] S. Li, Z. Zong, R. Zhou, S.J. Zhou, Y. Huang, Z. Song, et al. Howard S. Meyer, Methane Selective Membranes for Nitrogen Removal from Low Quality Natural Gas – High Permeation Is Not Enough. Available from: http://www.ecs.umass.edu/che/henson_group/research/membrane/t-04163.pdf

. Journal of Membrane Science, 487 (2015) 141.

[137] Ralph L. Amey and Robert H. Cole. Dielectric constants of Noble Gases and Methane. The journal of chemical physics. 40, 146 (1964).

[138] L.M. Robeson. The upper bound revisited. Journal of Membrane Science, 320 (2008) 390.

[139] D.F. Sanders, Z.P. Smith, R. Guo, L.M. Robeson, J.E. McGrath, D.R. Paul, et al. Energy-efficient polymeric gas separation membranes for a sustainable future: A review. Polymer, 54 (2013) 4729.

[140] B.W. Rowe, B.D. Freeman, and D.R. Paul. Physical aging of ultrathin glassy polymer films tracked by gas permeability. Polymer, 50 (2009) 5565.

[141] K. Kim, S. Park, W. So, D. Ahn, and S. Moon. CO2 separation performances of composite membranes of 6FDA-based polyimides with a polar group. Journal of Membrane Science, 211 (2003) 41.

[142] J. Jiang, L. Zhu, L. Zhu, B. Zhu, and Y. Xu. Surface Characteristics of a Self-Polymerized Dopamine Coating Deposited on Hydrophobic Polymer Films. Langmuir : the ACS journal of surfaces and colloids, 27 (2011) 14180.

[143] K. Vanherck, G. Koeckelberghs, and I.F.J. Vankelecom. Crosslinking polyimides for membrane applications: A review. Progress in Polymer Science, 38 (2013) 874.

[144] T. Chung, L. Shao, and P.S. Tin. Surface Modification of Polyimide Membranes by Diamines for H2 and CO2 Separation. Macromolecular Rapid Communications, 27 (2006) 998.

[145] L. Shao, C. Lau, and T. Chung. A novel strategy for surface modification of polyimide membranes by vapor-phase ethylenediamine (EDA) for hydrogen purification. International Journal of Hydrogen Energy, 34 (2009) 8716.

[146] H. Wang, D.R. Paul, and T. Chung. Surface modification of polyimide membranes by diethylenetriamine (DETA) vapor for H2 purification and moisture effect on gas permeation. Journal of Membrane Science, 430 (2013) 223.

[147] J. Won, M.H. Kim, Y.S. Kang, H.C. Park, U.Y. Kim, S.C. Choi, et al. Surface modification of polyimide and polysulfone membranes by ion beam for gas separation. Journal of Applied Polymer Science, 75 (2000) 1554.

[148] K. Kakitani, H. Koshikawa, T. Yamaki, S. Yamamoto, Y. Sato, M. Sugimoto, et al. Preparation of conductive layer on polyimide ion-track membrane by Ar ion implantation. Surface & Coatings Technology, 355 (2018) 181.

[149] M. Galizia, W.S. Chi, Z.P. Smith, T.C. Merkel, R.W. Baker, and B.D. Freeman. 50th Anniversary Perspective: Polymers and Mixed Matrix Membranes for Gas and Vapor Separation: A Review and Prospective Opportunities. Macromolecules, 50 (2017) 7809.

Appendix. 1

Appendix 1. Gas permeabilities and selectivities of polyimide and TR-polyimide membranes.

Polyimide Name	$\alpha(CO_2/CH_4)$	$\alpha(N_2/CH_4)$	$\alpha(CO_2/N_2)$	Ref.
t-PBO-1-6FDA-BisAPAF	55.4	25.9	2.1	[1]
t-PBO-2-6FDA-BisAPAF	27.8	14.8	1.9	[2]
t-PBO-3-6FDA-BisAPAF	44.2	23.1	1.9	[3]
t-PBO-2-BPDA-BisAPAF	39.8	29.9	1.3	[4]
t-PBO-3-ODPA-BisAPAF	73	31.7	2.3	[1]
t-PBO-4-BTDA-BisAPAF	46.9	31.3	1.5	[1]
t-PBO-5-PMDA-BisAPAF	41.4	28	1.5	[1]
a-PBO-1(1)-6FDA-BisAPAF	33.2	20.9	1.6	[2]
a-PBO-1(2)-6FDA-BisAPAF	46.6	21.5	4.3	[5]
aPBO-2-6FDA-BisAPAF	28.6	24.3	1.2	[6]
aPBO-3(1)-6FDA-pHAB	31.2	24	1.8	[7]
aPBO-3(2)-6FDA-mHAB	23.2	21.2	1.1	[7]
aPBO-3(3)-6FDA-HAB	36.9	26.8	1.4	[5]
aPBO-4-ODPA-BisAPAF	9	12.6	0.7	[8]
aPBO-5-BPDA-BisAPAF	24.7	21.1	1.2	[9]
cPBO-1-6FDA-BisAPAF	22.1	12.9	1.7	[2]
cPBO-2-6FDA-HAB	22.5	16.2	1.4	[10]
cPBO-cardo-1-6FDA-95%HAB-5%BisAPAF	25.9	18.9	1.4	[11]
cPBO-cardo-2-6FDA-90%HAB-10%BisAPAF	23.7	18.4	1.3	[11]
cPBO-cardo-3-6FDA-85%HAB-15%BisAPAF	22.2	18.8	1.2	[11]
cPBO-cardo-4-6FDA-70%HAB-30%BisAPAF	20.5	18.2	1.1	[11]
cPBO-cardo-5-6FDA-50%HAB-50%BisAPAF	21.2	19	1.1	[11]
sPBO-1-6FDA-BisAPAF	22.7	16.9	1.3	[2]
sPBO-2-6FDA-HAB	31.2	24	1.3	[12]
sPBO-3-6FDA-HAB-ACETIC ANHYDRIDE	30.1	22.6	1.3	[12]
sPBO-4-6FDA-DMAB	30	1.3	23.5	[12]
sPBO-5-6FDA-DAP-CL-MPD	37	1.9	20	[13]
sPBO-6-6FDA-DAP-CL-MPD	39.8	1.8	21.6	[13]
EA-PBO-1-6FDA-HAB	38.7	1.8	21.5	[14]
EA-PBO-2-ODPA-BisAPAF	33.3	1.3	24.1	[14]
EA-PBO-Ac-1-6FDA-HAB	34.1	2.6	12.9	[14]
EA-PBO-Ac-2-6FDA-BisAPAF	17.3	0.8	22.9	[15]
EA-PBO-Ac-3-BTDA-BisAPAF	38.2	1.8	21.1	[15]
EA-PBO-Ac-4-ODPA-BisAPAF	35	1.3	26.2	[15]
EA-PBO-PAc-6FDA-HAB	18.5	-	-	[16]
TR-PBI-1-6FDA-DAB	46.4	1.8	26.2	[17]
CTR-1-6FDA-HAB-Allyl	49.6	1.9	26.1	[18]
PBOI-1(1)-10%6FDA-5%BisAPAF-5%DAM	16.1	1.4	11.5	[19]
PBOI-1(2)-10%6FDA-5%BisAPAF-5%DAM	32.5	1.5	21.4	[5]
PBOI-2-10%6FDA-5%BisAPAF-5%DAM	13.3	0.6	12	[19]
PBOI-3(1)-10%6FDA-5%BisAPAF-5%DAM	27.6	1.3	21.1	[19]
PBOI-3(2)-10%6FDA-5%BisAPAF-5%DAM	32.5	1.3	24.7	[5]
PBOI-4-10%6FDA-5%BisAPAF-5%DAM	23.3	1.4	17.2	[19]
PBOI-5-10%6FDA-8%BisAPAF-2%DAM	43.9	1.6	27.3	[8]
PBOI-6-10%6FDA-8%BisAPAF-2%DAM	48.6	1.6	28.6	[8]

PBOI-7-10%6FDA-8%BisAPAF-2%DAM	41	1.5	26	[8]
TR-**α**-PBOI-8-10%ODPA-8%BisAPAF-2%DAM	54.7	1.98	29.7	[8]
TR-**α**-PBOI-9-10%ODPA-8%BisAPAF-2%OT	52.5	1.90	29.5	[8]
TR-**α**-PBOI-10-10%ODPA-8%BisAPAF-2%BAP	54.1	1.95	30.5	[8]
TR-**α**-PBOI-11-10%ODPA-8%BisAPAF-2%TPE-R	59	2.10	29.5	[8]
TR-**α**-PBOI-12-10%ODPA-8%BisAPAF-2%BAPP	45.9	1.55	30.3	[8]
TR-**α**-PBOI-13-10%ODPA6FDA-8%BisAPAF-2%DAM	36	1.67	21.6	[5]
TR-**α**-PBOI-14-10%6FDA-2%BisAPAF-8%DAM	31.2	1.49	20.9	[5]
TR-**α**-PBOI-15-10%6FDA-8%BisAPAF-2%ODA	46.3	1.92	23.8	[5]
TR-**α**-PBOI-16-10%6FDA-5%BisAPAF-5%ODA	49.6	1.80	26.4	[5]
TR-**α**-PBOI-17-10%6FDA-2%BisAPAF-8%ODA	52.7	1.93	28.5	[5]
TR-**α**-PBOI-18-10%6FDA-8%HAB-2%DAM	35.1	1.39	25.3	[5]
TR-**α**-PBOI-19-10%6FDA-2%HAB-8%DAM	28.3	1.29	21.9	[5]
TR-**α**-PBOI-20-10%6FDA-8%HAB-2%ODA	41.1	1.57	26.6	[5]
TR-**α**-PBOI-21-10%6FDA-5%HAB-5%ODA	46.8	1.63	29.1	[5]
TR-**α**-PBOI-22-10%6FDA-2%HAB-8%ODA	51.4	1.67	29.3	[5]
TR-**α**-PBOI-23-10%BPDA-8%BisAPAF-2%ODA	27.8	1.29	21.6	[9]
TR-**α**-PBOI-24-10%BPDA-8%BisAPAF-5%ODA	38.5	1.17	30.5	[9]
TR-**α**-PBOI-25-10%BPDA-2%BisAPAF-8%ODA	36.7	1.33	27.5	[9]
TR-**α**-PBOI-26-100%BPDA-95%BisAPAF-5%ODA	27.5	1.62	17	[20]
XTR-PBOI-1-100%6FDA-95%BisAPAF-5%DABA	34.4	1.54	22.3	[20]
XTR-PBOI-2-100%6FDA-90%BisAPAF-10%DABA	37.8	1.55	24.3	[20]
XTR-PBOI-3-100%6FDA-85%BisAPAF-15%DABA	33.1	1.48	22.4	[20]
XTR-PBOI-4-100%6FDA-80%BisAPAF-20%DABA	34.1	1.57	21.7	[20]
XTR-PBOI-5-100%6FDA-75%BisAPAF-25%DABA	28.8	0.90	20.2	[20]
XTR-PBOI-6-100%6FDA-95%BisAPAF-(5%DABA+diol)	37.5	1.49	25.2	[21]
XTR-PBOI-7-100%6FDA-90%BisAPAF-(10%DABA+diol)	29.7	1.54	19.3	[21]
XTR-PBOI-8-100%6FDA-85%BisAPAF-(15%DABA+diol)	34.4	1.54	22.4	[21]
XTR-PBOI-9-100%6FDA-80%BisAPAF-(20%DABA+diol)	35.5	1.59	22.3	[21]
TR-**α**-PBO-co-PPL-1-10%6FDA-8%BisAPAF-2%DBZ	37.5	1.88	19.9	[22]
TR-**α**-PBO-co-PPL-2-10%6FDA-5%BisAPAF-5%DBZ	39.2	1.85	21.2	[22]
TR-**α**-PBO-co-PPL-3-10%6FDA-2%BisAPAF-8%DBZ	78.4	2.68	29.2	[22]
TR-**β**-PBO-1-BPDC-BisAPAF	18.4	1.05	17.6	[23]
TR-**β**-PBO-2-IPCI-BisAPAF	44	0.80	55	[24]
TR-**β**-PBO-3-TPCI-BisAPAF	37.9	1.68	22.5	[24]

TR-**β**-PBO-4-6FCl-BisAPAF	29.3	3.71	7.9	[24]
TR-**α,β**-PBO-1-TAC-BisAPAF	26.2	1.36	19.2	[25]
TR-**β**-PBOA-1-10%IPCl-8%HBA-2%ODA	37.6	1.32	26.7	[26]
TR-**β**-PBOA-2-10%IPCl-2%HBA-8%ODA	52.3	3.13	17.2	[26]
PIM-TR-PBO-1-6FDA-Spiro-bis-indane	19.9	0.88	22.5	[27]
PIM-TR-PBO-2-PMDA-Spiro-bis-indane	17.5	0.73	23.9	[27]
PIM-TR-PBO-3-BPDA-Spiro-bis-indane	15.3	0.91	16.7	[27]
PIM-TR-PBO-4-BPADA-Spiro-bis-indane	16.6	0.90	19.6	[27]
TR-**α**CD-6FDA	21.7	1.08	19	[28]
TR-**β**CD-1-6FDA	17.3	1.13	15.3	[29]
TR-**β**CD-2-6FDA	22.2	1.19	18.7	[28]
TR-**γ**CD-6FDA	22.4	1.23	18.2	[28]
TR-glucose-1-6FDA	27	1.30	20.8	[30]
TR-glucose-2-6FDA	24.8	1.57	15.8	[30]
TR-sucrose-6FDA	27.2	1.59	17.1	[30]
TR-raffinose-6FDA	21.1	1.44	14.6	[30]
TR-1 (6FDA+bisAPAF)	55.41	2.14	25.9	[8]
TR-2 (BPDA+bisAPAF)	39.8	1.33	29.2	[5]
TR-3 (ODPA+bisAPAF)	73	2.3	31.7	[5]
TR-4 (BTDA+bisAPAF)	46.9	1.5	31.3	[5]
TR-5 (PMDA+bisAPAF)	41.4	1.5	28	[5]
TPBO (6FDA+bisAPAF)	27.8	1.9	14.8	[5]
APBO (6FDA+bisAPA)	33.2	1.6	21	[5]
CPBO (6FDA+bisAPA)	22.1	1.7	12.9	[5]
CPBO (6FDA+bisAPA)	22.7	1.3	16.8	[5]
TR400 (6FDA+HAB-EA)	36.4	-	-	[5]
TR400 (6FDA+HAB-Ac)	34.1	-	-	[5]
TR400 (6FDA+HAB-Pac)	18.5	-	-	[9]
TR450 (6FDA+HAB)	22.5	1.4	16.2	[9]
6FDA+APAF	17.3	1.3	12.9	[9]
BTDA+APAF	38.2	1.7	22.9	[20]
ODPA+APAF	35	1.7	21.1	[20]
PBO (6FDA+HAB)	32.2	1.5	20.8	[20]
CPBOC (6FDA+HAB (95)+bisAHPF (5)	25.9	1.4	18.9	[20]
CPBOC (6FDA+HAB (90)+bisAHPF (10)	23.7	1.3	18.3	[20]
CPBOC (6FDA+HAB (85)+bisAHPF (15)	22.2	1.2	18.8	[20]
CPBO (6FDA+bisAHAP(cardo))	27.7	1.3	21.6	[21]
PHAB-6FDA (6FDA+HAB PI)	62.5	2.2	28.5	[21]
PTR450 (6FDA+HAB PBO)	31.2	1.3	24	[21]
MHAB-6FDA (6FDA+mHAB PI)	66.7	2.3	29.2	[21]
MTR450 (6FDA+mHAB PI)	23.2	1.1	21.1	[22]
TR-PBO (6FDA+BISAPAF)	34.8	1.7	20.7	[22]
XTR-PBO-5 (6FDA+bisAPAF+DABA(5))	37.5	1.5	25.2	[22]
XTR-PBO-10 (6FDA+bisAPAF+DABA(10))	29.7	1.5	19.3	[23]
XTR-PBO-15 (6FDA+bisAPAF+DABA(15))	34.4	1.5	22.4	[24]
XTR-PBO-20 (6FDA+bisAPAF+DABA(20))	25.5	1.6	22.3	[30]
450-1 (6FDA+6FBAHPP)	5.3	29	0.98	[29]
450-3 (6FDA+6FBAHPP)	4.4	29	0.99	[38]
PBI (6FDA+DAB)	5.4	46	1	[3]

References

[1] Y. Kobayashi, W. Zheng, E. F. Meyer, J. McGervey, A. Jamieson and R. Simha., Macromolecules, 1989, 22, 2302.

[2] C. W. Frank, V. Rao, M. M. Despotopoulou, R. F. W. Pease, W. D. Hinsberg, R. D. Miller and J. F. Rabolt, Science, 1996, 273, 912.

[3] S. D. Kelman, B. W. Rowe, C. W. Bielawski, S. J. Pas, A. J. Hill, D. R. Paul and B.D. Freeman, J. Membr. Sci., 2008, 320, 123.

[4] A. J. Hill, K. J. Heater and C. M. Agrawal, J. Polym. Sci. Part B: Polym. Phys., 1990, 28, 387.

[5] D. Cangialosi, H. Schut, A. van Veen and S. J. Picken, Macromolecules, 2003, 36, 142.

[6] M. E. Rezac, P. H. Pfromm, L. M. Costello and W. J. Koros, Ind. Eng. Chem. Res., 1993, 32, 1921.

[7] J. H. Kim, W. J. Koros and D. R. Paul, Polymer, 2006, 47, 3104.

[8] P. H. Pfromm and W. J. Koros, Polym. Mater. Sci. Eng., 1994, 71, 401.

[9] P. H. Pfromm and W. J. Koros, Polymer, 1995, 36, 2379.

[10] H. A. Lorentz, The Theory of Electrons, Dover Publications, Inc., New York, 1952.

[11] Y. Huang and D. R. Paul, Macromolecules, 2006, 39, 1554.

[12] R. Suzuki et al., Jpn. J. Appl. Phys., Part 2, 1991, 30, L532.

[13] D. J. Enscore, H. B. Hopfenberg, V. T. Stannett and A. R. Berens, Polymer, 1977, 18, 1105.

[14] S. D. Kelman, S. Matteucci, C. W. Bielawski and B. D. Freeman, Polymer, 2007, 48, 6881.

[15] L. Baayens and S. L. Rosen, J. Appl. Polym. Sci., 1972, 16, 663.

[16] S. J. Tao, J. Chem Phys., 1972, 56, 5499.

[17] A. R. Berens and I. M. Hodge, Macromolecules, 1982, 15, 756.

[18] C. A. Scholes, G. Q. Chen, G. W. Stevens and S. E. Kentish, J. Membr. Sci., 2010, 346, 208.

[19] A. J. Kovacs and J. M. Hutchinson, J. Polym. Sci. Polym. Phys. Ed., 1979, 17, 2031.

[20] C. M. Agrawal, K. J. Heater and A. J. Hill, J. Mater. Sci. Lett., 1989, V8, 1414.

[21] Y. Huang, X. Wang and D. R. Paul, J. Membr. Sci., 2006, 277, 219.

[22] Y. Huang and D. R. Paul, Polymer, 2004, 45, 8377.

[23] K. Nagai, B. D. Freeman and A. J. Hill, J. Polym. Sci. Part B: Polym. Phys., 2000, 38, 1222.

[24] C. J. Ellison and J. M. Torkelson, Nat. Mater., 2003, 2, 695.

[25] A. H. Chan and D. R. Paul, J. Appl. Polym. Sci., 1980, 25, 971.

[26] D. W. V. Krevelen, Properties of Polymers, Elsevier, Amsterdam, 1990.

[27] S. M. Jordan, W. J. Koros and G. K. Fleming, J. Membr. Sci., 1987, 30, 191.

[28] J. M. S. Henis and M. K. Tripodi, Sep. Sci. Technol., 1980, 15, 1059.

[29] J. H. Kim, W. J. Koros and D. R. Paul, Polymer, 2006, 47, 3094.

[30[G. Reiter, G. Reiter, M. Hamieh, P. Damman, S. Sclavons, S. Gabriele, T. Vilmin and E. Raphae¨l, Nat. Mater., 2005, 4, 754.

CHAPTER 3: PHYSICOCHEMICAL AND THERMAL EFFECTS OF PENDANT GROUPS, SPATIAL LINKAGES AND BRIDGEING GROUPS ON THE FORMATION AND PROCESSING OF POLYIMIDES

3.1 Abstract

Aromatic polyimides are known for their remarkable thermal and chemical properties which are greatly influenced by their precursors. In this study, we report synthesis and characterization of four different aromatic polyimides. The four different dianhydrides (ODPA, BTDA, BPDA and PMDA) were reacted with a diamine (BisAPAF) via azeotropic imidization under same conditions. FTIR analysis confirmed the formation of aromatic polyimides and all but one polyimide (HPI-BPDA) were found to be completely soluble in common solvents. The obtained molecular weights were between 16,000-32,000 Da, glass transition temperatures were between 250-275°C, degradation temperatures were above 550°C and the *d*-spacing values were around 5Å. These properties are promising and can be beneficial for various applications such as thin films and membranes.

3.2 Introduction

Aromatic polyimides are well known for their good thermal stability, chemical resistance and outstanding mechanical properties [1]. These properties are mainly attributed to the strong intermolecular forces between the polymer chains such as the polar interactions, aromatic stacking and charge transfer complexation [1, 2]. Hence, aromatic polyimides are available in a variety of commercial forms and used in a wide range of demanding applications such as high performance fibers, films, thermosetting or thermoplastic resins, heat-resistant adhesives and coatings as well as foamed plastics [1, 2].

Aromatic polyimides are prepared from aromatic diamines via a two-step synthesis process: (1) poly(amic-acids) synthesis then (2) poly(amic-acids) to polyimides conversion.[1, 3] The poly(amic-acid) is mainly prepared by the condensation reaction of a diamine and a dianhydride in an appropriate solvent at relatively low temperatures because the reaction is exothermic. This step aims to prepare a *soluble* poly(amic acid) which is crucial because fully aromatic polyimides have low solubilities due to their high chain rigidity and strong interchain interactions, causing applicability limitations due to poor processability [4]. The poly(amic acid) is then converted into polyimide through the imidization reaction which could be performed via three routes: azeotropic (*Az*), thermal (*T*) or chemical (*Ch*) imidization [4-9]. It is worth mentioning that for the three aforementioned imidization routes, the sequence of adding the diamine first followed by the dianhydride is important due to the moisture sensitivity of the dianhydride [10, 11]. An undesired side reaction between the dianhydride and any trace amounts of moisture could, most likely, lead to incomplete imidization [10, 11]. Despite the imidization route chosen, the final synthesized polyimide must have identical chemical structures. Nevertheless, the route choice has an impact on the physical properties of the synthesized polyimides [10, 11]. Among the three imidization routes, the most commonly used imidization route seems to be the azeotropic imidization mainly due to its simplicity and the efficient dehydration of the water formed from the condensation reaction.

The aim of this study is to synthesize four different aromatic polyimides using four different dianhydride precursors and investigate the potential variation in their chemical and physical properties. One aromatic diamine (BisAPAF) is reacted with four aromatic dianhydride (ODPA, BPDA, BTDA and PMDA) via an azeotropic imidization route to form aromatic polyimides. These aromatic precursors were chosen based upon three primary factors:

type of pendant group, type of spatial linkages and type of bridging groups. These factors have a direct effect on several physiochemical and thermal properties of the polyimide.

Pendant groups are groups of molecules attached to the backbone chain of a polymer; they have a major impact on the mobility of the polymer chains [12-14]. For instance, a precursor with high rigidity, bulkiness or polarity mainly result in high packing efficiency which is attributed to the stiffness of the chains which restrict their rotational freedom [12-14]. Moreover, having a high packing efficiency results in elevated T_g [15, 16]. Furthermore, the introduction of bulky pendant side groups, or bridging groups, to a polymer backbone chain constrains crystallinity which causes the molecular weight of the polymer to increase [15]. Additionally, the inhibition of crystallinity could result in soluble polyimides [15].

Spatial linkage groups are those that link and space the pendant group. They, like the pendant groups, also play a role in determining the T_g [12, 17]. *Para*-substitutions usually have high T_g and thus high packing efficiency because this position inhibits chain mobility [12]. On the other hand, spatial linkages with *ortho*-positions are usually expected to be flexible because the chains tend to have more freedom resulting in low T_g. However, that is not the case with polyimides because spatial linkages with *ortho*-positions result in high T_g, which is substantially due to the strong dipolar attractions between the imide linkages and the diamine [12]. *Meta*-spatial linkages, like *para*-spatial linkages, also tend to have high packing efficiency due to the increased rigidity it imparts on the chains [18, 19] and consequently result in high T_g. It is worth mentioning that, beside the presence of spatial linkages, the number of benzene rings in the precursors have a significant effect on the T_g as well [12, 20].

Bridging groups have major influence on electrophilicity of the dianhydrides which is usually evaluated in terms of electron affinity (E_a) of the molecules [12]. In other words,

62

bridging groups govern the reactivity of the precursors which also impacts T_g. Among the four considered dianhydrides, PMDA has the highest E_a (1.90 eV) followed by BTDA (1.55 eV), BPDA (1.38 eV) and ODPA (1.30 eV) [21]. Moreover, the presence of any bridging groups in the dianhydrides have a strong impact on the glass transition because the bridging groups change the E_a which possibly promotes the formation of charge transfer complex [12]. Nonetheless, as the bridging group in the dianhydride becomes longer, the T_g becomes insensitive to E_a [12]. Generally, diamines with bridging groups that enhances crystallinity mainly causes the packing density to decrease which consequently reduces T_g [12, 22]. The properties of the precursors used in this study are summarized in Table. 9.

Table 9. Physical properties of used precursors [10].

Precursor	Rigid	Flexible	Bulky	Unbulky
BisAPAF	✓	-	✓	-
ODPA	-	✓	-	✓
BTDA	✓	-	-	✓
PMDA	✓	-	-	✓
BPDA	✓	-	-	✓

3.3 Experimental section

3.2.1 Materials

Diamine: 2,2-Bis(3-amino-4-hydroxyphenyl)-hexafluoro-propane (bisAPAF-98%) was purchased from Matrix Scientific (USA). Dianhydrides: 4,4'-oxydiphthalic anhydride (ODPA-97%), 3,3',4,4'- benzophenone tetracarboxylic dianhydride (BTDA-96%), 3,3',4,4'-biphenyl tetracarboxylic dianhydride (BPDA-97%), and benzene-1,2,4,5-tetracarboxylic dianhydride, also known as pyromellitic dianhydride (PMDA-97%) were purchased from Sigma Aldrich Co. LLC (USA). N-methyl-2-pyrrolidinone ReagentPlus (NMP-99%), o-xylene (>98%) reagent grade, diethylene glycol anhydrous (DEG-99.5%), dimethylformamide anhydrous (DMF-99.8%), methanol histological grade, acetone histological grade and tetrahydrofuran, HPLC grade

(THF->99.9%) were also purchased from Sigma Aldrich Co. LLC (USA). Mineral oil and anti-bumping granules were bought from Sigma Aldrich Co. LLC (USA). All diamines and dianhydrides were dried in a vacuum oven for 24 hours at 60°C temperature before use. All the glassware was dried for 24 hours in an oven at 80°C and then purged with Nitrogen for one hour before being used. All the reagents were used as received without further purification. The chemical structures of the used monomers are presented in Figure. 24.

Diamine

2,2-Bis(3-amino-4-hydroxyphenyl)-
hexafluoro-propane (bisAPAF)

Dianhydrides

4,4'-oxydiphthalic anhydride
(ODPA)

3,3',4,4'- benzophenone
tetracarboxylic dianhydride (BTDA)

3,3',4,4'-biphenyl tetracarboxylic
dianhydride (BPDA)

pyromellitic dianhydride
(PMDA)
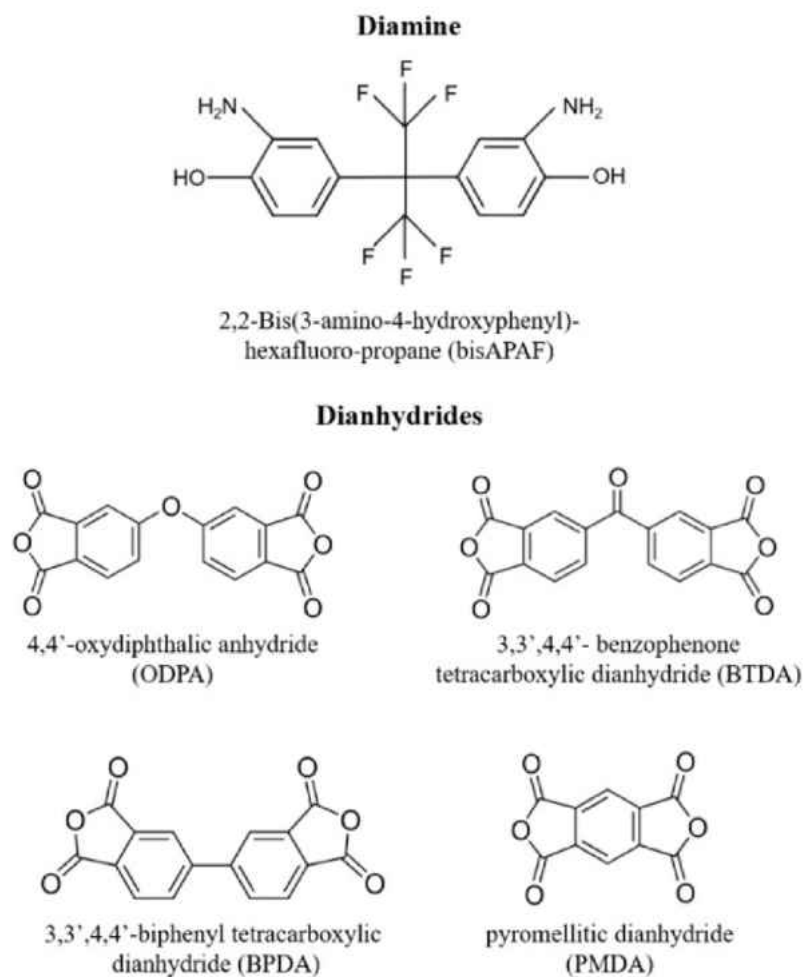
Figure 24. Chemical structures of the monomers used to synthesize the hydroxyl-polyimides (HPIs).

3.2.2 Polymer synthesis

3.2.2.1 Hydroxyl polyamic acid (HPAA) synthesis

The polymers were synthesized using an azeotropic imidization method previously describes by several articles [23, 24]. 10 mmol of APAF was inserted into a 500 ml round bottom flask which was purged with dry nitrogen for 1 hour prior to the reaction. The final monomer solution concentration is 20 wt%; hence, half of the total amount of the solvent (NMP) was added to the AFAP and was allowed to dissolve completely using a magnet stirrer for 1 hour under a nitrogen atmosphere. The diamine solution was then cooled to below 10°C in an ice bath. Next, 10 mmol of the dianhydride was gradually added in three batches each 2-3 minutes apart and then the remaining NMP was added for an overall 20 wt% monomer solution. The diamine and dianhydride were allowed to react below 10°C for 48 hours resulting in the formation of a viscous yellow HPAA solution. This procedure was repeated for each of the dianhydrides.

3.2.2.2 Hydroxyl polyimide (HPI) synthesis

In this stage, the water resulting from the condensation reaction was distilled off continuously under o-xylene reflux in the form of a water/o-xylene azeotropic mixture. First, an equivalent volumetric amount of o-xylene as NMP was added to the HPAA solution. Then, a couple of anti-bumping agent granules were added to the round-bottom flask to sooth the boiling of the solution. After that, a dean-stark trap with a circulated condenser was equipped on top of the round-bottom flask containing the HPAA solution and o-xylene. The solution was then placed in a 700 mL mineral oil bath which was heated to a temperature between 160-180°C for around 6 hours. This resulted in an orange to brown solution that was then cooled to room temperature. This solution was then precipitated in an 800 mL beaker filled with 3:1

water:methanol solution (600 mL and 200 mL respectively) that was cooled to around 13°C. A vortex was then created in the water:methanol solution using a stirrer and the orange to brown solution was slowly poured into the solution. This resulted in a precipitant that floated at the top of the beaker and was left for 12 hours at a temperature of around 13°C. Afterwards, the precipitant was filtered and soaked again in deionized water for another 12 hours. Finally, the precipitant was filtered using a vacuum filter and dried in a vacuum oven for 24 hours at around 70°C.

3.2.3 Characterizations

3.2.3.1 Solubility

About 100 mg of each HPI was put in contact with 3 mL of various solvents under continuous mixing for 48 hours, or until completely dissolved, at room temperature. Polymer solubility was determined to be either soluble, partially soluble, or insoluble. This was determined visually, where completely soluble polymers were completely dissolved before 48 hours, partial solubility refers to a noticeable dissolution, but undissolved polymer remaining after 48 hours, and insolubility refers to no visible dissolution after 48 hours. The solubility parameters were calculated according to EQs (15) to (18):

$$\delta_d = \frac{\sum F_{di}}{V} \qquad\qquad EQ. 15$$

$$\delta_p = \frac{\sqrt{\sum F_{pi}^2}}{V} \qquad\qquad EQ. 16$$

$$\delta_h = \sqrt{\frac{\sum E_{hi}}{V}} \qquad\qquad EQ. 17$$

$$\delta_t = \sqrt{\delta_d^2 + \delta_p^2 + \delta_h^2} \qquad\qquad EQ. 18$$

Where δ_d, δ_p, δ_h are the dispersive, polar, and hydrogen bonding solubility parameters respectively. F, E and V are polar attractive constant, cohesive energy and molar volume respectively. Also, δ_t is the total solubility parameter.

3.2.3.2 Fourier transform infrared spectroscopy (FTIR)

The chemical compositions of the HPIs were investigated using the Thermo Scientific NIcolet NEXUS 460 FTIR equipped with a ZnSe crystal and DTGS detector. The samples were tested in attenuated total reflection mode with a resolution of 2 cm^{-1} and 16 scans per sample.

3.2.3.3 Differential scanning calorimetry (DSC) & thermogravimetric analysis (TGA)

The glass transition temperatures (T_g) of the HPIs were initially investigated using PerkinElmer DSC. The DSC method consisted of three cycles each started at 25°C and ramped up to 300°C at a rate of 20°C.min^{-1} and the temperature was held for 2 minutes at 300°C. The obtained temperatures were then confirmed and corrected using TA Instruments SDT Q 600 TGA from room temperature to 900°C at a heating rate of 10°C.min^{-1} under nitrogen atmosphere with flow rates of 100 mL.min^{-1} using around 15 mg of HPI powder samples.

3.2.3.4 Gel permeation chromatography (GPC)

The molecular weight of the HPI powders were evaluated using a Varian Prostar GPC with a TSK^{TM} SuperMultipore HZ-M column and a refractive index detector in THF.

3.2.3.5 X-ray diffraction (XRD)

The XRD analysis was conducted using a diffractometer with Cn Ka radiation of λ = 1.5406 Å, voltage of 60 kV and current of 30 mA. The samples were scanned in 2θ from 5˚ to 40˚ at a rate 1˚.min^{-1}. The *d*-spacing values of the HPIs were calculated using the XRD patterns via Bragg's law [25]:

$$n\lambda = 2dsin\theta \qquad\qquad EQ.\ 19$$

Where *n* is the order of reflection (*n*=1), *λ* is the X-ray wavelength, *d* is the *d*-spacing and *θ* is the X-ray diffraction angle.

3.4 Results and discussion

3.4.1 Solubility

All the HPIs were found to be completely or partially soluble in the organic solvents tested as seen in Table. 10. Their solubility can be attributed to bulky hexafluoroisopropylidene monieties in the diamine monomer as well as the flexibility of the HPI chains [21]. The solubility is also a result of intermolecular interactions between the main chains of the HPIs and the solvents. Specifically, there are three intermolecular interactions present between the polymers and solvents, dispersion, polarity, and hydrogen bonding forces.

Table 10. Solubility of HPIs in common organic solvents: (+) represents complete solubility and (+/-) represents partial solubility.

Solubility in Organic Solvents

Solvent	ODPA	BPDA	BTDA	PMDA
NMP	+	+/-	+	+
DEG	+	+/-	+	+
DMF	+	+/-	+	+
MeOH	+	+/-	+	+
THF	+	+/-	+	+

To gain insight into the solubility and the level of interaction between HPIs and the solvents selected, the solubility parameters were calculated. The dispersive, polar, and hydrogen bonding solubility parameters were determined by the group contribution approach based on Krevelin [26]. The functional groups present in the HPIs, their frequency in the polymer monomers, and their energy contribution are recorded in Table. 11.

Table 11. Solubility parameter component group contributions from Hoftyzer-Van Krevelen method [26].

Material	Functional Group	Frequency	Components		
			F_{di} (MJ$^{1/2}$m$^{2/3}$mol^{-1})	F_{Pi} (MJ$^{1/2}$m$^{2/3}$mol^{-1})	E_{hi} (Jmol^{-1})
HPI-ODPA	⬡	4	1270	110	0
	Ring	2	190	0	0
	>N-	2	20	800	5000
	-C=O-	4	270	770	2000
	-O-	1	100	400	3000
	-OH	2	210	500	20000
	-F	6	220	0	0
	>C>	1	-70	0	0
HPI-BPDA	⬡	4	1270	110	0
	Ring	2	190	0	0
	>N-	2	20	800	5000
	-C=O-	4	270	770	2000
	-OH	2	210	500	20000
	-F	6	220	0	0
	>C>	1	-70	0	0
HPI-BTDA	⬡	4	1270	110	0
	Ring	2	190	0	0
	>N-	2	20	800	5000
	-C=O-	5	270	770	2000
	-OH	2	210	500	20000
	-F	6	220	0	0
	>C>	1	-70	0	0
HPI-PMDA	⬡	3	1270	110	0
	Ring	2	190	0	0
	>N-	2	20	800	5000
	-C=O-	4	270	770	2000
	-OH	2	210	500	20000
	-F	6	220	0	0
	>C>	1	-70	0	0

The dispersive, polar, and hydrogen bonding solubility parameters, molar attractive constant and cohesive energy used in the solubility calculations were taken from Table. 11, and the molar volumes were calculated by dividing the monomer molecular weight by the density. It is important to note that the molar volumes were determined to be 457.379, 445.950, 465.957, and 391.621 for HPI-ODPA, HPI-BPDA, HPI-BTDA, and HPI-PMDA, respectively. Table. 12 shows the calculated parameters for each HPI and solvents.

Table 12. Hoftyzer-Krevelen solubility parameters of HPIs and various solvents.

Name	δ_d (MPa$^{1/2}$)	δ_p (MPa$^{1/2}$)	δ_h (MPa$^{1/2}$)	δ_t (MPa$^{1/2}$)	Source
HPI-ODPA	18.256	8.003	11.549	23.037	This work
HPI-BPDA	18.500	8.159	11.404	23.214	This work
HPI-BTDA	18.285	9.250	11.348	23.424	This work
HPI-PMDA	17.823	9.262	12.170	23.485	This work
NMP	15.970	16.281	8.520	24.346	[25]
DEG	15.603	8.455	7.953	19.447	[25]
DMF	14.853	20.277	9.508	26.874	[25]
MeOH	15.2	12.3	22.3	29.7	[26]
THF	16.8	5.7	8.0	19.5	[26]

The solubility parameters for each HPI are similar to each other, and similar to experimentally determined, and calculated parameters for other polyimides [27-29]. Interestingly, due to the closeness of the total solubility parameters of each HPI with the solvents, all HPIs are expected to be soluble in each solvent investigated. However, HPI-BTDA was only partially soluble in all solvents, indicating intermolecular interactions were not completely responsible for solubility. The chain rigidity is the probable cause for the partial solubility of the HPI-BTDA as it has a rigid bridging group. Another potential explanation is the extent of cross-linking that takes place at 160-180°C while distilling the water formed during the reaction (prior to precipitation). As the degree of cross-linking increases due to the elevated temperatures, the solubility tends to decrease [30]. Moreover, considering that the

70

solubility parameters for each HPI are similar to each other, they would be viable options for polymer blends and would interact well in solution together. Due to the partial solubility of HPI-BPDA in THF, GPC analysis was not carried. Also, XRD analysis was not shown due to incompatibilities between the sample and sample preparation requirements.

3.4.2 FTIR analysis

The chemical structures and the completion of the imidization processes were revealed via the FTIR analysis. Figure.25 represents the IR spectra for HPI-ODPA, HPI-BTDA, HPI-PMDA and HPI- BPDA powders imidized azeotropically. The four dianhydride precursors have very similar structures which resulted in homopolymers with relatively similar structures in terms of characteristic vibrational bands [4]. Therefore, no significant differences between the HPIs were observed and only some minor differences in composition were detected. For all HPIs, an incomplete cyclization was evident due to the presence of amides at wavelengths of ~1515 cm^{-1} [4]. Moreover, all the HPIs have O-H stretching (~3400 to ~2400 cm^{-1}) and the C-F stretch (~1300 to ~1000 cm^{-1}) which are mainly attributed to the diamine. Additionally, the presence of the C-N stretch in all HPIs (~1518 cm^{-1}) indicate the presence of imide functional groups demonstrating that the polyimide is cured and the more abundant the C-N stretch is, the more fully cured the polyimide is. Also, the presence of C=O stretching (~1778 cm^{-1} and ~1714 cm^{-1}) could indicate the presence of anhydrides and ketones. For instance, in the case of HPI-BTDA, the C=O stretch most likely indicates the presence of ketones due to the presence of the clear aryl ketone in its structure. Whereas, the C=O stretch in the HPI-PMDA most likely indicates an anhydride functional group not a ketone again due to its structure that lacks of a clear ketone functional group. Finally, C-H stretch at <1000 cm^{-1} corresponds to aromatic functional groups such as benzene. Moreover, somewhere at ~714 cm^-

[1] usually corresponds to imide ring deformation. Therefore, the FTIR analysis indicates the formation of polyimides form the different dianhydride precursors and the similarity between the spectra is significant. The minor differences in the HPI-ODPA are mainly due to the presence of the ether functional group in its structure.
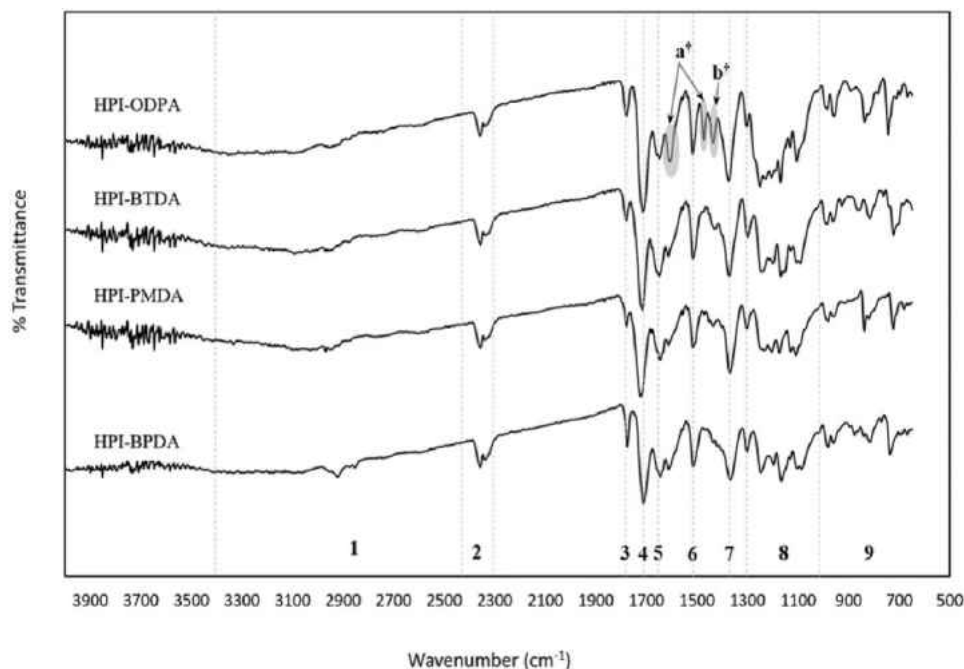
Figure 25. FTIR spectra of HPI-ODPA, HPI-BTDA, HPI-PMDA and HPI-BPDA.

Table 13. HPI-ODPA wavelengths and corresponding functional groups and molecular motion.

Peak	Wavelength (λ) [cm^{-1}]	Functional Group	Molecular Motion
1	3400-2400	Carboxylic Acids	OH Stretch
2	2352 & 2328	Hydroxyl Group	OH Stretch
3	1778	Anhydride	C=O Stretch
4	1714	Ketone	C=O Stretch
5	1645	Alkenes	C=C Stretch
6	1518	Amides	N-H Bend (1°)
7	1375	Alkenes	C-C In-Plane Bend
8	1300-1000	Halogenated Organic Molecules	C-F Bond
9	<1000	Aromatics (Benzene Rings)	C=C
a†	1608 & 1473	Aromatics	C=C Stretch
b†	1435	Carboxylic Acids	OH Stretch

3.4.3 Proton NMR analysis [1]

The ^{1}H NMR studies provided an in-depth analysis regarding the success of the imidization process as well as the final structures of the synthesized HPIs. Figures (26-28) represent ^{1}H NMR spectra for the HPI-ODPA, HPI-BTDA and HPI-PMDA. The structures of the HPIs were identified; however, there was a major overlap between some peaks between 2.7 to 4 ppm resulting in a broad peak which caused some uncertainties regarding the final structure of the HPIs. The peaks at 9.59 ppm, 9.67 ppm and 9.79 ppm in HPI-ODPA, HPI-BTDA and HPI-PMDA respectively could be assigned to the appearance of the –OH group indicating that the functionalization of the hydroxyl group was incomplete. The expected structures of the HPI have 14, 15 and 10 protons in HPI-ODPA, HPI-BTDA and HPI-PMDA respectively and all the protons were assigned to given peaks as shown in Figures (26-28). Nevertheless, those same peaks could also be assigned to aromatics protons of dianhydrides and diamines that typically appear at 8.6 to 7.3 ppm and 7.6 to 7.1 ppm respectively. If this is the case, it is an indication that the imidization process was incomplete.[18] Hence, ^{13}C NMR is needed in order to eliminate those possibilities.

---

[1] Please note that the ^{1}H NMR results and discussion were not included in the published virsion due to page limit where FTIR and NMR mainly provide similar information.
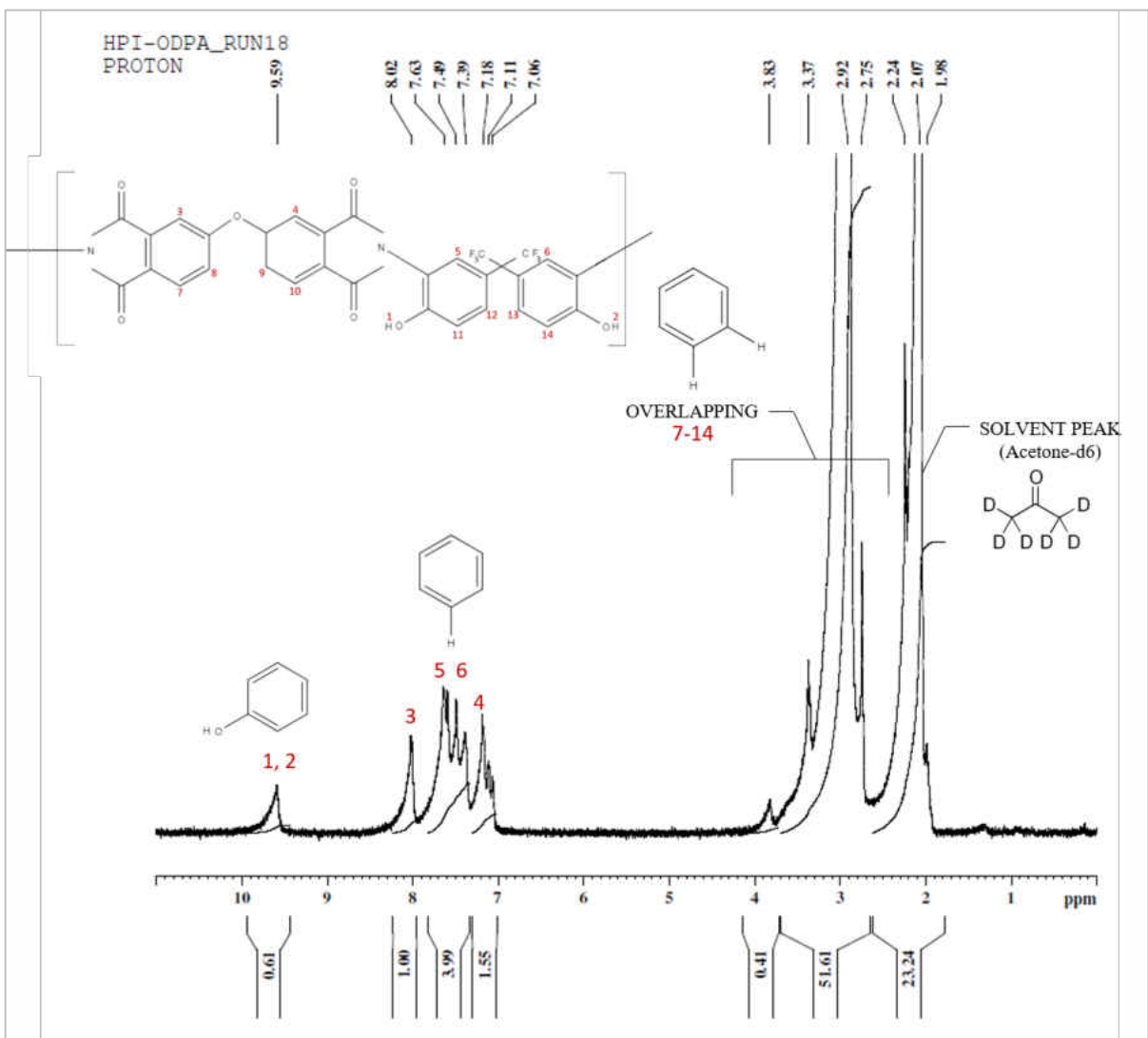
Figure 26. 1H NMP for HPI-ODPA.
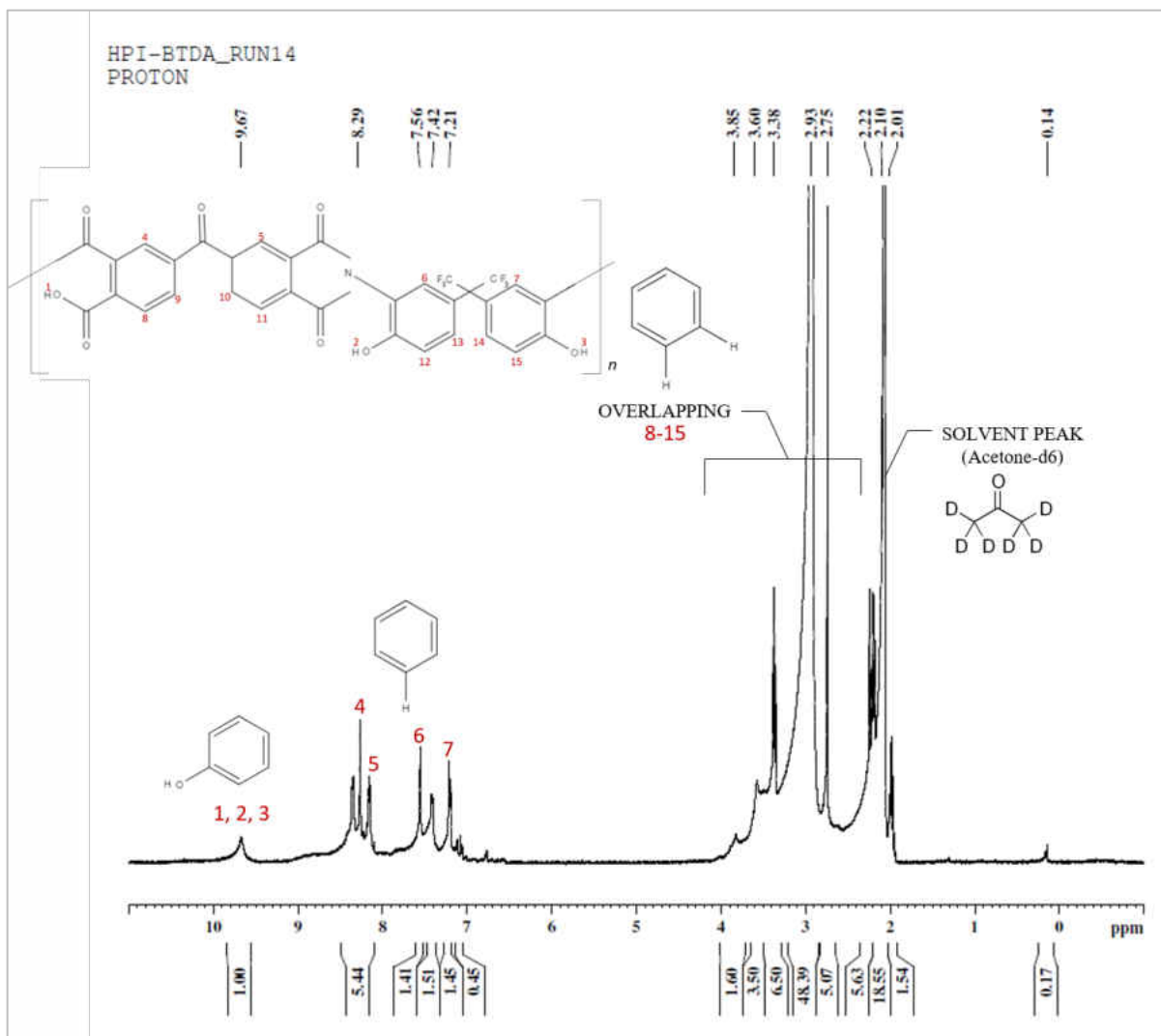
Figure 27. [1]H NMP for HPI-BTDA.
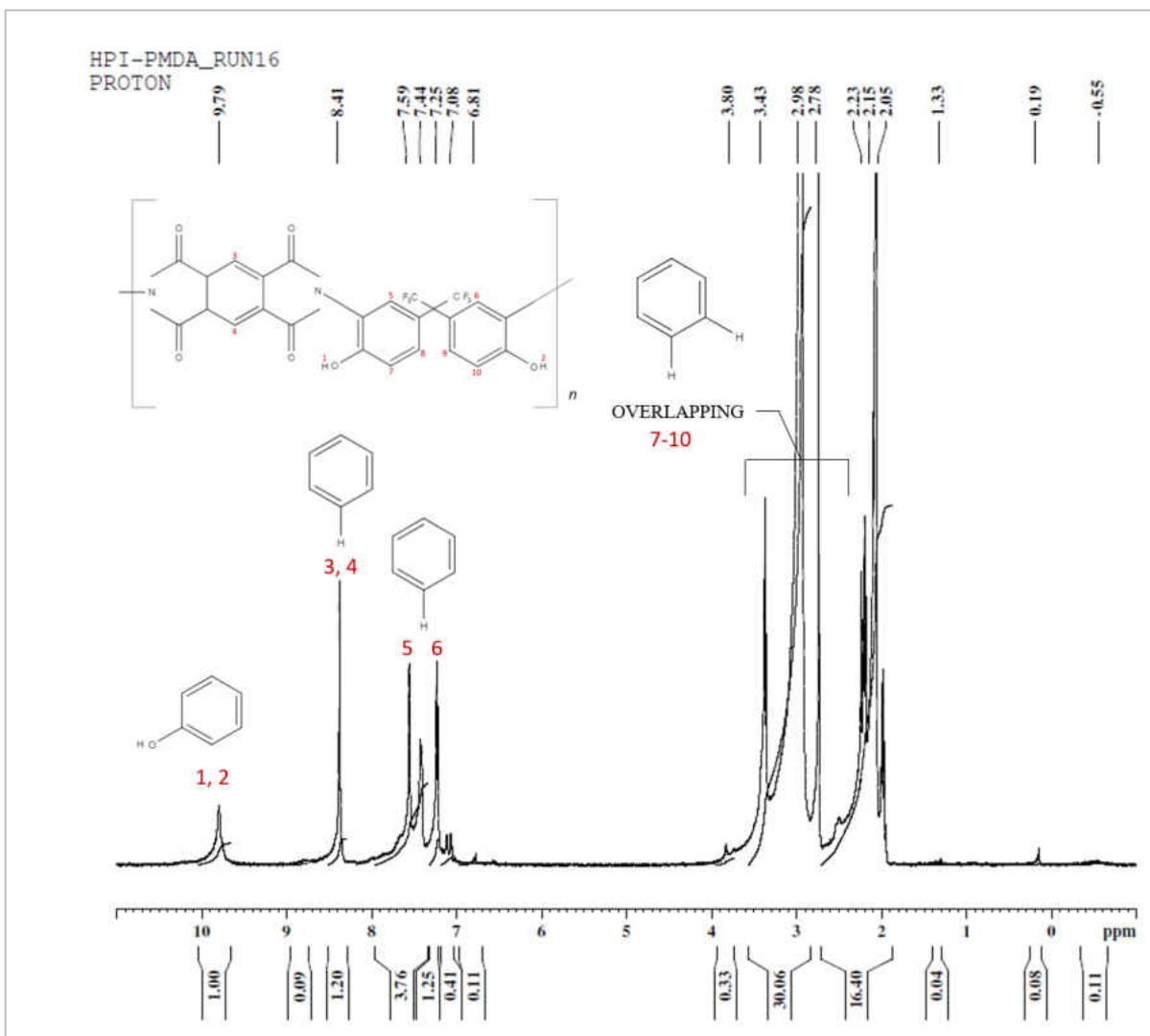
Figure 28. [1]H NMP for HPI-PMDA.

3.4.4 GPC, DSC, TGA & XRD analyses

The two main properties of a polymer that significantly affect their performance are molecular weight and glass transition temperature (T_g). For instance, in order for polymers to be used in gas separation membranes, they need to have medium to high molecular weights because higher molecular weights usually correspond to better mechanical properties [31]. The molecular weights of the HPI powders, displayed in Table. 15, are discussed in terms of M_w. Homopolymers, like the ones synthesized in this study, generally have low M_w of below 50,000 Da [23]. In this case, this is mainly attributed to the presence of several bulky 6 fluorine (6F)

groups that originate from the BisAPAF diamine. These bulky groups restrict the amine group and make it harder for the amine group to react with another dianhydride [25]. Moreover, it is clearly observed that the M_w of the HPI-ODPA is significantly lower than the others and that is attributed to the flexibility of dianhydride pendant groups. All in all, the obtained M_w are consistent with previously reported values [23, 31, 32].

The rigidity of the polymer chains, or flexibility, could be directly measured using T_g. This becomes crucial in the application of HPIs when they are fabricated into films or membranes, for example, because the rigidity or flexibility affects the thermal rearrangement kinetics and could consequently affect the gas permeabilities and selectivities [23]. The glass transition temperatures presented in Table. 14 are consistent with those in the literature since the average expected T_g of other polyimides is in the range of 230-330ºC [23, 33]. As mentioned earlier, precursors with rigid and bulky groups tend to result in high T_g. Hence, the high T_g could be attributed to the rigidity of the dianhydrides and the presence of several bulky 6F groups that originate from the BisAPAF diamine. Moreover, the synthesized polymers showed fairly high thermal stability where no weight loss was detected before a temperature of around 550˚C in nitrogen [34]. This could be observed from the degradation temperatures (T_d) in Table. 14.

Table 14. Properties of the HPI powders.

	GPC	GPC	GPC	DSC	TGA*	TGA	XRD
Polymer	Mn	Mw	PDI	T_g (˚C)	T_g (˚C)	T_d (˚C)	d-spacing (Å)
HPI-ODPA	10,124	16,281	1.6082	230	246	566	4.9734
HPI-BTDA	14,187	30,648	2.1603	226	266	561	5.1394
HPI-PMDA	20,369	32,243	1.5829	233	274	566	5.5764
HPI-BPDA	-	-	-	271	277	557	-

* Based on mass corrected heat flow due to moisture losses.

A broad and undefined peak was observed between 2θ values of 10° and 22° for HPI-ODPA, HPI-BTDA and HPI-PMDA indicating an amorphous structure. The 2θ values at the maximum peaks found from the XRD analysis are expected to be positioned somewhere in the centre with the *d*-spacing, or average interchain distance, of around 5 Å [35]. The 2θ values for HPI-ODPA, HPI-BTDA and HPI-PMDA were found to be 17.82°, 17.24° and 15.88° respectively. This corresponds to d-spacing values of 4.9734 Å, 5.1394 Å and 5.5764 Å respectively as shown in Table. 14. Among the three HPIs, HPI-PMDA was found to have the highest *d*-spacing which is a measure of the molecular distance between chains.

3.5 Conclusions

Four different dianhydride precursors (ODPA, BPDA, BTDA and PMDA) and a diamine (BisAPAF) were used to synthesize four different aromatic HPIs at a 1:1 dianhydride:diamine molar ratio via two-step method of hydroxyl poly(amic acid) and azeotropic imidization. Three dianhydrides (ODPA, BTDA and PMDA) out of the four were successfully synthesized into *soluble* HPIs. HPI-BPDA was not soluble potentially due to the occurrence of intensive crosslinking during the azeotropic imidization stage. The chemical and physical properties of the three soluble HPIs were investigated intensively. It was found that the chemical composition of the HPIs indicate the formation of polyimides with a likely incomplete cyclization due to the presence of amide functional groups. Moreover, the obtained molecular weights, glass transition temperatures, degradation temperatures and d-spacing values agree with other polyimides. Therefore, this detailed analysis provides sufficient characterization that would facilitate implementing these polyimides for various applications.

Acknowledgements

References

[1] Edward P. Savitski , Fuming Li , Sheng-Hsien Lin , Kevin W. McCreight , William Wu , Elaine Hsieh , Roland F. Rapold , Mark E. Leland , Donald M. McIntyre , Frank W. Harris , Stephen Z. D. Cheng , Simon Chi Man Kwan & Chi Wu. 1997. Investigation of the Solution Behavior of Organosoluble Aromatic Polyimides, International Journal of Polymer Analysis and Characterization, 4:2, 153-172.

[2] Migdalia Alvarado & Issifu I. Harruna. 2005. Characterization of HighPerformance Polyimides Containing the Bicyclo[2.2.2]oct-7-ene Ring System, International Journal of Polymer Analysis and Characterization, 10:1-2, 15-26.

[3] Sroog, C. E. 1976. Polyimides. J. POLYMER SCI. 11:161-208.

[4] Tena, A. Shishatskiy, S. Meis, D. Wind, J. Filiz, V and Abetz, V. 2017. Influence of the composition and imidization route on the chain packing and gas separation properties of fluorinated copolyimides. Macromolecules. 50: 5839-5849.

[5] Bessonov, M. I.; Zubkov, V. A. 1993. Polyamic Acids and Polyimides: Synthesis, Transformations, and Structure. New York: Taylor & Francis.

[6] Okamoto, K.-i.; Fuji, M.; Okamyo, S.; Suzuki, H.; Tanaka, K.; Kita, H. 1995. Gas permeation properties of poly(ether imide) segmented copolymers. Macromolecules. 28 (20), 6950−6956.

[7] Furusho, Y.; Ito, Y.; Kihara, N.; Osakada, K.; Suginome, M.; Takata, T.; Takeuchi, D. 2004. Polymer Synthesis Berlin: Springer.

[8] Tena, A.; Marcos-Fernandez, A.; Lozano, A.; de Abajo, J.; Palacio, L.; Pradanos, P.; Hernaˊndez, A. 2013. Influence of the PEO lengthˊ in gas separation properties of segregating aromatic−aliphatic copoly (ether-imide). Chem. Eng. Sci. 104, 574−585.

[9] Coletta, E.; Toney, M. F.; Frank, C. W. 2015. Influences of liquid electrolyte and polyimide identity on the structure and conductivity of polyimide−poly (ethylene glycol) materials. J. Appl. Polym. Sci. 132 (12), 41675.

[10] Drioli, E., Barbieri, G., and Brunetti, A. 2013. Membrane Engineering for the Treatment of Gases volume 1: Gas-Separation Issues with Membranes. 2nd ed., p.276. Croydon: CPI Group (UK) Ltd.

[11] Wen-ke, Y., Fang-fang, L., Guo-min, L., En-song, Z., Yan-hu, X., Zhi-xin, D., Xue-peng, Q., and Xiang-ling, J. 2016. Comparison of Different Methods for Determining the Imidization Degree of Polyimide Fibers. Chinese Journal of Polymer Science. 34(2): 209-220.

[12] REVIEW Varun Ratta, "POLYIMIDES: chemistry & structure-property relationships – literature review", chap. 1, Dissertation Thesis, 1999, Faculty of Virginia Polytechnic Institute and State University.

[13] Tanaka K, Osada Y, Kita H, Okamoto K. Gas permeability and permselectivity of polyimides with large aromatic rings. Journal of Polymer Science Part B: Polymer Physics. 1995. 33(13):1907-1915.

[14] Woock, T. 2016. "Effects of bridging group of dianhydride precursor on resulting thermally rearranged polybenzoxazole for removal of nitrogen from natural gas." Master's thesis, University of North Dakota.

[15] St. Clair, A.K. and St. Clair, T.L. 1987. Polymers for High technology, Ed. Bowden, M.J. and Turner, S.R., Amer. Chem. Soc. Symposium Series, 483.

[16] Wook. T., Bjorgaard, S. Tande, B., and Alshami, A. 2016. Purification of natural gas using thermally rearranged polybenzoxazole and polyimide membranes- A review: Part 1. Membrane Technology. 9: 7-12.

[17] Wook. T., Bjorgaard, S. Tande, B., and Alshami, A. 2016. Purification of natural gas using thermally rearranged polybenzoxazole and polyimide membranes- A review: Part 2. Membrane Technology. 10: 7-12.

[18] Tanaka K, Kita H, Okano M, Okamoto K. 1992. Permeability and permselectivity of gases in fluorinated and non-fluorinated polyimides. Polymer. 33(3):585-592. 140.

[19] Kawakami H, Anzai J, Nagaoka S. 1995. Gas transport properties of soluble aromatic polyimides with sulfone diamine moieties. J Appl Polym Sci. 57(7):789-795.

[20] Tamai, S., Yamaguchi, A. and Ohta, M.1996. Polymer. 37, 3683.

[21] Takekoshi, T., 1996. Polyimides- Fundamentals and Applications, ed. M.K Ghosh, and K.L. Mittal, Chapter 2. New York: Marcel Dekker.

[22] Lee, C.J. 1989. J. Macrmol. Sci.- Rev. Macromol. Chem. Phys. 29 (4), 431.

[23] Soo, C.Y, Jo, H.J, Lee, Y.M, Quay, J.R and Murphy, M.K. 2013. Effect of the chemical structure of various diamines on the gas separation of thermally rearranged poly(benzoxazole-co-imide) (TR-PBO-co-I) membranes. Journal of Membrane Science. pp. 444: 365-377.

[24] Han, S.H. Misdan, N. Kim, S. Doherty, C.M. Hill, A.J and Lee, Y.M. 2010. Thermally rearranged (TR) polybenzoxazole: Effects of diverse imidization routs on the physical properties and gas transport behaviours. Macromolecules. 43(18): 7657-7667.

[25] Adewole, J.K., Ahmad, A.L., Ismail, S., Leo, C.P., Sultan, A.S. 2015. Comparative studies on the effects of casting solvent on physico-chemical and gas transport properties of dense polysulfone membrane used for CO2/CH4 separation. J Appl Poly Sci. 132: 1-10

[26] Van Krevelen, D.W., and Te Nijenhuis, K. 2009. Properties of Polymers Their Correlation with Chemical Structure; Their Numberical Estimation and Prediction from Additive Group Contributions 4th edition. New York: Elsevier.

[27] Lee, H.R., and Lee, Y.D. 1990. Solubility behavior of an organic soluble polyimide. J of Apl Poly Sci. 40, 2087-2099

[28] Liu, Y. and Shi, B. 2008. Determination of Flory interaction parameters between polyimide and organic solvents by HSP theory and IGC. Polymer Bulletin, 61, 501-509

[29] Jwo, S.L., Whang, W.T., and Liaw, W.C. 1999. Effects of the solubility parameter of polyimides and the segment length of siloxane block on the morphology and properties of poly(imide siloxane). J of Appl Polyr Sci, 74, 2832-2847

[30] Kim, Y. J., Glass, T. E., Lyle, G. D., and McGrath, J. E. 1993. Kinetic and mechanistic investigations of the formation of polyimides under homogeneous conditions. Macromolecules. 26 (6), 1344-1358

[31] Gowariker, V.R. Viswanathan, N.V and Sreedhar. 1986. Polymer science. New Delhi: New Age International (P) Ltd.

[32] Grubb, T.L. Ulery, V.L. Smith, T.J. Tullos, G.L. Yagci, H. Mathias, L.J. and Langsam, M. 1999. Highly soluble polyimides from sterically hindered diamines. Polymer. 40: 4279-4288.

[33] Calle, M, Chan, Y. Jo, H.J. and Lee, Y.M. 2012. The relationship between the chemical structure and thermal conversion temperatures of thermally rearranged (TR) polymers. Polymer. 48(7): 1313-1322.

[34] Chen, C.F., Qin, W.M., and Huang, X.A. 2008. Characterization and Thermal Degradation of Polyimides Derived from ODPA and Several Alicyclic-Containing Diamines. Polymer engineering and Science. 48: 1151-1156.

[35] Chung, T. S., Ren, J., Wang, R., Li, D., Liu, Y., Pramoda, K. P., Cao, C., and Loh, W. W. 2003. J. Membr. Sci, 214, 57.

CHAPTER 4: GAS SEPRATION USING POLYBENZOXAZOLE (PBO) MEMBRANES DERIVED FROM BISAPAF POLYIMIDES AND THE INFLUENCE OF DIANHYDRIDE PENDANT GROUPS

4.1 Abstract

Soluble aromatic polyimide membranes were synthesized via azeotropic imidization and fabricated into membranes using three different dianhydrides (PMDA, ODPA and BTDA) with the same diamine (BisAPAF). Those membranes were then characterized before and after thermal rearrangement (TR) in order to investigate the influence of the chosen precursors on the ideal selectivity properties. The molecular weights of the polyimides were found to be between 25,000 and 94,000 g/mol. Moreover, the glass transition temperatures varied between 250 ºC and 270 ºC, and the degradation temperatures were at an average of 550ºC. Furthermore, the gas separation performance of all membranes improved after TR especially APAF-BTDA polyimide which surpassed the 2008 Robeson upper bound while testing CO_2/CH_4, N_2/CH_4 and CO_2/N_2 gas pairs.

4.2 Introduction

Gas separation using polymeric membranes continue to be the object of intensive research in chemical and physical molecular separation processes. Membranes are considered a staple at industrial scales owing to their effectiveness stemming from their low cost, high efficiency and simple operation [1]. In general, polymers are one of the most commonly used class of materials in the fabrication of membranes for applications which range from water, vapor and gas separation to fuel cells and sensor [2-6]. Of particular interest to gaseous

separations are the aromatic, glassy, and relatively rigid polymers, such as polyimides. The extent of separation of polyimide membranes remains to be dependent upon the nature of the physical and chemical interactions of the gases with the material, and upon the membrane-formation characteristics [1].

Polyimides are classified as glassy polymers and are known as "a class of high-performance materials" due to their remarkable thermal, mechanical and chemical properties [7]. These outstanding properties are mainly attributed to the strong intermolecular forces, such as polar interactions, aromatic stacking and charge transfer complexation, between the polymer chains [7]. Polyimides can be either aliphatic or aromatic which is governed by the nature of the monomers used. Aliphatic polyimides are prepared from aliphatic diamines via a process known as melt fusion of salt where the reactants are initially reacted at around 110-138 ºC forming a low molecular weight product that is then heated for several hours at around 250-300 ºC; however, this method is limited to polyimides that have low melting points in order for them to stay molten under the polymerization conditions [8]. Aromatic polyimides, on the other hand, are prepared from aromatic diamines via a two-step synthesis process: (1) synthesis of poly(amic-acids) and (2) conversion of poly(amic-acids) to polyimides through an imidization reaction which can be performed via three different routes: azeotropic, thermal or chemical imidization [7-11]. Between the two types, aromatic polyimides generally have better gas selectivity properties and that is mainly because of the large differences in the mobility of the pendant groups which is attributed to the stiffness of the polymer chains [5,12].

One of the major issues associated with polyimide synthesis is low solubility. This is due to the stiffness, rigidity and the strong interchain interactions, which ultimately results in poor processability and, consequently, applicability limitations [7]. Some techniques suggested

to address this issue include introducing flexible linkages, bulky substituents and alicyclic or noncoplanar monomers resulting in the disruption of the chain linearity of the polymer where backbone rigidity, chain packing and charge transfer complex are minimized [7,13-18]. Despite the applicability limitations associated with polyimides, they are among few membrane materials that can operate at elevated temperatures above 300 ºC [2,12]. Such a property is rare among most glassy polymeric membranes which usually cannot be used at temperatures above 100 ºC because glassy polymers are usually in a non-equilibrium state both at room temperature as well as near and above their glass transition temperatures [2]. This causes the equilibrium process to shorten, which results in increasing the chain mobility and decreasing gas selectivity [2].

Aromatic polyimides containing ortho-positioned functional groups can undergo thermal rearrangement (TR) to form polybenzoxazole (PBO), which is known for having a rigid rod-like structure with high-torsional energy barriers to rotational energy between two individual phenylene-heterocyclic rings [2,13]. Such a feature is crucial when considering gas separation applications because it could lead to large differences in the mobility of the pendant groups depending on their size and, hence, result in higher selectivities [2]. Moreover, PBOs have very high thermal and chemical stability, making them suitable for potential separation applications under harsh conditions such as the purification of hydrogen from steam reforming or the separation of carbon dioxide from flue gases [2]. Thermally rearranged aromatic polyimides can also reduce the permeability/selectivity tradeoff [19,20]. During TR, the fractional free volume (FFV) distribution of membranes made from aromatic polyimides is changed, forming large cavities that are separated by narrow necks and resulting in higher permeabilities [21]. Moreover, TR increases the rigidity of the polymer chains where the rigid-

rod benzoxazole structure is responsible for slightly increasing and mostly maintaining a relatively unchanged selectivity [22]. Hence, polyimide membranes which undergo TR witness a significant increase in permeability of gases while maintaining their selectivities.

This work concerns, first, the synthesis and characterization of three aromatic polyimides and, second, the fabrication, characterization and evaluation of the fabricated polyimides membranes. Synthesis and characterization of the polyimides were accomplished to compare their physiochemical and separation properties based on their structure. One diamine (BisAPAF) and three different dianhydrides (PMDA, ODPA and BTDA) were used to synthesize the polyimides via azeotropic imidization. These aromatic precursors were selected based on the type of pendant groups, spatial linkages and bridging groups that they have, which affects the way they react and, thus, will vary their gas separation properties. Testing the fabricating membranes was conducted to assess their gas separation performance before and after TR in order to investigate the change in properties due to the thermal treatment.
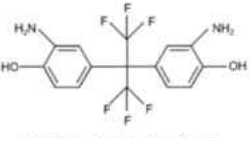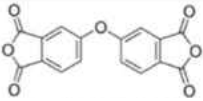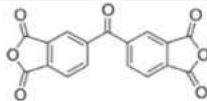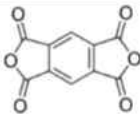
4.3 Experimental Section

4.3.1 Materials

The diamine: 2,2-Bis(3-amino-4-hydroxyphenyl)-hexafluoro-propane (APAF-98%) was purchased from Matrix Scientific (USA). The dianhydrides: 4,4'-oxydiphthalic anhydride (ODPA-97%), 3,3',4,4'- benzophenone tetracarboxylic dianhydride (BTDA-96%) and benzene-1,2,4,5-tetracarboxylic dianhydride, also known as pyromellitic dianhydride (PMDA-97%), were purchased from Sigma Aldrich Co. LLC (USA). The solvents used include N-methyl-2-pyrrolidinone ReagentPlus (NMP-99%), o-xylene (>98%) reagent grade, dimethylformamide anhydrous (DMF-99.8%), methanol histological grade and tetrahydrofurane HPLC grade (THF->99.9%), were also purchased from Sigma Aldrich Co.

LLC (USA). Mineral oil, anti-bumping granules, drying agent calcium hydride (powder, 99.99% trace metals basis) and molecular sieves 4Å (beads, 8-12 mesh) were bought from Sigma Aldrich Co. LLC (USA). Chemical structures and the physical properties of the used monomers are presented in Table. 15.

Table 15. Chemical structures and physical properties of the monomers used to synthesize the hydroxyl-polyimides (HPIs) [11,23].

	APAF	ODPA	BTDA	PMDA
Precoursors				
Properties	Rigid	Flexible	Rigid	Rigid
	Bulky	Unbulky	Unbulky	Unbulky

4.3.2 Materials Preparation

The diamine and dianhydrides were dried in an oven for 24 hours at 100°C and 180°C, respectively, and were used as received without further purification. All the glassware used was dried for 24 hours in an oven at 105°C, purged with nitrogen and used in a controlled atmospheric chamber. The NMP solvent was dried using calcium hydride via a distillation setup (Figure. 29) for 24 hours, where it was under vacuum first and then under inert nitrogen in order to remove as much latent water in the solvent as possible. The dried NMP was then stored over activated 4Å molecular sieves. Drying the solvent and the precursors is crucial because the dianhydrides are extremely sensitive to moisture, otherwise an undesirable side reaction of the dianhydride and moisture tends to take place and results in incomplete polymerization reactions.

Number	Label
1	Hot/ Stirring Plate
2	Mineral Oil Bath
3	Drying Agent (CaH$_2$)
4	Solvent (NMP)
5	Thermometer
6	Condenser
7	Dried Solvent
8	Molecular Sieves
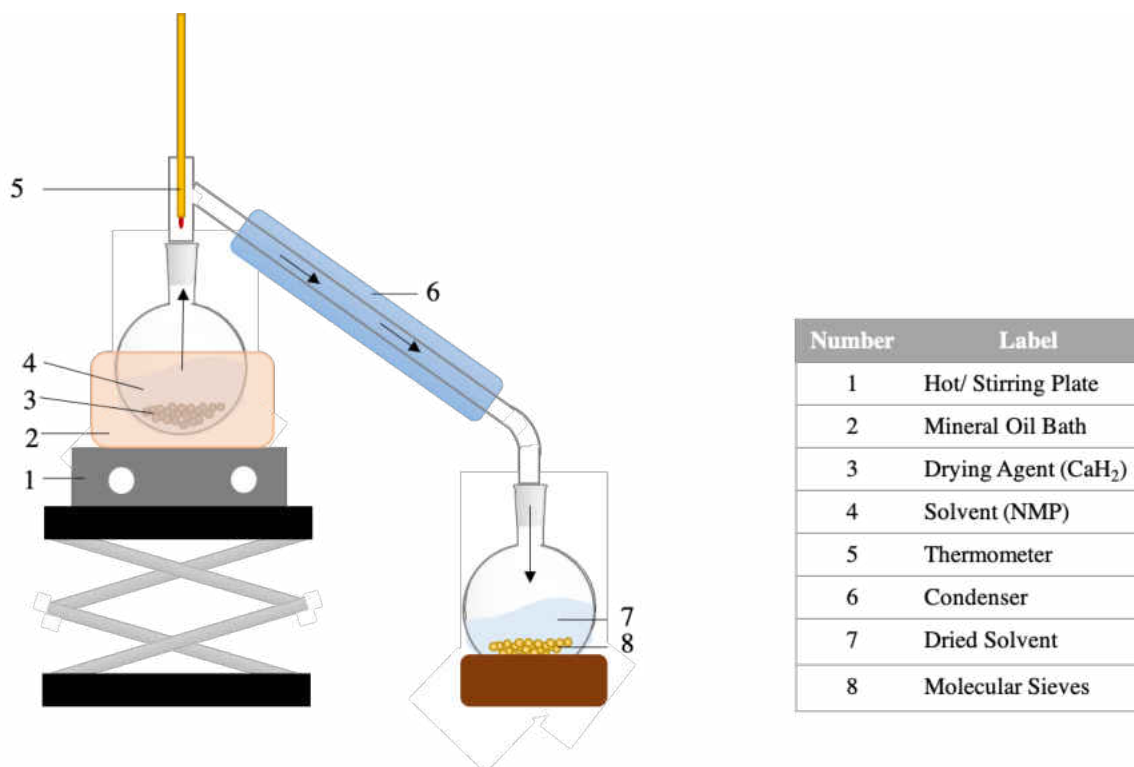
Figure 29. Solvent distillation setup.

4.4 Polymer Synthesis

4.4.1 Hydroxyl polyamicacid (HPAA) synthesis

The most commonly used method for processing polyimides is via soluble polyamic acid precursors primarily because fully aromatic polyimides have high chain rigidity and strong interchain interactions. The polyamic acid is converted into polyimide through the imidization reaction which in this work was done via the azeotropic imidization method per previous work [7,11,24,25]. First, 10 mmol of BisAPAF diamine was allowed to dissolve for 1 hour in half the final amount of NMP needed, where the final monomer solution concentration is 20 wt%. This took place in a glove box in an inert atmosphere. Then, the flask was tightly sealed and the diamine solution was cooled to below 10°C. An equal ratio of dianhydride (10 mmol) was then incrementally added to the diamine solution in 3 intervals, 3 minutes apart. The remaining amount of NMP was then added to obtain the final 20 wt%

monomer solution. Finally, the diamine and dianhydride were allowed to react for 48 hours at a temperature of below 10°C which resulted in the formation of a yellow, viscous HPAA solution. The same procedure was repeated for each of the dianhydrides.

4.4.2 Hydroxyl polyimide (HPI) synthesis

The reaction of the diamine and dianhydride is a condensation polymerization reaction, which means that water is formed. To remove this excess water, a dean-stark extractor equipped with a condenser was used where a continuous distillation under o-xylene reflux in the form of a water/o-xylene azeotropic mixture took place. This was done by adding an equivalent amount of o-xylene as NMP to the HPAA solution together with some anti-bumping granules. The solution was then heated to a temperature between 160-180°C for around 4 hours inside a 700 mL mineral oil bath, resulting in an orange solution, and was allowed to cool slowly to room temperature. The literature mostly states that the distillation should be allowed to continue for around 6 hours [24,25]. However, it was observed that when distillation time exceeds 4 hours, the solution tended to turn dark brown and when precipitated it formed a highly insoluble polyimide. Reducing the distillation time to around 4 hours or less resulted in a flaky highly soluble polyimide powders.

The next step involves the precipitation of the solution which was done in an 800 mL beaker filled with a cooled solution (~13°C) of 3:1 ratio deionized water:methanol (600 mL and 200 mL, respectively). A stir bar was then used to create a vortex in the precipitation solution while the orange solution was added slowly, resulting in a floating precipitant. The floatation of the precipitant is a good sign of a porous, flaky powder. The precipitant was first allowed to soak for 12 hours at a temperature of around 13°C in the precipitation solution and then for another 12 hours in deionized water. Finally, the HPI precipitant was vacuum filtered,

rinsed with deionized water until it was odorless, and then dried in an oven at 120°C for 24 hours.

4.5 Membrane Formation & Thermal Rearrangement

The polyimide membranes were formed via the solvent evaporation method where the dried HPI powders were each dissolved in DMF at 30 wt% over 24 hours. Each viscous solution was then casted on Kapton support, and placed in an oven where it was slowly heated to 250°C at a rate of 1°C/ minute. The temperature was held for 1 hour at 60°C, 155°C and 250°C. Afterwards, the oven was allowed to cool to room temperature. The membranes were then peeled off the Kapton and free-standing polyimide membranes were formed. During this process, the additional solvent in the membrane evaporates due to the elevated temperatures. A muffle furnace was used to thermally rearrange the membranes where each membrane was sandwiched between two ceramic plates to prevent curling. Each membrane was heated to 300°C and then 400°C at a rate of 5°C/minute where the temperature was held for 1 hour and 2 hours, respectively. During this process, the polyimide was converted to polybenzoxazole (PBO) and the membrane changed color from yellow-orange to dark-orange-brown. The whole synthesis method is visually summarized in Figure. 30 and the resulted HPIs, polyimide membrane and TR polyimide (PBO) membranes are presented in Figure. 31.
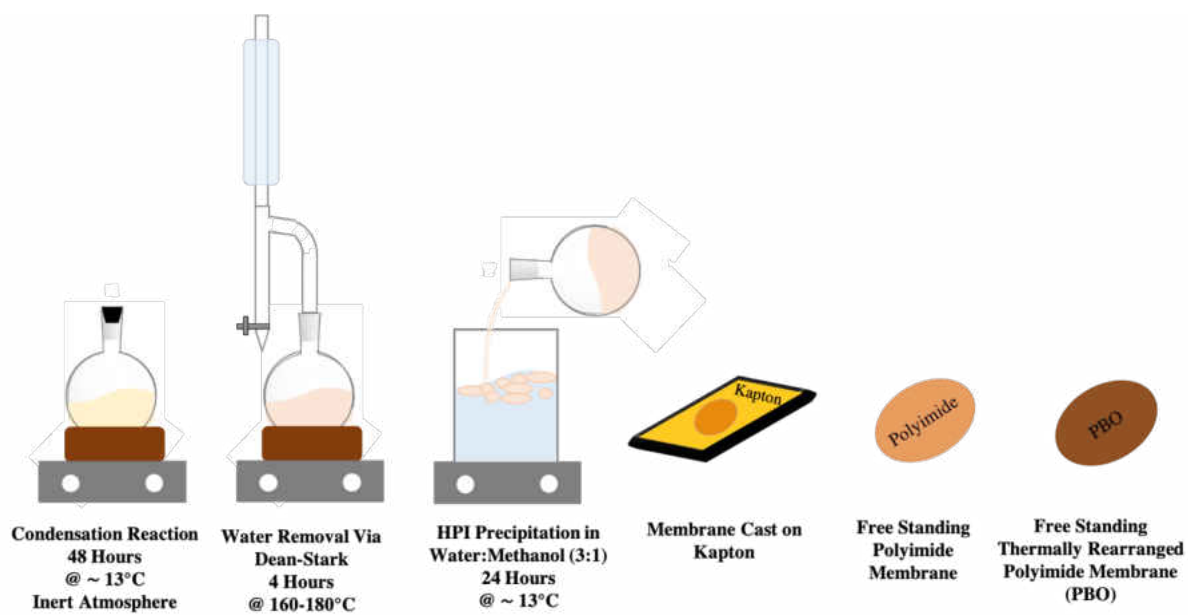
Figure 30. Polymer synthesis and membrane fabrication scheme.
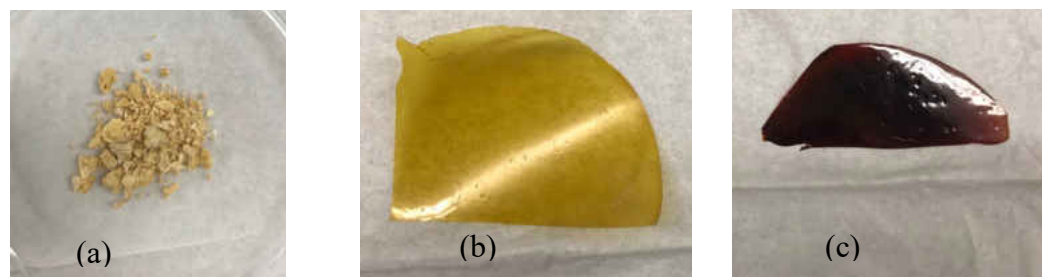
Figure 31. The obtained (a) HPI, (b) polyimide membrane and (c) PBO.

4.6 Characterization

Fourier transform infrared spectroscopy (FTIR) was used to examine the chemical composition of the HPI powders, polyimide membranes and the thermally rearranged membranes. A Thermo Scientific Nicolet NEXUS 460 FTIR equipped with a ZnSe crystal and DTGS detector was used in an attenuated total reflection mode with a resolution of 2 cm^{-1} and 16 scans per sample.

A Hitachi SU8010 field emission scanning electron microscope (FE-SEM) was used to investigate the morphology of the polyimide membranes before and after TR. The samples

90

were fractured to reveal a cross section and sputter coated for 30 seconds with carbon using an automated sputter coater.

An EcoSEC HLC-8320 GPC (Tosoh Bioscience, Japan) gel permeation chromatography (GPC) system with a differential refractometer (DRI) detector was used to determine the molecular weight of the polyimides. Separations were performed using two TSKgel SuperH3000 6.00 mm ID× 15 cm columns with an eluent flow rate of 0.35 ml min^{-1}. The columns and detectors were thermostated at 40 ºC, and the eluent used was tetrahydrofuran (THF). Samples were prepared at nominally 4 mg ml^{-1} in an aliquot of the eluent and allowed to dissolve at ambient temperature for several hours and the injection volume was 40µL for each sample. Calibration was conducted using PS standards (Agilent EasiVial PS-H 4ml).

A PerkinElmer differential scanning calorimeter (DSC) was used to investigate the glass transition temperature (T_g) of the HPIs and the membranes. The DSC method consisted of three cycles each starting at 25°C and ramping up to 400°C at a rate of 10°C/min. The samples were held isothermal for 2 minutes after ramping to ensure equilibrium.

A TA Instruments SDT Q 600 thermogravimetric analyzer (TGA) was used to determine the extent of thermal rearrangement of the membranes. The method used involved heating an 8 mg sample from 25°C to 900°C at a heating rate of 10°C/min under nitrogen atmosphere. Moreover, the analysis was used to find the degradation temperature (T_d) of the polyimide membranes.

A Rigaku SmartLab X-Ray Diffractometer (XRD) with Cu Kα radiation of $\lambda = 1.5406$ Å, current of 44 mA and voltage of 40 kV. The membranes were scanned in 2θ from 5° to 40° at a rate of 2°/minute. It was used to calculate the d-spacing of the membranes using the XRD patterns via Bragg's law EQ (20) [26]:

$$n\lambda = 2d sin\theta \qquad\qquad EQ. \; 20$$

Where n is the order of reflection ($n = 1$), λ is the X-ray wavelength, d is the d-spacing and θ is the X-ray diffraction angle.

4.7 Gas Permeation Measurements

The gas permeabilities of the membranes before and after thermal rearrangement were determined by a constant pressure, variable volume method where the permeate flow rate was measured using a bubble flow meter. The gas permeabilities were calculated using EQ (21) at steady-state conditions [26, 27]:

$$P = \frac{22,414}{A} \frac{l}{(p_2 - p_1)} \frac{p_1}{RT} \frac{dV}{dt} \qquad\qquad EQ. \; 21$$

where 22,414 is the number of cm^3 at standard temperature and pressure of penetrant per mole, A is the membrane area (cm^2), l is the membrane thickness (cm), p_1 & p_2 are permeate and feed pressures respectively, R is the universal gas constant (6236.56 $cm^3 cmHg/molK$), T is the absolute temperature (K) and $\frac{dV}{dt}$ is the the volume displacement rate of the soap-bubble in the bubble flow meter.

The gases tested were CH4, N2 and CO2 which have kinetic diameters of 0.380 nm, 0.364 nm and 0.330 nm respectively [2] and the setup used is shown in Figure. 32. The tested membranes were sealed with a Teflon washer that with an area of 2.27 cm^2, and the feed side was controlled with a pressure regulator form the gas cylinder while the permeate was left at atmospheric pressure. The setup was purged with the tested gas through the purge valve to ensure that there were no impurities. The setup was then pressurized to 50 psi and was maintained while the flow rate was measured using the bubble meter. The ideal selectivity of the membranes was then calculated using EQ (22): [26,27]

$$\propto_{i/j} = \frac{P_i}{P_j} \qquad\qquad EQ.\ 22$$

where $\propto_{i/j}$ is the selectivity of gas pair i/j and P_i and P_j are the permeabilities of gas species i and j respectively [26, 27].

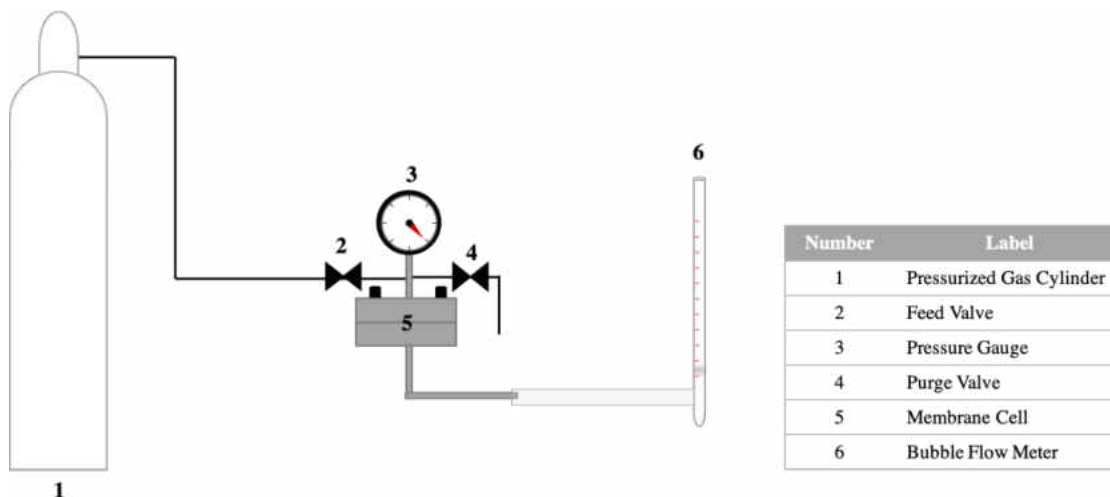| Number	Label
1	Pressurized Gas Cylinder
2	Feed Valve
3	Pressure Gauge
4	Purge Valve
5	Membrane Cell
6	Bubble Flow Meter

Figure 32. Sketch of the permeation test setup.

4.8 Results and Discussion

The FTIR was used to investigate the chemical compositions of the HPI powders as well as the synthesized membranes before and after TR. The chemical compositions of the HPI powders were identical to those powders obtained and reported in our previous work [11]; hence, they will not be discussed in this paper.

The FTIR spectrum of the APAF-BTDA membrane before TR is shown in Figure. 33 and all the membranes were thermally synthesized and treated to 250ºC and they have fairly similar composition. The most important peaks are labelled in the figure where a strong broad absorption band is observed at a wavenumber of around (a) 3200 and 3600 cm^{-1} and it corresponds to an OH-phenyl functional group which could be attributed to the diamine. Moreover, there is some indication that thermal imidization of the polyimide started taking place during the membrane synthesis which is evident by wavenumbers at around (b) 1788 cm^{-}

^{1} and (c) 1718 cm^{-1} which correspond to symmetric and asymmetric C=O stretching respectively. Actually, the chemical composition of the HPI powders discussed in our pervious paper [11] , shows the presence of peaks (b) and (c) indicating that the thermal treatment of the polyimide seems to have started earlier during the azeotropic distillation of the HPAA solution.
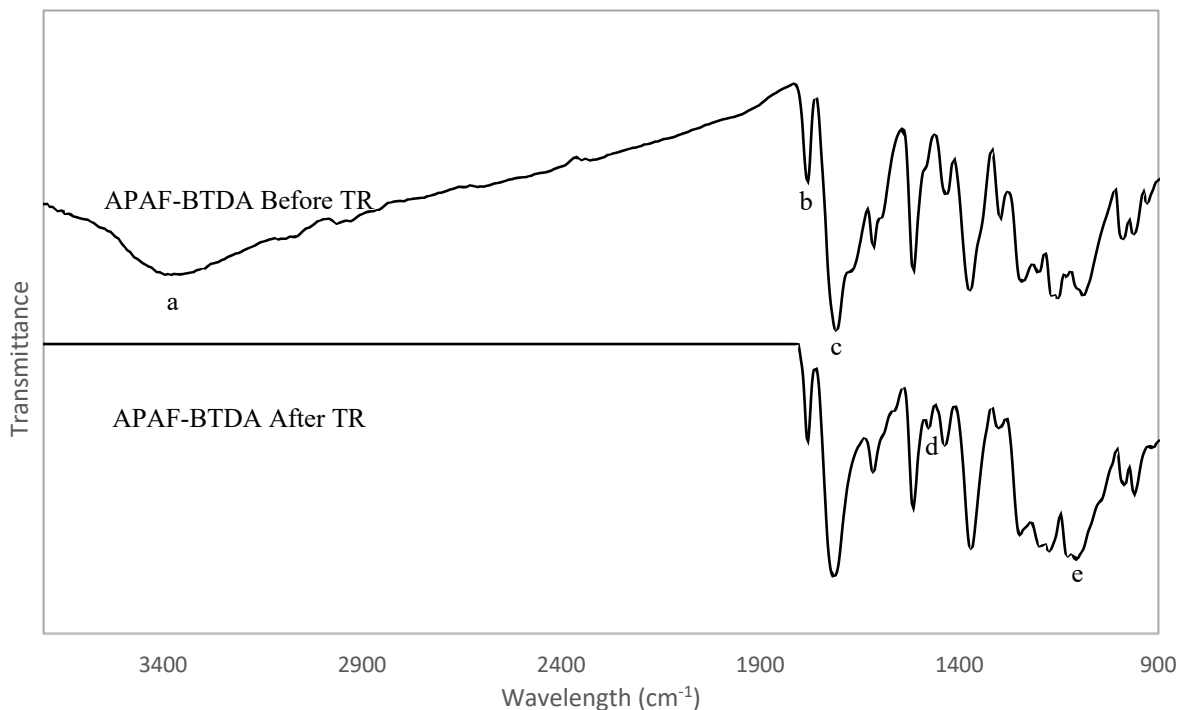
Figure 33. FTIR spectra of APAF-BTDA membranes before and after TR.

The FTIR spectrum of the APAF-BTDA membrane after TR is also presented in Figure. 33 and the most important peaks are labelled. During this step, the polyimide is converted to polybenzoxazole thermally somewhere between 300 and 400°C. Peaks (d) and (e) at 1474 cm^{-1} and 1059 cm^{-1}, respectively, correspond to the benzoxazole bands indicating that thermal conversion did indeed take place.

Some other peaks that can be observed but not labelled include wavenumbers between around 1300 cm^{-1} and 1000 cm^{-1} corresponds to C-F stretching and is attributed to the diamine

structure. Additionally, the absence of a peak at around 1515 cm^{-1} indicate that the cyclization is complete [7,11]. Also, there are multiple imide groups at wavenumbers around 1778, 1724, 1373 and 1091 cm^{-1} indicating the presence of imide and hence emphasizes that polyimides were synthesized successfully [28].

SEM was used to investigate the morphology of the polyimide membranes before and after TR (Figures. 34). All of the synthesized membranes had similar morphology of a dense layer. Further observation reveals that there are slightly different morphologies between the surface side, or the side of the membrane which was in contact with the material it was cast on, and the exposed side, or the side of the membrane that was exposed to atmosphere, of the membrane. The surface side shows a rougher morphology which could be due to sample preparation, however, this is unlikely due to the rough patterned morphology observed at the exposed side of the membrane. This dichotomy means that the rough morphology of the surface side is most likely due to some surface tension between the polyimide and the surface on which it was cast (Kapton) which could have been caused by the interaction of the phases with the solvent used (DMF). Looking at the TR membrane SEM, it is clearly observed that the two layer morphology disappeared. This could be due to the relaxation of the polymer chains during TR which caused the polymer chains to become more rigid.
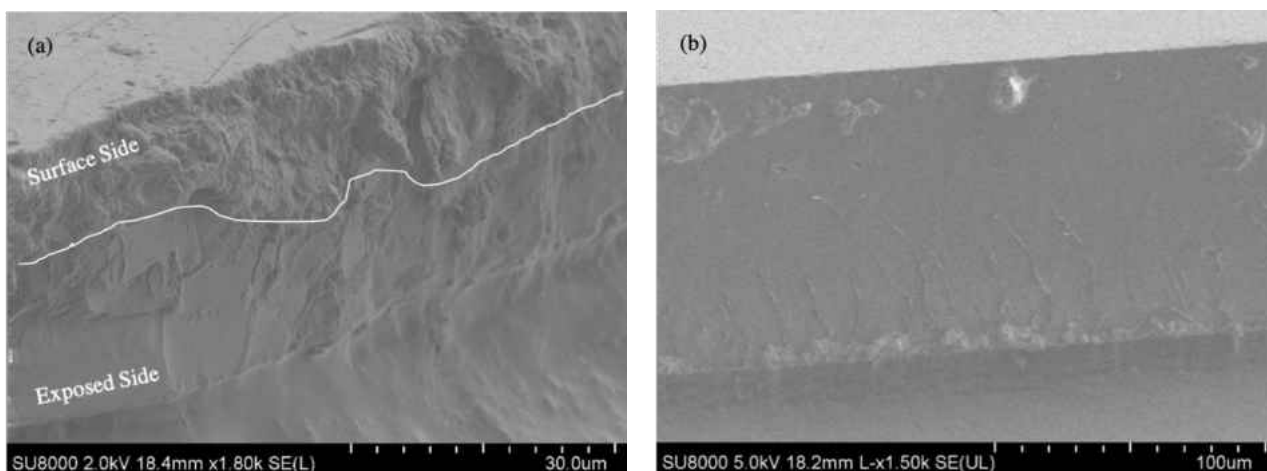
Figure 34. SEM images of polyimide membrane, (a) before TR and (b) after TR, showing the dense cross-section.

Polymeric properties for each membrane are displayed in Table. 16. Glass transition temperatures (T_g) of the synthesized polyimide membranes were determined by DSC. The T_g is considered one of the most significant properties when dealing with polymer synthesis primarily because it directly measures the extent of rigidity or flexibility of the polymer chains [8,11,25]. Knowing the extent of rigidity is crucial when fabricating membranes for gas separation because it affects the kinetics of thermal rearrangement and ultimately the gas separation properties of the membranes [11,25]. The APAF-PMDA polyimide membrane was found to have the highest Tg (271ºC), followed by APAF-BTDA (268ºC) and APAF-ODPA (250ºC), making the average Tg 263ºC which is consistent with other polyimides [11,25,29]. The APAF-ODPA has the lowest T_g mainly due to the flexibility of the dianhydride pendant groups whereas the other polyimides have rigid pendant groups that usually result in higher T_g values [25,29].

Table 16. Properties of the synthesized polyimides membranes.

Polymer	DSC T$_g$ (°C)	GPC Mw (g/mol)	GPC Mn (g/mol)	GPC PDI	TGA T$_d$ (°C)
APAF-PMDA Pre TR	271	35,642	16,000	2.2	556.07
APAF-ODPA Pre TR	250	25,337	11,072	2.2	547.45
APAF-BTDA Pre TR	268	94,417	47,912	2.0	548.91

GPC was used to determine the molecular weight (*Mw*) of the synthesized HPI powders. Testing the powders instead of the membranes ensured a more accurate measurement since the HPIs are highly soluble compared to the insoluble thermally treated membranes due to the crosslinking that takes place during membrane fabrication. It was found that the *Mw* values of APAF-PMDA and APAF-ODPA (35,642 g/mol and 25,337 g/mol) are within the expected *Mw* values for homopolymers [11,25]. Such *Mw* is considered relatively low mainly due to the bulkiness of the diamine limiting its reaction with the dianhydride together with the less stable pendant groups [26]. Among the two, APAF-ODPA has the lowest *Mw* which is believed to be due to the flexible nature of this dianhydride which makes the dianhydride unstable causing low conversion efficiencies. The APAF-PMDA polyimide is more stable than ODPA but not as stable at BTDA, meaning it has more freedom to interact with the diamine which leads to a higher *Mw*. The *Mw* value for APAF-BTDA is considered very high (94,417 g/mol) which could be attributed to both its rigid nature and its very stable pendant group. The combination of rigidity and stability potentially led the reaction to higher conversion efficiencies and could explain the increase in *Mw*. Generally, polymers with higher *Mw* values often correspond to enhanced mechanical properties, hence, APAF-BTDA has the best mechanical properties among the three polyimides. This has a significant impact on the TR of the membranes as discussed later. Moreover, the average polydespersity index (PDI), or the distribution of polymer chain molecular weights in a given polymer, is around 2.1 which is a

typical value for condensation polymerization [30]. A PDI that is greater than 1 usually means that the polymer growth was not controlled and is not monodisperse.

Comparing the results of this paper with our previous work [11] generally shows that the values of T_g and Mw obtained in this work are higher. This was expected and is mainly attributed to the drying step of the NMP solvent where it was not dried in our previous work [11]. Drying the NMP solvent reduces the amount of moisture considerably which is significant because dianhydrides are highly sensitive to moisture where side reactions between the dianhydride and moisture are more likely to take place than the main reaction [23,31]. This does not allow the polymerization reaction to reach high conversion efficiencies and, thus, incomplete polymerization takes place. The fact that T_g and Mw values are higher indicate that the condensation polymerization reaction indeed reached higher conversion efficiencies.

The degradation temperatures (T_d) of the polyimide membranes refers to the temperature at which the functional groups break off and they were determined using the TGA. In other words, T_d could be used to determine the thermal stability of the polymers which ultimately dictates their applications. Again, APAF-PMDA was found to have the highest T_d (556.07ºC), followed by APAF-BTDA (548.81ºC) and finally APAF-ODPA (548.45ºC). These values are considered very high for glassy polymer like polyimide. This means that these polyimide membranes can be used in various applications that require thermal resilience.

The TGA was also used to investigate the extent of TR of the synthesized membranes as they thermally convert from polyimides to polybenzoxazole. This conversion is determined by monitoring the weight loss which is due to CO_2 evolution as the hydroxyl-imide rings thermally rearrange to benzoxazole rings [2,31]. Generally, it seems like all the polyimide membranes are stable up to 300-350ºC where afterwards weight loss is observed to occur

mainly between 400ºC and 450ºC (Figure. 35) at which point CO_2 evolution is at maximum. These temperatures indicate both that the thermal cyclization reaction takes place to form polybenzoxazole [2] and that this is the optimum temperature to convert polyimide to polybenzoxazole. Since the TR in this work was done at temperature up to 400ºC, it is safe to assume that the membranes were not thermally rearranged completely. However, the extent of TR was found to be very close to completion as shown in Table. 17 which presents both the theoretical and experimental weight loss percentages of polyimide membranes. The experimental values obtained in this work found to be relatively close to the theoretical values, indicating that the thermal conversion was near completion.
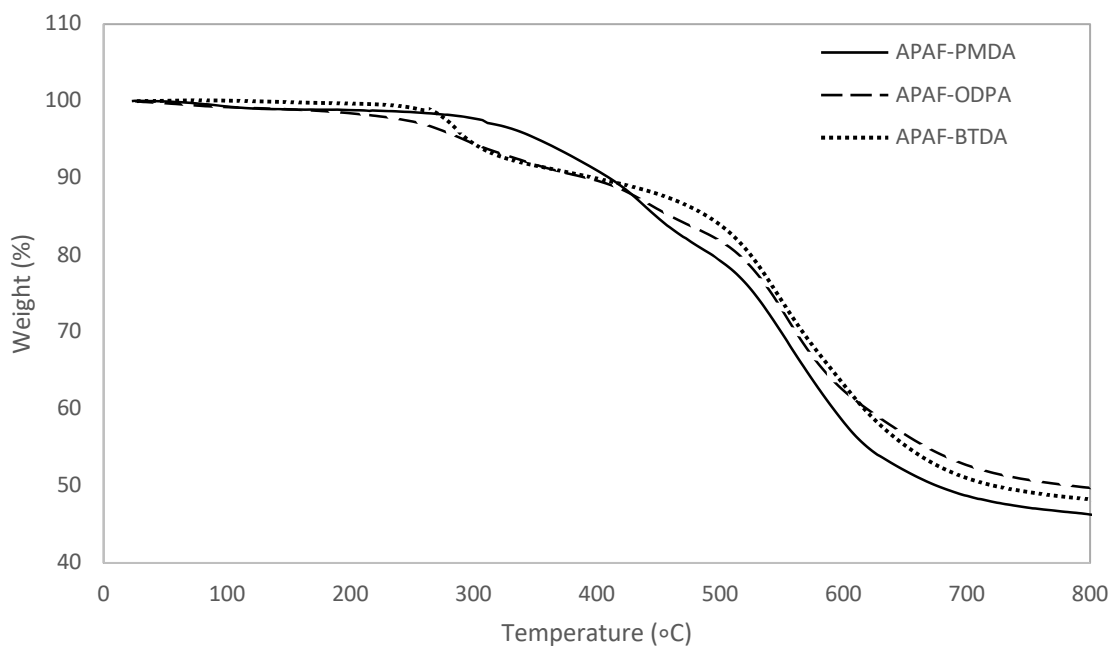
Figure 35. The weight (%) of the polyimide membranes under N2 atmosphere.

Table 17. Theoretical and experimental weight loss values of polyimide membranes at 400-450ºC.

Polyimide	Theoretical Weight Loss [31]	Experimental Weight Loss	Extent of TR
APAF-PMDA	15.8%	12.9%	82%
APAF-ODPA	13.6%	10.9%	80%
APAF-BTDA	13.3%	13.1%	99%

The separation properties of the synthesized polyimide membranes before and after TR (Table. 18) are compared to the 2008 Robeson upper bound [32] (Figures.36-38). Generally, TR enhanced the gas separation performance of polyimide membranes due to the fact that the backbone segments of thermally rearranged polymers have limited mobility, giving them strong selective functions [2].

Table 18. Gas permeation data of polyimide membranes before and after TR.

Polymer	$P(N_2)$ Barrer	$P(CH_4)$ Barrer	$P(CO_2)$ Barrer	$\propto (CO_2/CH_4)$	$\propto (N_2/CH_4)$	$\propto (CO_2/N_2)$
APAF-PMDA Pre TR	0.9	0.8	27	35.1	1.2	29.5
APAF-PMDA Post TR	32	22	904	41	1.4	28.3
APAF-ODPA Pre TR	5.3	3.3	133	39.9	1.6	25.4
APAF-ODPA Post TR	3.6	1.3	101	80.8	2.9	28.2
APAF-BTDA Pre TR	6.3	3.1	133	43.3	2.1	21
APAF-BTDA Post TR	17	13	676	51.9	3.1	39.2

In the case of CO_2/CH_4 gas pair, it is clearly observed that the gas separation performance of the three polyimide membranes are significantly enhanced where they exceed the 2008 upper bound, which is consistent with literature [2,5,7]. This is mainly due to the kinetic diameter difference between CO_2 (0.330 nm) and CH_4 (0.380 nm) which favors the diffusion of CO_2 explaining its higher permeability compared to CH_4.Moreover, the polarity of CO_2 is higher than that of CH_4 which makes it more soluble in the polyimide membrane.

The separation of N_2 and CH_4 is very challenging mainly because the two species have very similar kinetic diameters and dielectric constants. Among the two gases, nitrogen has a slightly smaller kinetic diameter of 0.364 nm compared to methane (0.380 nm) which means that nitrogen is more favored to diffuse through the membrane [2,33]. Nevertheless, methane has a slightly higher dielectric constant of 1.1 compared to nitrogen (1.0) which means that methane is more condensable and hence solubility favors methane since the dielectric constant

of polyimide films is typically around 3.4 [34,35]. This means that the low selectivity of the membranes is due to this solution-diffusion mechanism. Since the difference between the kinetic diameters is more significant than that of the dielectric constants, gas diffusion plays a leading role than that of the solubility which explains the higher permeabilities of nitrogen compared to methane. Among the three membranes tested, only the APAF-BTDA polyimide membrane barely crossed the upper bound. This noteworthy performance could be linked to the high *Mw* of APAF-BTDA which has a significant impact on the kinetic of TR and thus the final separation performance.

Examination of the CO_2/N_2 gas pairs reveals a noticeable increase in selectivity, where all of the membranes have ideal selectivities above 10. Furthermore, there is a significant increase in CO_2 permeation for APAF-PMDA and for APAF-BTDA, which additionally brushes the upper bound.

Comparing the data obtained in this paper to that presented by Park et al. [2], it is observed that our work resulted in slightly better sepation properties and that is primarly attributed to the imidization routes used. While they [2] used the thermal imidization routes, we used the azeotropic imidization route. Between the two routes, azeotropic usually results in higher permeabilities because the polymer chains during azeotropic imidization have higher freedom to mobilize [7]. This results in better packing of polymer chains and thus a higher diffusivity selectivity parameter, which is clearly evident in the CO_2/CH_4 gas pair [7].
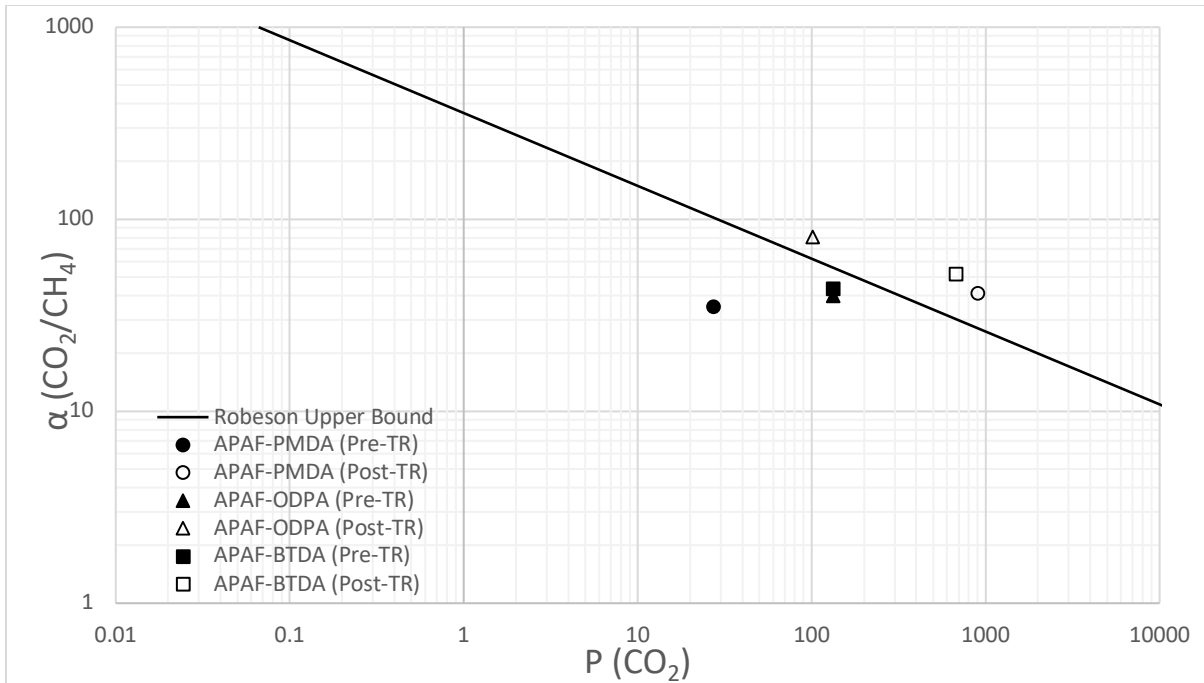
Figure 36. CO_2/CH_4 selectivity and CO2 permeability performance of polyimide membranes before and after TR plotted with the 2008 upper bound.
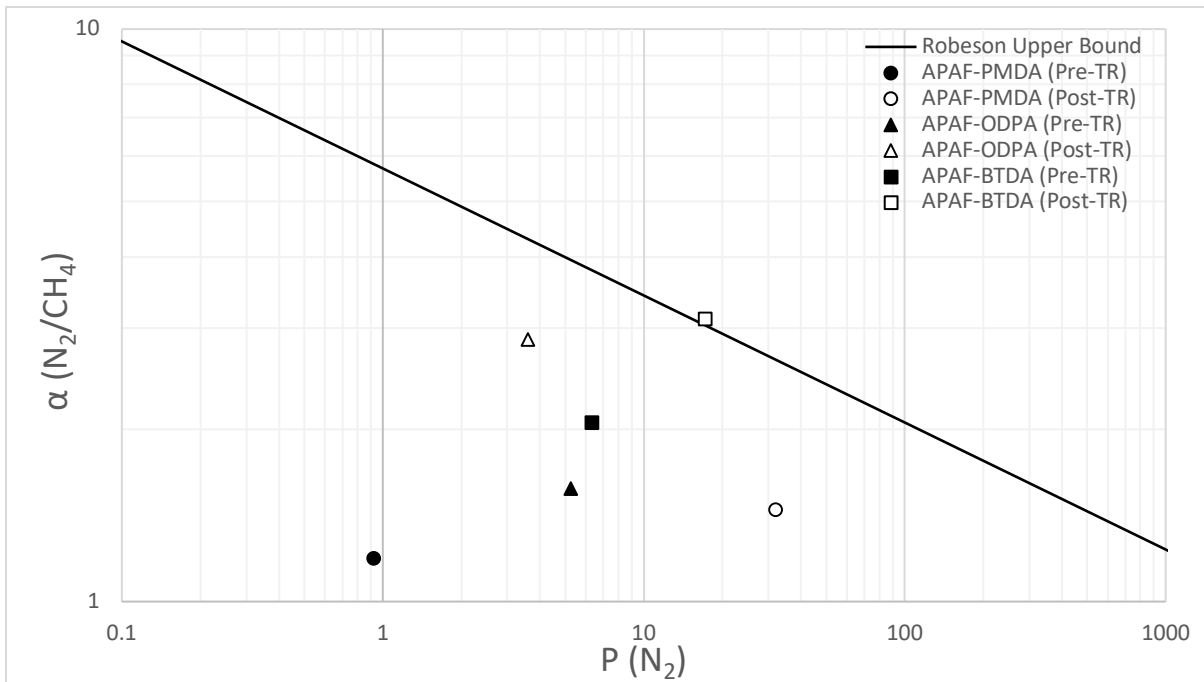

Figure 37. N_2/CH_4 selectivity and N2 permeability performance of polyimide membranes before and after TR plotted with the 2008 upper bound.
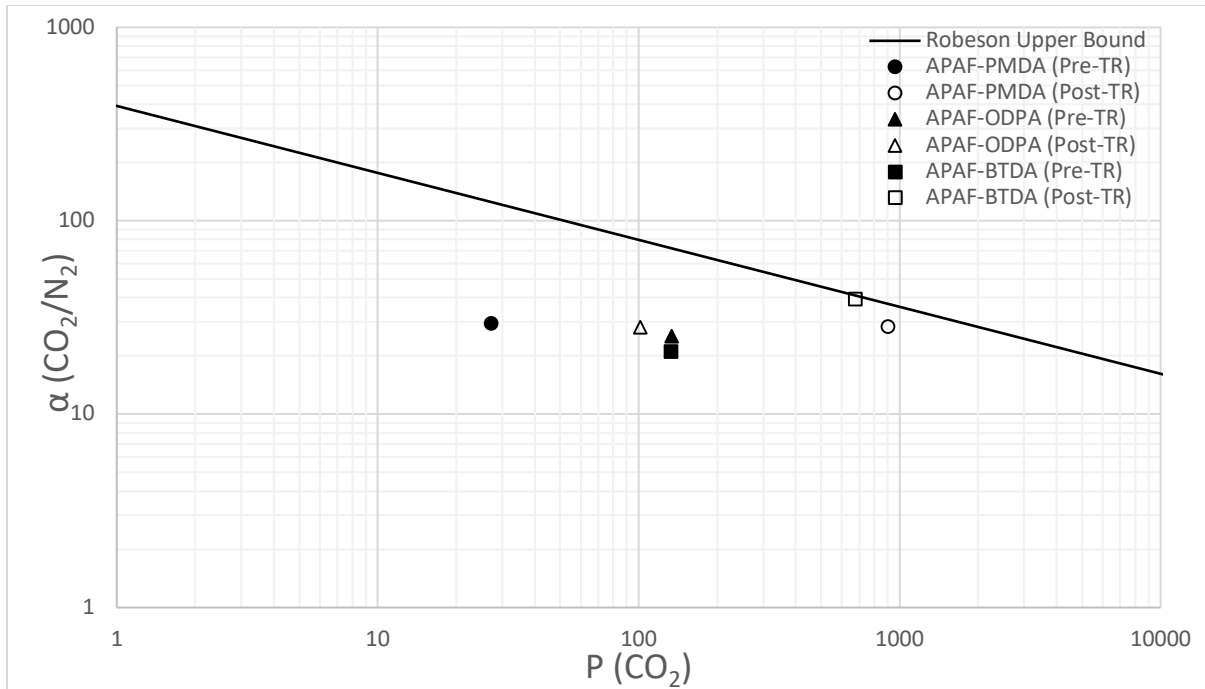
Figure 38. CO_2/N_2 selectivity and CO2 permeability performance of polyimide membranes before and after TR plotted with the 2008 upper bound.

Among the three polyimide membranes, APAF-BTDA showed superlative performance followed by APAF-PMDA and APAF-ODPA. The noticeable increase in gas permeabilities could potentially be attributed to the percentage of hydroxyl group (-OH) present in each of the polyimides which depends on both the percentage of diamine used [7,31,36] and on the molecular weight of the polyimides according to EQ. 23 [7]:

$$mol\ \%\ OH\ groups = \frac{\left(\frac{2 \times Mw\ OH \times 100}{MW\ APAF}\right) \times APAF\ content\ (\%)}{MW\ of\ the\ polymer} \qquad EQ.\ 23$$

Since a 1:1 ratio of diamine to dianhydride was used in this work, the content of APAF is 50% and the *Mw* of the synthesized membranes are presented in Table. 1. It was found that mol % of OH groups in APAF-BTDA is 0.5%, APAF-PMDA is 1.3% and APAF-ODPA is 1.8%. This means that a higher OH percentage lead to lower performance, which explains the ranking of the polyimides membranes studied in this work.

The preformance of the membranes could also be expalined by investigating the *d*-spacing which is the average intersegmental distance of the polymer chains or, in other words, the FFV [26]. The greater the shift in the broad peak X-ray pattern, the greater the change in *d*-spacing and hence FFV which effects the gas permeabilities significantly. Table. 18 shows that APAF-BTDA has the highest change in *d*-spacing followed by APAF-PMDA and APAF-ODPA. Form Figure. 39, it is clear that the broad peak of APAF-BTDA shifted to the left after TR indicating that the FFV increased which explains its much improved prefoemance. Moreover, the extent of the peak shift could also be linked to the extent of TR where APAF-BTDA had the highest weight loss and thus the highest conversion from polyimide to PBO, as previously shown in Table. 18. This shows that the higher the conversion from polyimide to PBO, the higher the *d*-spacing and, consequently, the higher the pemeation values are.

Table 19. Calculated d-spacing from polyimide membranes before and after TR.

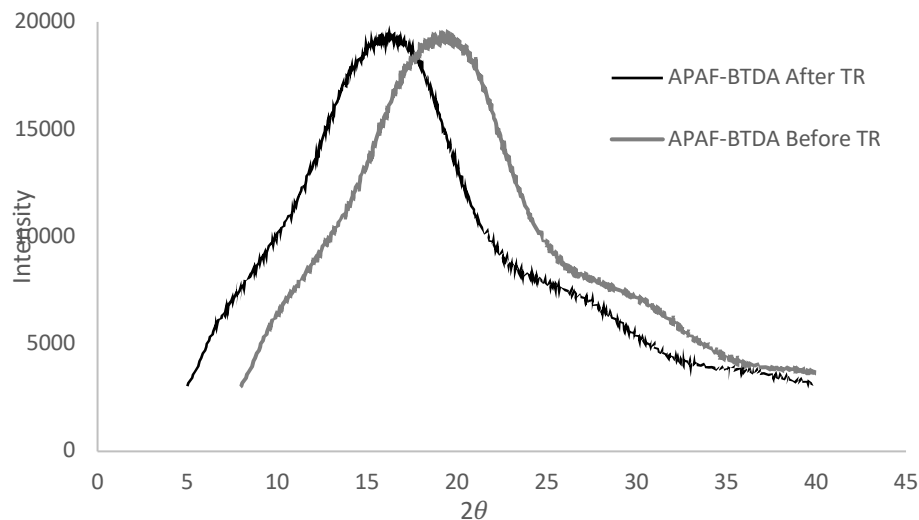| Polyimide	XRD Before TR *d*-spacing (Å)	XRD After TR *d*-spacing (Å)	% Change in *d*-spacing
APAF-PMDA	4.924	5.535	12.4
APAF-ODPA	4.973	5.132	3.2
APAF-BTDA	4.544	5.211	14.7

Figure 39. XRD pattern of APAF-BTDA before and after TR.

4.9 Conclusions

Three different dianhydride precursors were reacted azeotropically with diamine to form polyimide membranes. These membranes were then thermally converted to polybenzoxazole via a mechanism known as thermal rearrangement (TR), which is a mechanism that involves a random chain configuration of dense polymeric membranes resulting in refined microvoids which significantly improved selective molecular gas species transport. In this work, the gas separation performance of synthesized polyimide membranes using CO_2/CH_4, N_2/CH_4 and CO_2/N_2 gas pairs was improved between 1.5 to 2 orders of magnitude through TR. The chemical characterization of the membranes before and after TR showed that first polyimide and then polybenzoxazole were successfully synthesized. Furthermore, other characterization properties such as the molecular weight, glass transition temperature, degradation temperature, permeation tests and *d*-spacing provide detailed information explaining the reasons behind the improved performance. In conclusion, the TR mechanism enables the synthesis of membranes that have outstanding thermal, mechanical and chemical properties which makes them viable candidates for various applications under a wide range of conditions.

Reference

[1] A.F. Ismail, K.C. Khulbe, T. Matsuura, K.C. Khulbe, and A.F. Ismail, Gas Separation Membranes : Polymeric and Inorganic, Cham, Springer, 2015.

[2] H.B. Park, S.H. Han, C.H. Jung, Y.M. Lee, and A.J. Hill, Thermally rearranged (TR) polymer membranes for CO2 separation, Journal of Membrane Science, 359 (2010) 11.

[3] H.B. Park, B.D. Freeman, Z. Zhang, M. Sankir, and J.E. McGrath, Highly chlorine-tolerant polymers for desalination, Angewandte Chemie (International ed. in English), 47 (2008) 6019.

[4] S. Matteucci, Y. Yampolskii, B.D. Freeman, and I. Pinnau, Transport of Gases and Vapors in Glassy and Rubbery Polymers, in Anonymous , Materials Science of Membranes for Gas and Vapor Separation, Chichester, UK, John Wiley & Sons, Ltd, 2006, pp. 1-47.

[5] H.B. Park, Y.M. Lee, Polymeric Membrane Materials and Potential Use in Gas Separation, in Anonymous , Advanced Membrane Technology and Applications, Hoboken, NJ, USA, John Wiley & Sons, Inc, 2008, pp. 633-669.

[6] Y. Sakai, M. Matsuguchi, and N. Yonesato. Humidity sensor based on alkali salts of poly(2-acrylamido-2-methylpropane sulfonic acid). Electrochimica Acta, 46 (2001) 1509.

[7] A. Tena, S. Shishatskiy, D. Meis, J. Wind, V. Filiz, and V. Abetz, Influence of the Composition and Imidization Route on the Chain Packing and Gas Separation Properties of Fluorinated Copolyimides, Macromolecules, 50 (2017) 5839.

[8] C.E. Sroog. Polyimides. Progress in Polymer Science, 16 (1991) 561.

[9] M.I. Bessonov, Polyamic acids and polyimides, Boca Raton [u.a.], CRC Press, 1993.

[10] Y. Furusho, Polymer synthesis, Berlin [u.a.], Springer, 2004.

[11] M.A.Q. Al-Sayaghi, J. Lewis, C. Buelke, and A.S. Alshami. Physicochemical and thermal effects of pendant groups, spatial linkages and bridging groups on the formation and processing of polyimides. International Journal of Polymer Analysis and Characterization, 23 (2018) 566.

[12] D.R. Pesiri, B. Jorgensen, and R.C. Dye. Thermal optimization of polybenzimidazole meniscus membranes for the separation of hydrogen, methane, and carbon dioxide. Journal of Membrane Science, 218 (2003) 11.

[13] X. Hu, S.E. Jenkins, B.G. Min, M.B. Polk, and S. Kumar, Rigid-Rod Polymers: Synthesis, Processing, Simulation, Structure, and Properties, Macromolecular Materials and Engineering, 288 (2003) 823.

[14] M. Kusama, T. Matsumoto, and T. Kurosaki, Soluble Polyimides with Polyalicyclic Structure.3. Polyimides from (4arH,8acH)-Decahydro-1t,4t:5c,8c-dimethanonaphthalene-2t,3t,6c,7c-tetracarboxylic 2,3:6,7-Dianhydride, Macromolecules, 27 (1994) 1117.

[15] J.P. Chen, A. Natansohn, Synthesis and Characterization of Novel Carbazole-Containing Soluble Polyimides, Macromolecules, 32 (1999) 3171.

[16] J.V. Grazulevicius, P. Strohriegl, J. Pielichowski, and K. Pielichowski. Carbazole-containing polymers: synthesis, properties and applications. Progress in Polymer Science, 28 (2003) 1297.

[17] D. Liaw, F. Chang, M. Leung, M. Chou, and K. Muellen. High Thermal Stability and Rigid Rod of Novel Organosoluble Polyimides and Polyamides Based on Bulky and Noncoplanar Naphthalene−Biphenyldiamine. Macromolecules, 38 (2005) 4024.

[18] M.S. Butt, Z. Akhter, and M.z. Zaman. Synthesis and Characterization of Polyimides Based on Flexible Diamine. (2013).

[19] B.D. Freeman, Basis of Permeability/Selectivity Tradeoff Relations in Polymeric Gas Separation Membranes, Macromolecules, 32 (1999) 375.

[20] T. Woock, S. Bjorgaard, B. Tande, and A. Alshami. Purification of natural gas using thermally rearranged polybenzoxazole and polyimide membranes – a review: part 2. Membrane Technology, 2016 (2016) 7.

[21] D.F. Sanders, Z.P. Smith, C.P. Ribeiro, R. Guo, J.E. McGrath, D.R. Paul, et al. Gas permeability, diffusivity, and free volume of thermally rearranged polymers based on 3,3′-dihydroxy-4,4′-diamino-biphenyl (HAB) and 2,2′-bis-(3,4-dicarboxyphenyl) hexafluoropropane dianhydride (6FDA). Journal of Membrane Science, 409-410 (2012) 232.

[22] Y.M. Xu, N.L. Le, J. Zuo, and T. Chung. Aromatic polyimide and crosslinked thermally rearranged poly(benzoxazole-co-imide) membranes for isopropanol dehydration via pervaporation. Journal of Membrane Science, 499 (2016) 317.

[23] E. Drioli, E. Drioli, and G. Barbieri, Membrane engineering for the treatment of gases (volume 1, Cambridge, NBN International, 2011.

[24] S.H. Han, N. Misdan, S. Kim, C.M. Doherty, A.J. Hill, and Y.M. Lee, Thermally Rearranged (TR) Polybenzoxazole: Effects of Diverse Imidization Routes on Physical Properties and Gas Transport Behaviors, Macromolecules, 43 (2010) 7657.

[25] C.Y. Soo, H.J. Jo, Y.M. Lee, J.R. Quay, and M.K. Murphy. Effect of the chemical structure of various diamines on the gas separation of thermally rearranged poly(benzoxazole-co-imide) (TR-PBO-co-I) membranes. Journal of Membrane Science, 444 (2013) 365.

[26] J.K. Adewole, A.L. Ahmad, S. Ismail, C.P. Leo, and A.S. Sultan, Comparative studies on the effects of casting solvent on physico-chemical and gas transport properties of dense polysulfone membrane used for CO2/CH4separation, Journal of Applied Polymer Science, 132 (2015).

[27] M. Sadrzadeh, M. Amirilargani, K. Shahidi, and T. Mohammadi. Pure and mixed gas permeation through a composite polydimethylsiloxane membrane. Polymers for Advanced Technologies, 22 (2011) 586.

[28] Diego Guzman-Lucero, Jorge Froylan Palomeque-Santiago, Claudia Camacho-Zúñiga, Francisco Alberto Ruiz-Treviño, Javier Guzman, Alberto Galicia-Aguilar, et al, Gas Permeation Properties of Soluble Aromatic Polyimides Based on 4-Fluoro-4,4'-Diaminotriphenylmethane, Materials, 8 (2015) 1951.

[29] M. Calle, Y. Chan, H.J. Jo, and Y.M. Lee. The relationship between the chemical structure and thermal conversion temperatures of thermally rearranged (TR) polymers. Polymer, 53 (2012) 2783.

[30] Agilent, Polymer Molecular Weight Distribution and Definitions of MW Averages .

[31] Chul Ho Jung, Young Moo Lee. Gas Permeation Properties of Hydroxyl-Group Containing Polyimide Membranes. Macromol. Res, 16 (2008) 555.

[32] L.M. Robeson. The upper bound revisited. Journal of Membrane Science, 320 (2008) 390.

[33] D.W. Breck, Zeolite molecular sieves, New York [u.a.], Wiley, 1974.

[34] A. Harvey, E. Lemmon. Method for Estimating the Dielectric Constant of Natural Gas Mixtures. Int J Thermophys, 26 (2005) 31.

[35] Dupont Kapton, Dupont Kapton. General Specification: Polyimide Film. (2018). Available from: https://www.dupont.com/content/dam/dupont/products-and-services/membranes-and-films/polyimde-films/documents/DEC-Kapton-general-specs.pdf.

[36] N. Alaslai, B. Ghanem, F. Alghunaimi, E. Litwiller, and I. Pinnau. Pure- and mixed-gas permeation properties of highly selective and plasticization resistant hydroxyl-diamine-based 6FDA polyimides for CO2/CH4 separation. Journal of Membrane Science, 505 (2016) 100.

CHAPTER 5: SUPPLEMENTARY INFORMATION

Completing this research project was challenging because a lot of issues emerged while preforming the experiments. As previously mentioned in the executive summary, this research project consisted of three main goals which demonstrated the three main stages of this research:

- Stage (1): Synthesis of the polyimide powders

- Stage (2): Fabrication of free-standing polyimide membranes

- Stage (3): Conducting gas permeation tests using the fabricated membranes

The major issues encountered during each stage and the attempted potential solutions for each of the issues are discussed in this chapter.

5.1 Stage (1): Synthesis issues

Synthesizing the polyimide powders was the most challenging part of this project and that is mainly because the resulting product was not a flaky powder but rather a hard chunk of solids. Moreover, the resulting hard chunk of solids were in most cases insoluble in any of the solvents used (NMP or DMF) which made continuing to stage (2) impossible because the processability of the polymer was very poor. It is important to note that each experiment took an average of 5 days to be completed and the first 187 experiments failed. This corresponds to around 80% of the experiments. Only the last 72 experiments were successful (20%). In an attempt to address this major issue, the following potential solutions were tested:

5.1.1 Changing the amount of solvent

Changing the amount of solvent used during the condensation reaction was the first variable that was tested because the literature papers that were considered were not very clear regarding the exact amount of solvent to be used. Therefore, the procedure followed was revised again with the assistance a chemist. There was one main part of the procedure that was confusing which states: '… **enough** NMP was added to dissolve the diamine' and then later in the procedure it states that 'Additional NMP was then poured into the flask until a 20 wt% monomer solution is obtained'. But the main question is, does the 'enough' amount added initially count towards the 20 wt% or not? If it does account for it, then the total amount of NMP put is around 26.4 mL only. Whereas, if it does not account for it, the total amount is 77.8 mL of NMP. To test this, three different solvent amounts (70, 50 and 26 mL) were used to synthesize one polyimide (BisAPAF-ODPA). The resulting HPI powders using the three different amounts of solvent had different morphologies (Figure. 40) and they were visually different too (Figure. 41). When only 26 mL was added, the resulting HPIs were very hard to a point where a ball mill had to be used to crush it. Whereas, when 77 mL of NMP was added the resulting HPIs were softer and could be crushed by hands which made it dissolve better than the other one. However, both HPIs would not synthesize a membrane.
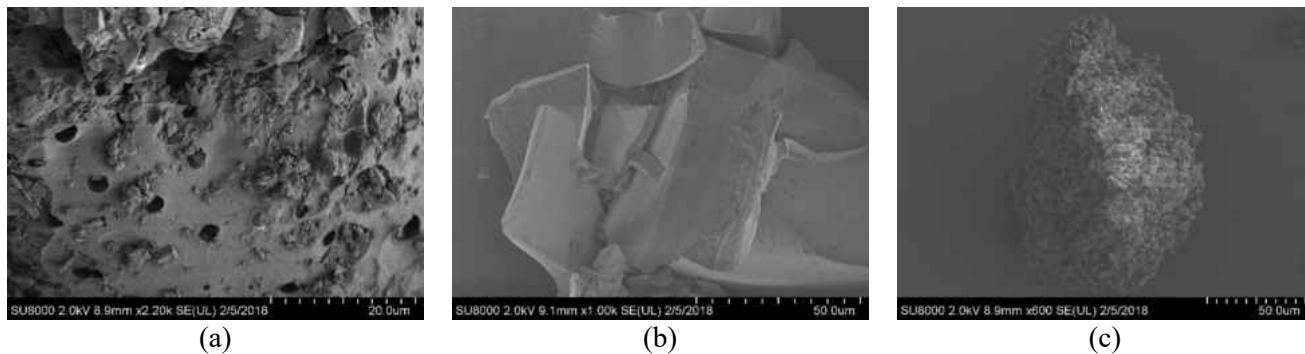

(a)   (b)   (c)

Figure 40. SEM image of: (a) HPI-ODPA made using 70 mL of NMP, (b) HPI-ODPA made using 50 mL of NMP and (c) HPI-ODPA made using 26 mL of NMP.
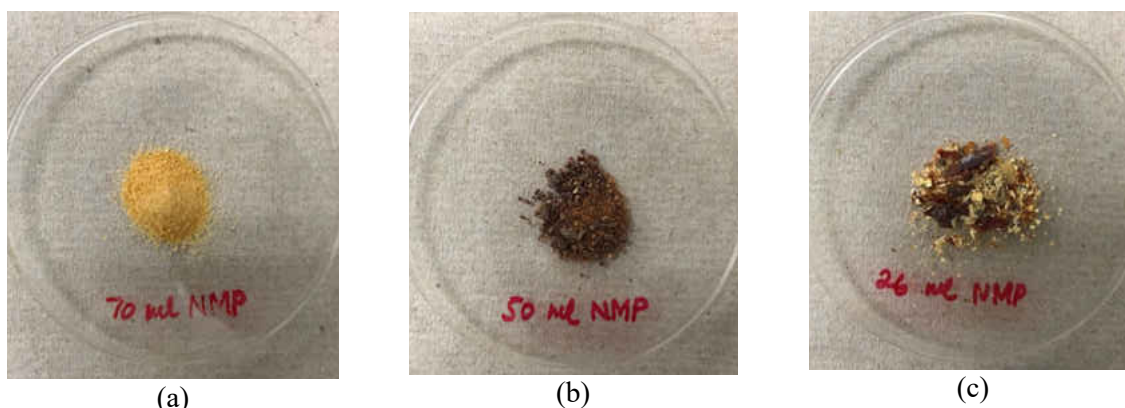
Figure 41. Photographs of: (a) HPI-ODPA made using 70 mL of NMP, (b) HPI-ODPA made using 50 mL of NMP and (c) HPI-ODPA made using 26 mL of NMP.

However, the chemical composition of these HPI indicated that polyimides were indeed synthesized. From the spectrums presented in Figure. 42 and peaks identified in Table. 20 it is clearly noticed that all of the HPI-ODPAs are similar but have slightly different intensities. The peaks in region (a) (2900 cm^{-1} to 3500 cm^{-1}) in Fig. 4, are assigned to the hydroxyl group that comes from the BisAPAF. The peaks at 1788 cm^{-1} and the peaks in region (b) (1720 cm^{-1} to 1735 cm^{-1}) both indicate the presence of C=O stretching. In region (c), the peaks at around 1108 cm^{-1} to 1230 cm^{-1} represent C-C stretch and C-C(O)-C stretch respectively. Whereas, peaks in region (c) at around 1475 cm^{-1} is mostly O-H bend. All of these peaks show that the HPI samples have characteristic structures of polyimide. This means that the condensation reaction of the diamine with the dianhydride did indeed take place and resulted in polyimide.
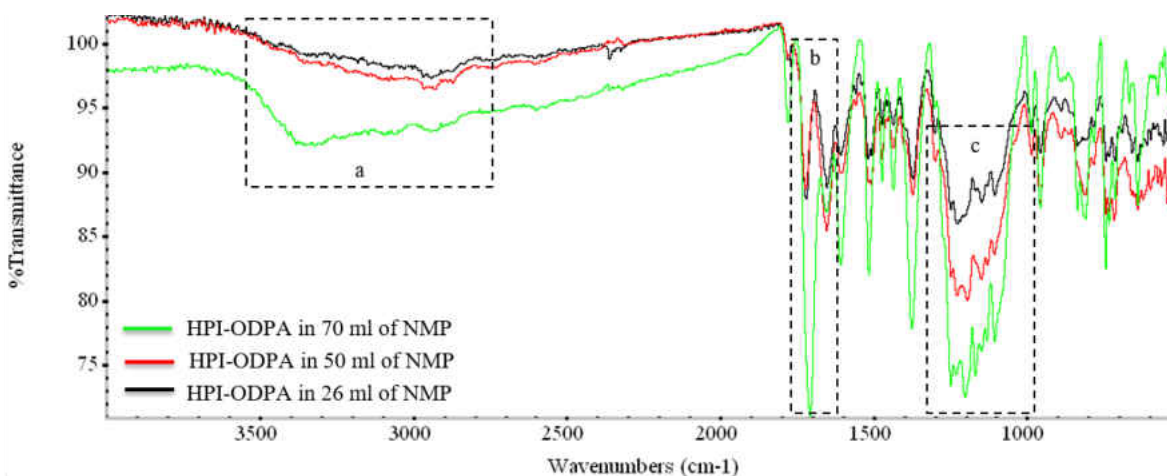

Figure 42. FTIR spectrum of HPI-ODPA powders made in 70ml, 50 ml and 26 ml of NMP.

Table 20. Infrared spectra of HPI-ODPA powders made in different amounts of NMP.

Functional group	Wave number recorded (cm⁻¹)
Hydroxyl group (OH)	2900-3500
C=O stretching	1720-1735 and 1788
C-C stretch	1108
C-C(O)-C stretch	1230
O-H bend	1475

Moreover, the molecular weights of the synthesized polyimides using the three different amounts of solvents ranged between around 2900 to 4200 which is considered extremely low as shwon in Table. 21. The main thing that did not make sense was that the low molecular weights obtained should result in soluble polymers; however, that was not case. This was finally expalied by the wrong precipitation method initially used and the high temperature that was used to dry the HPI which might have encourouged cross-linking to some extent.

Table 21. Properties of BisAPAF-ODPA HPI synthesized using three solvent amounts (70, 50 and 26 mL).

Polymer	Amount of NMP (mL)	M_n	M_w	PDI	Tg (°C)
HPI-ODPA	70	2787	4206	1.51	150
HPI-ODPA	50	1989	2939	1.48	145
HPI-ODPA	26	2015	2929	1.45	150

5.1.2 Changing the reactant ratios

Changing the reactant ratios was the second approach tested in an attempt to ge soluble polyimide powders. The reactant ratios of the monomers used were changed form 1:1 to 1:0.5 of diamine: dianhydride. The resulting HPIs dissolved and casted better but no membranes were fabricated because the caseted membrane looked as shown in Figure. 43. The membranes alomost disappeared potentailly because the casted solution had s lot of water and solvent in it which evaporated at the elvated temperatures leaving parts of the polyimide behind.

Figure 43. Resulting polyimide "membrane" synthesized form reactant ratio of 1:0.5 of diamine: dianhydride.

5.1.3 Diamine purification

The third and final approach attempted was the recrystallization of the diamine in order to purify it because the impurities present it could lead to branching or cross-linking of the polymer. The purity of the used diamine BisAPAF is 98% which might have affected the reaction and hence it was recrystallized in an attempt to boost the purity to about 99.9% and that was done using different non-polar solvents such as toluene, benzene and hexane as well as some polar solvents such as methane, deionized water and THF. Since diamine is more polar, a nonpolar solvent had to be used and among the three solvents used, toluene seemed to result in a diamine that is whiter in color compared to the yellowish initial color and hence it was used (Figure. 44). The resulting membrane was slightly modified (Figure. 45) but were very fragile. The moment they were picked up, they broke down into small pieces a shown in the circled part of Figure. 45.
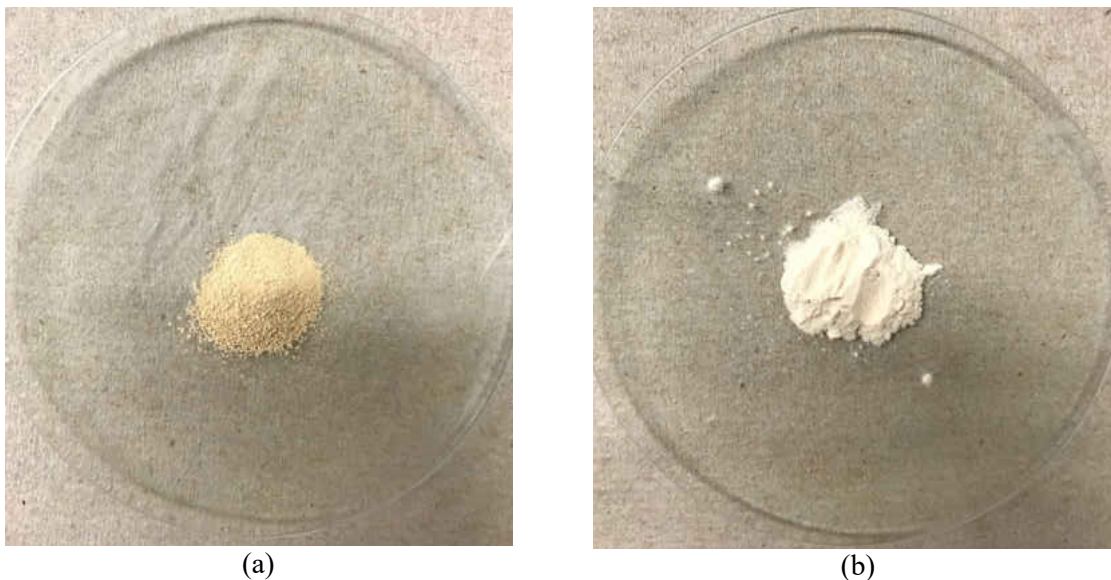
|(a)|(b)|

Figure 44. Photographs of the same diamine (a) before and (b) after recrystallizing in in Toluene.

Figure 45. Image of the membrane fabricated using the recrystallized diamine with ODPA.

5.1.4 Precipitation method

The issue of getting a soluble polyimide powder was finally overcome by using another precipitation method. The initial precipitation method used involved adding the HPAA solution after the azeotropic imidization to a small beaker (50 mL) of water: methanol and then water at room temperature. This always resulted in hard insoluble chunks of polyimide.

However, by using more solvent (700 mL) of water: methanol that was cooled to around 10 ºC in combination with creating a vortex resulted in flaky soluble polyimide (Figure. 46).
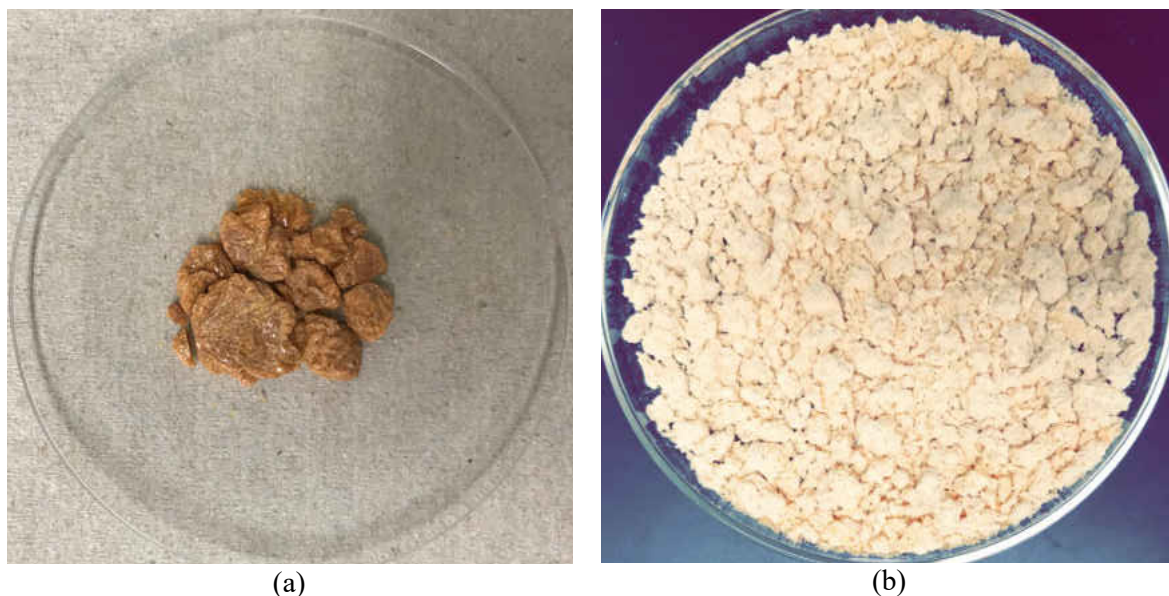

<div align="center">(a)   (b)</div>

Figure 46. Physical structure of BisAPAF-ODPA (a) precipitated in the 50 mL and at room temperature, (b) precipitated in 700 mL, at 10 ºC and with vortex.

5.1.5 Drying the solvent

Even after solving the solubility issue, the membranes would not form and the last approuch used was drying the NMP solvent using a drying agent as described in details in section (4.3.2). This finally solved the issue of polyimide that were brittle, evaporating leaving behind bits and easily tearing into very small pieces. The issue was found to be the amount of mositure in the solvent used which caused undesiered side reactions with the dianhydrides to take place. This resulted in low conversion efficiencies and incomplete polymerization. The polymers obtained after drying the solvent were close to those expected from polyimides as discussed perviously in sections (3.4) and (4.8). Samples of the powders produced are presented in Figure. 47.
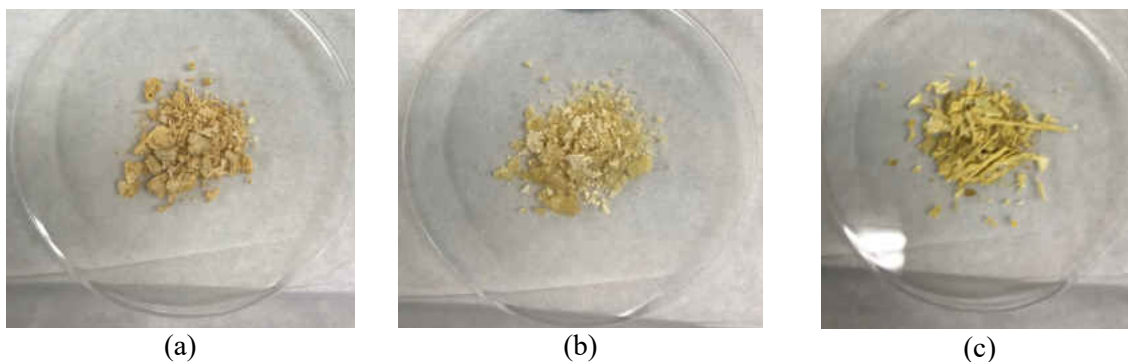
Figure 47. Samples of the synthesized polyimide powders: (a)APAF-PMDA, (b) APAF-ODPA and (c) APAF-BTDA.

5.2 Stage (2): Casting issues

After overcoming the issues associated with the synthesis stage of the research, a new issue emerged and that is fabricating the membrane. After obtaining the HPIs, they were dissolved in NMP and casted on different support materials. However, they would adhere to the material they were cast on very hard and any attempt of peeling them resulted in taring the membrane into small pieces. The materials used as a support included quartz plates, Pyrex plates, silicon sheets, Teflon paper and Teflon thick sheet.

5.2.1 Changing the support material

When quartz plates and the Pyrex plates were used, the membrane would stick completely as shown in Figure. 48. This was later believed to be due to the harshness of the NMP solvent used during the casting stage in combination with the elevated temperature might have triggered a bond between the membrane and the support material. This issue was attempted to be solved by used the silicon sheets, Teflon paper and Teflon thick sheet. Nevertheless, the solution would seem to show a hydrophilic-like behavior would it could break into smaller droplets all over the sheet.
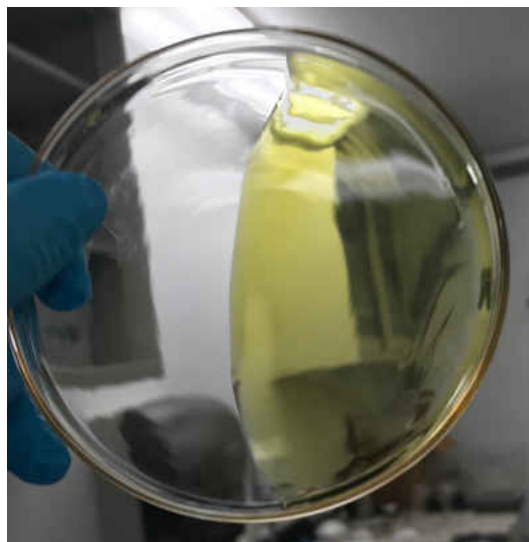
116

Figure 48. The dissolved polyimide powder solution adhered to the Pyrex glass after being thermally treated.

5.2.2 Functionalizing the support material

Another method used to overcome the issue of the membrane sticking to the support material was the functionalizing of the support material (i.e. the plat on which the membrane is cast) using sodium hydroxide (NaOH). This was done by submerging a Pyrex plate in NaOH and then drying it, washing it and drying it again. The membrane solution was then casted and thermally treated as usual. By doing this, only a part of the membrane did not stick but the rest of it was adhered. Therefore, the whole plate containing the membrane was then submerged into the NaOH for several hours as shown in Figure. 49a. The membrane was successfully detached from the plate as shown in Figure. 49b. However, the membrane obtained started developing cracks which made it impossible to test.
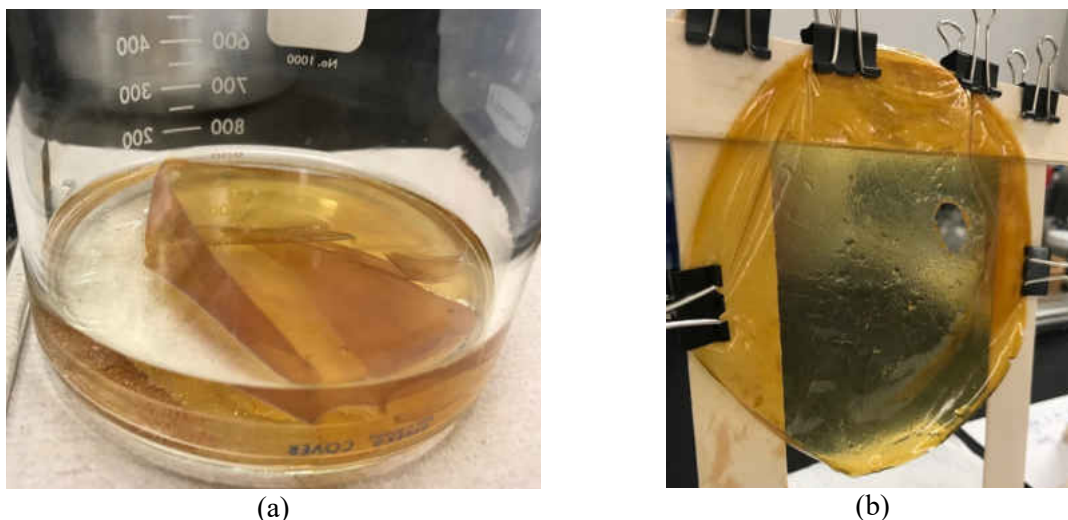
<div align="center">(a)   (b)</div>

Figure 49. Polyimide membrane (a) submerged in NaOH for several hours detaching and forming (b) free-standing membrane with many defects.

5.2.3 Changing the solvent and using Kapton®

The final approach used was changing the solvent used to dissolve the polyimide solvent from NMP to DMF. The is mainly because DMF is one of the most commonly used solvents in polymer synthesis and because it is considered a less harsh solvent with a boiling point of around 153 ºC compared to NMP which has s boiling point of around 202 ºC. In addition to that, Kapton® was used as a supporting base on which the solution is poured onto which provided a guaranteed on-stick medium (Figure. 50). This finally resulted in intact free-standing membranes that were easily peeled off as shown in Figure. 51.
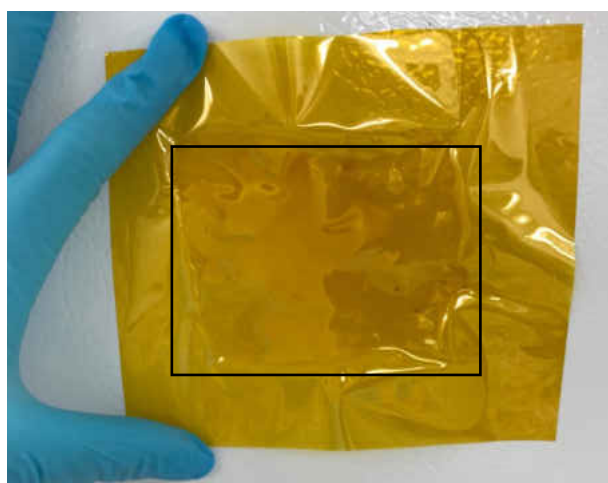

Figure 50. Casting the polyimide dissolved in DMF on a piece of Kapton®.
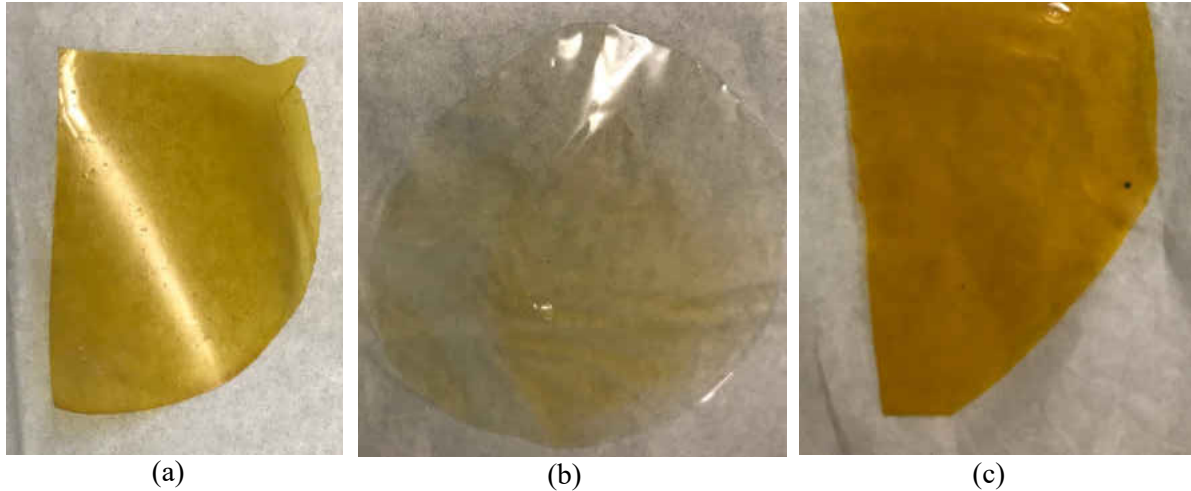
<div align="center">118</div>

Figure 51. Fabricated free-standing polyimide membranes: (a) APAF-PMDA, (b) APAF-ODPA and (c) APAF-BTD.

5.3 Stage (3): Premeation tests issues

One of the main issues faced during preforming the permeation tests was testing thin membranes (less than 50 μm). This was addressed by maintain a membrane thickness of between 50-75 μm and that was achieved by pouring an exact amount of 5g of solution for every membrane. Most of the membranes produced via this method were in good condition which enabled moving to the third stage where the permeation test was run. Another issue that emerged was while attempting to test mixed gases which resulted in the failure of the membranes due to plasticization. This caused the membranes to tear very easily although the withstood high pressures and testing time when testing the pure gases.

CHAPTER 6: CONCLUSIONS AND FUTURE RECOMMENDATIONS

The main objective of this thesis was to *study the effect of varying the dianhydride precursors on the synthesis and gas separation properties of polyimide membranes* where one diamine and three different dianhydrides were used to synthesize hydroxyl-polyimides and thermally rearrange them to polybenzoxazoles. The synthesis of the hydroxyl-polyimide powders was the most challenge stage of this project because polymer synthesis is very sensitive. The polyimide powders were synthesized successfully via the azeotropic imidization route and they were characterized intensively using FTIR, GPC, TGA, SEM, NMR and XRD. The powders were then fabricated into free-standing membranes which were tested before and after their thermal rearrangement to polybenzoxazoles. The characterization analysis proved that polyimides and polybenzoxazoles were indeed synthesized and the gas permeabilities and selectivities obtained were within the expected range according to literature. Among the three used precursors, the membranes made from BTDA showed superior physiochemical and gas separation properties followed by those made from PMDA and finally ODPA. Moreover, it is important to note that ideal selectivities using pure gases were used during the permeation testing and when mixed gases were used, the membranes failed.

Some of the future recommendations that could further this research are listed below:

- Avoid in-lab synthesis of polymers because the reactions are very sensitive and tricky and requires a lot of experience and more advanced equipment. Some of the main equipment needed to make the synthesis easier and more consistent include a proper

glass glove-box that is kept at constant conditions at all times and that detects both air and moisture contents. Moreover, having an automated casting equipment would overcome some of the issues associated with the consistency of the membrane fabrication. Buying off-shelf polymers will ensure that the integrity and consistency of the polymer is good and will save a lot of time since engineers are interest more in the applications side of this project.

- Explore new combination of monomers (some of which were listed in Table. 8) because the ones tested in this project are already considered very well established.

- Try experimenting co-polymer and blends because that would allow for more manipulation of properties and will result in even more superior performances.